DESIGN AND CHARACTERIZATION OF ELECTROMAGNETIC WAVE ABSORBING STRUCTURAL COMPOSITES

A THESIS SUBMITTED TO
THE GRADUATE SCHOOL OF NATURAL AND APPLIED SCIENCES
OF
MIDDLE EAST TECHNICAL UNIVERSITY

BY

GÖKSU GÜRER

IN PARTIAL FULFILLMENT OF THE REQUIREMENTS
FOR
THE DEGREE OF MASTER OF SCIENCE
IN
METALLURGICAL AND MATERIALS ENGINEERING

SEPTEMBER 2010

Approval of the thesis:

DESIGN AND CHARACTERIZATION OF ELECTROMAGNETIC WAVE ABSORBING STRUCTURAL COMPOSITES

submitted by **GÖKSU GÜRER** in partial fulfillment of the requirements for the degree of **Master of Science in Metallurgical and Materials Engineering Department, Middle East Technical University** by,

Prof. Dr. Canan ÖZGEN ___________
Dean, Graduate School of **Natural and Applied Sciences**

Prof. Dr. Tayfur ÖZTÜRK ___________
Head of Department, **Metallurgical and Materials Engineering**

Assoc. Prof. Dr. Arcan Fehmi DERİCİOĞLU ___________
Supervisor, **Metallurgical and Materials Engineering Dept., METU**

Examining Committee Members:

Prof. Dr. Muharrem TİMUÇİN _______________
Metallurgical and Materials Engineering Dept., METU

Assoc. Prof. Dr. Arcan Fehmi DERİCİOĞLU _______________
Metallurgical and Materials Engineering Dept., METU

Prof. Dr. Kadri AYDINOL _______________
Metallurgical and Materials Engineering Dept., METU

Assoc. Prof. Dr. Caner DURUCAN _______________
Metallurgical and Materials Engineering Dept., METU

Assoc. Prof. Dr. Özlem AYDIN ÇİVİ _______________
Electrical and Electronics Engineering Dept., METU

Date: 13.09.2010

I hereby declare that all information in this document has been obtained and presented in accordance with academic rules and ethical conduct. I also declare that, as required by these rules and conduct, I have fully cited and referenced all material and results that are not original to this work.

Name, Last name : Göksu GÜRER

Signature :

ABSTRACT

DESIGN AND CHARACTERIZATION OF ELECTROMAGNETIC WAVE ABSORBING STRUCTURAL COMPOSITES

Gürer, Göksu

M.Sc., Department of Metallurgical and Materials Engineering

Supervisor: Assist. Prof. Dr. Arcan Fehmi Dericioğlu

September 2010, 101 pages

Electromagnetic interference (EMI) is one of the most common problems encountered in microwave applications. Interaction of electromagnetic (EM) waves from different sources may result in device malfunction due to misinterpretation of the transferred data or information loss. On the other hand, development of materials with reduced radar detectability is desired in defense applications. Considering the limitations in weight and thickness, development of lightweight structural materials with enhanced electromagnetic absorption potential is needed. In this study, development and characterization of glass fiber-reinforced polymer (GFRP) composite materials to be used in EM wave absorbing or EMI shielding applications was aimed. Incorporation of electromagnetic wave absorption characteristic has been achieved by the application of conductive thin film on fiber glass woven fabric reinforcement layers. Characterization of EM wave absorption potential was conducted using “free-space method” in 18 – 27 GHz frequency range. Single and multilayered combinations of surface-modified fiber glass woven fabrics were characterized in terms of their EM wave interaction properties and design principles for efficient broadband EM wave absorbing multilayered GFRP composite material have been presented. A computer aided computation method has also developed in order to predict EM wave transmission, reflection, and hence absorption characteristics of multilayered structures from single layer properties. Estimated results were verified compared to free-space measurement results. In the current study, up to 85% electromagnetic wave absorption has been obtained within 18-27 GHz frequency range (K band). Enhancement of EM wave absorption potential of multilayer structure has also been demonstrated by computer aided computation.

Keywords: Fiber glass woven fabrics, electromagnetic wave absorption, electromagnetic interference, glass fiber reinforced plastic (GFRP) composites, free-space method.

ÖZ

ELEKTROMANYETİK DALGA SOĞURUCU YAPISAL KOMPOZİTLERİN TASARIMI VE KARAKTERİZASYONU

Gürer, Göksu
Yüksek Lisans, Metalurji ve Malzeme Mühendisliği Bölümü
Tez Yöneticisi: Yrd. Doç. Dr. Arcan Fehmi Dericioğlu

Eylül 2010, 101 sayfa

Mikrodalga uygulamalarında en çok karşılaşılan problemlerden bir tanesi elektromanyetik karışmadır. Farklı kaynaklardan yayınlanmakta olan elektromanyetik dalgaların birbirleriyle olan etkileşimi, bilgi aktarımında kayıplara ve yanlış aktarım sonucu oluşan cihaz arızalarına yol açmaktadır. Diğer yandan, radar görünürlükleri azaltılmış malzemelerin gelişimi savunma uygulamaları açısından önem teşkil etmektedir. Ağırlık ve kalınlıkla ilgili kısıtlamalar göz önüne alınarak, elektromanyetik soğurma özellikleri geliştirilmiş, hafif ve yapısal malzemelerin üretimi hedeflenmiştir. Cam takviyeli plastik (CTP) kompozit malzeme uygulamalarında takviye malzemesi olarak kullanılan cam elyaf dokumalar üzerine iletken ince film kaplanmış ve bu sayede elektromanyetik dalga soğurma özelliği cam dokumalara kazandırılmıştır. 18 - 27 GHz frekans aralığındaki elektromanyetik dalga soğurma potansiyeli “free-space metodu” ile tayin edilmeye çalışılmıştır. Tek katmanlı ve çok katmanlı örneklerin karakterizasyonu üzerine yapılan incelemeler sonucunda çok katmanlı CTP kompozitlerin tasarımında uyulacak bir takım prensipler açıklanmıştır. Çalışma kapsamında ayrıca bilgisayar destekli hesaplamalar aracılığıyla, çoklu katman özelliklerinin öngörülmesine çalışılmıştır. Tek katman özelliklerinden yola çıkılarak elde edilen çoklu katman özellikleri, “free-space” ölçümleri ile karşılaştırılmış ve uyumlu sonuçlar elde edilmiştir. Çalışmada geniş bant aralığında etkin, %85 seviyesinde elektromanyetik soğurma elde edilmiştir. Çalışma kapsamında ayrıca, elektromanyetik dalga soğurma özelliklerinin bilgisayar destekli hesaplamalar aracılığıyla geliştirilmesi gösterilmiştir.

Anahtar Kelimeler: Cam fiber dokumalar, elektromanyetik dalga soğurma, elektromanyetik karışma, cam takviyeli plastik kompozitler, free - space metodu.

To My Family,

ACKNOWLEDGEMENTS

I would like to express my sincere appreciation to Assoc. Prof. Dr. Arcan Dericioğlu and Assoc. Prof. Dr. Özlem Aydın Çivi for their supervision, guidance, support and encouragement throughout the study.

I am grateful to the researchers Caner Güçlü, Ozan Doğan Gürbüz and Ramazan Çetin of the Department of Electrical and Electronics Engineering for their support in free-space measurements. I must also express my great thanks to Prof. Dr. Raşit Turan and researcher Mustafa Kulakçıoğlu of the Department of Physics and researcher Okan Öner Ekiz for their support and consultancy in surface coatings.

I am grateful to all the staff of the Department of Metallurgical and Materials Engineering and my labmates Burcu Kayıplar, Derya Erdem, Eda Aydoğan, Elvan Tan, Gökçe Şen, Gökhan Kıdıl, Nurdan Gürkan Evcimen, and Selen Gürbüz Güner.

Finally, I owe a depth to my family for their endless love, support and encouragement throughout my life.

TABLE OF CONTENTS

LIST OF TABLES

TABLES

LIST OF FIGURES

FIGURES

CHAPTER 1

INTRODUCTION

After development of electromagnetic theory in 19^{th} century, technological devices utilizing electromagnetic (EM) waves became widespread in engineering applications. Electromagnetic waves emitted by power sources with certain wavelength is used for different objectives like wireless information transfer, broadcasting, medical applications, imaging, foreign object detection etc. Considering its interaction with the atmospheric air, electromagnetic waves can provide information transfer between distant terminals such as satellites, space shuttles etc.

Increasing demand on EM wave based systems has been causing common service problems in engineering applications. Interference of EM waves from different sources results in misinterpretation of information carried by the electromagnetic wave. As a result, development of shielding structures has become obligatory in order to eliminate electromagnetic interference (EMI) and provide information security[1]. Furthermore, EM waves are also used for “radio detection and ranging” (RADAR) in military and commercial applications. Advances in radar applications have focused on detailed imaging within a sufficient distant range. Methods offered decrease in radar cross section (RCS) including electronic, geometric and materials engineering solutions. Additional parts attached to the main body of a system caused performance problems for mobile structures [2]. As a result, fabrication and development of EM wave absorbing materials with structural performance gained a strategic importance especially in military applications.

EM wave absorption applications aim suppression of incident EM energy. EM energy stored by the material is dissipated as heat. Earlier examples of EMI shielding focused on geometrical arrangements in order to scatter EM energy carried by incident waves, and thus to cause reflection loss. Due to problems related to uncontrollable thickness, weight and geometry of the EMI shields, studies have focused on modifications of magnetic and dielectric properties of candidate materials. Apart from considerations on thickness and weight, frequency effectiveness has also been considered. Need for EM wave absorbers effective within wide frequency range, has been attained by the application of multilayered structures [2].

In the present study, EM wave absorbing potential of surface-modified woven fiber glass fabrics has been investigated. Complex magnetic and dielectric properties of as - received woven glass fabrics were altered by the application of metallic surface coatings by thin film deposition methods. Effect of surface modification on the EM wave reflection and transmission properties of surface-modified woven fiber glass fabrics have been characterized by "free - space method" in 18 - 27 GHz frequency range described as K - band [3].

Woven fiber glass fabrics are being used as reinforcement layers in glass - fiber reinforced polymer matrix (GFRP) composites. To attain durable structures with a certain thickness, layers of woven fiber glass fabrics are stacked in a polymer matrix. Layer stacking is done according to composite materials' design procedures to attain mechanical requirements. There are various weave types commercially available for different design purposes. This study has focused on quadriaxially woven layers which are effective against tensile loadings from quadriaxial angles (0^{o} / $\pm45^{o}$ / 90^{o}).

Multilayered application of surface - modified woven fiber glass layers has been utilized to unite EM energy loss of each individual layer. In addition, interactions between reflected waves from differently modified layers are expected to cause frequency effectiveness to increase. In the present study, design principles for optimal EM wave absorbing multilayered reinforcement structure has been introduced. Mathematical models for cascading single layers to form multilayer structures have also been applied by computer computations. Via computer computations, fabrication of GFRP composite materials with predictable electromagnetic properties could be achieved.

Throughout this thesis, starting with the following chapter basic principles related to EM wave theory and fundamental information related to EM wave - matter interaction is presented. Advantages of the developed EM wave absorbing material over conventional absorbing materials are also discussed. In the third chapter, “Experimental Procedure” applied is presented. Information related to used fiber glass woven fabrics, applied surface modification, measurement setup and methodology is explained in detail. In the “Results and Discussion” chapter, results on the electromagnetic characterization of as-received and surface-modified fiber glass woven fabric layers are given. Effect of surface modification on the electromagnetic wave absorbing properties of single layered fabrics is discussed. A procedure for the design of multilayered EM wave absorbing reinforcement structures is given based on the data obtained from multilayered structures up to 5 layers. Finally, a comprehensive method for the processing of EM wave absorbing GFRP composite materials. As well as suggestions for future studies and possible applications are offered.

CHAPTER 2

THEORY AND LITERATURE REVIEW

This chapter includes basic information about electromagnetic (EM) waves and their interaction with matter and environment in microwave frequency applications. First of all, basic characteristics of EM waves and physical facts related to devices utilizing millimeter waves will be discussed. Possible effects of nanoscale surface modification and mechanisms effective on EM wave absorption will be explained. A literature review on commercially available EM wave absorbing materials and structures will be given. Methods for EM characterization of inhomogeneous and anisotropic media will be reviewed. Chapter is concluded with general fabrication routines and design principles for glass fiber reinforced plastic (GFRP) composite materials discussed in this study.

2.1. Electromagnetic Waves and Electromagnetic Spectrum

Fundamental laws of electromagnetism are first unified by Scottish physicist James Clerk Maxwell (1831 - 1879). Unifying the phenomena of electricity and magnetism, Maxwell’s Equations for understanding and exploiting electromagnetic wave (EM wave) behavior have been developed [4]. Maxwell’s Equations are mathematical expressions of Gauss’ law, Faraday’s law and Ampere’s law.

Gauss law for electricity represents the relation between electric charge , Q, and electric field intensity, **E**. Gauss’ statement for electric flux through a closed surface of area A is expressed in Equation 2.1;

$$\oint_A \mathbf{E}\,.\mathrm{d}\mathbf{A} = \frac{Q_{enclosed}}{\epsilon_0} \tag{2.1}$$

Where $Q_{enclosed}$ is the charge enclosed by the surface and ϵ_0 is the permittivity of free space which is 8.85 x 10^{-12} $C^2/N.m^2$.

Application of Gauss' law for magnetism results in Equation 2.2;

$$\oint_A \mathbf{B}\,.\mathrm{d}\mathbf{A} = 0 \tag{2.2}$$

where **B** is magnetic field. As Faraday's law of electromagnetic induction implies, time varying magnetic field through a closed loop of length l induces an electric current and vice versa. Relation between electric field (**E**) and magnetic flux (Φ_B) is expressed by Faraday's law of induction (Equation 2.3).

$$\oint_C \mathbf{E}\,.\mathrm{dl} = -\frac{d\Phi_B}{dt} \tag{2.3}$$

Mathematical relation for the dependence of produced magnetic field on electric flux change is given by Ampere's law. Generalized form of Ampere's law is given by Equation 2.4.;

$$\oint_C \mathbf{B}\,.\mathrm{dl} = \mu_0 I_{enclosed} + \mu_0 \epsilon_0 \frac{d\Phi_E}{dt} \tag{2.4}$$

where $I_{enclosed}$ is the change in current induced, μ_0 is the permeability of free space which is equal to 4π x 10^{-7} T.m/A and Φ_E is the electric flux through a closed path. It is also shown by "Generalized Ampere's Law" that generation of magnetic field is not only caused by an electric current, but also by a time varying electric field or changing electric flux.

Equation (2.1) - (2.4) are known as integral form of Maxwell's Equations in free - space. From Maxwell's Equations it is inferred that time varying electric field generates magnetic field with time varying magnitude and similarly changing magnetic fields promote generation of electric fields with changing magnitude. Direction of corresponding electric and magnetic fields are perpendicular to each other.

Consequently, electrical charges accelerated in an alternating electric field generate an alternating magnetic field. Such electric fields with sinusoidal alternations create electric field and magnetic field couples propagating through space in form of "*harmonic electromagnetic waves*" (EM waves) (Figure 2.1).

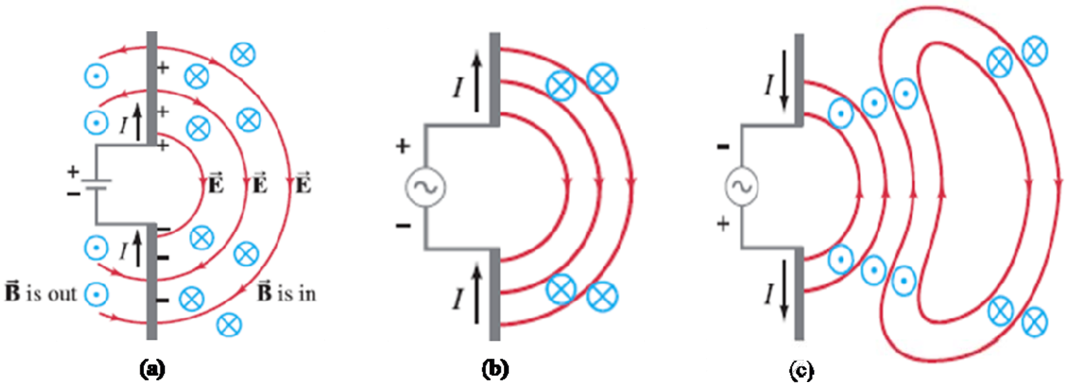

Figure 2.1 Electric field (E) and magnetic field (B) vectors around changing electric field (a); Generation and propagation of EM waves at near field of AC source (b,c) at two different time instants [4].

EM waves travel in free space with a velocity of 3.00 x 10^8 m/s which is the measured speed of light (c). Frequency (f) and wavelength (λ) of the EM wave is expressed by the Equation (2.5);

$$c = \lambda f \tag{2.5}$$

In order to demonstrate the relation between wavelength and corresponding frequency electromagnetic spectrum can be constructed as in Figure 2.2:

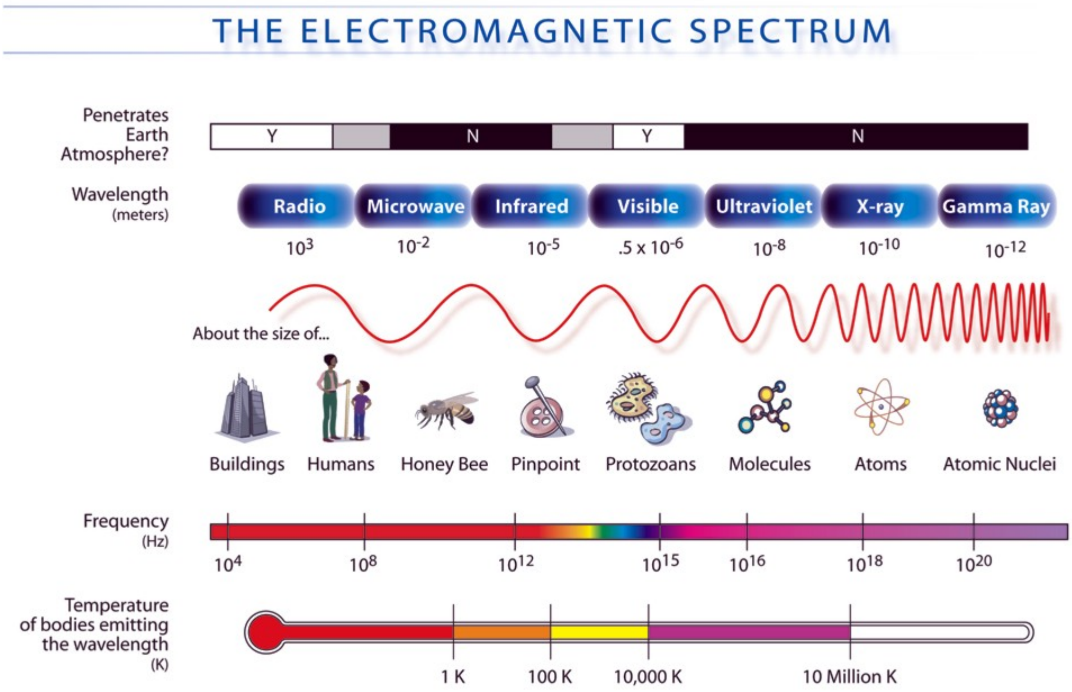

Figure 2.2 Electromagnetic spectrum [5].

Wavelength of EM wave is an important parameter. Interaction between physical objects and EM waves with comparable size is mainly utilized in engineering. Detection of objects from nanoscale to macro scale is done by electromagnetic methods.

EM waves are waves consisting of electric and magnetic energy fields. Therefore, EM wave propagation requires energy. In quantum mechanics, electromagnetic radiation is regarded as photonic energy where the energy of a photon is expressed by Equation (2.6)

$$E = hf = \frac{hc}{\lambda} \tag{2.6}$$

In terms of the Planck's constant, h, which is 6.63×10^{-34} J.s and frequency of EM wave, f. Energy of a photon can only have specific values. At higher frequencies energy on EM wave increases. Electronically, production of high frequency EM waves is rather difficult. High frequency EM waves are generally produced as a result of natural processes or by acceleration of electrons or charged particles.

EM waves can travel through space where most of the wireless systems transfer information and energy between terminals using them. Distance travelled by EM wave is dependent on variables such as frequency (or wavelength) emitter power, emitter specifications etc. In atmospheric conditions, constituents inside atmospheric air may interact with travelling EM waves. Atmospheric window represents opacity of atmospheric media against EM wave transmission between wavelengths from 0.1nm and 1km (Figure 2.3). EM wave applications are widespread from several centimeters to meters where the atmospheric window is fully transparent. As technology develop, systems operating at higher frequencies and lower wavelengths become advantageous. For this reason EM wave applications in millimeter wavelength range, where atmosphere is semi - transparent to EM waves, has potential.

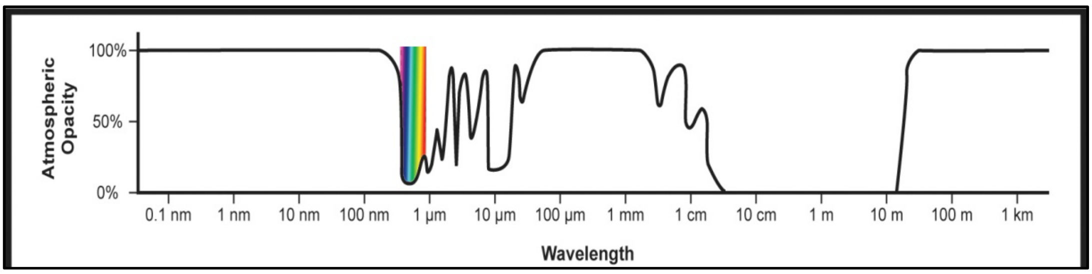

Figure 2.3 Atmospheric window [6].

Another important characteristic of EM waves is their interaction with each other. As a result of wave characteristic, EM waves have superposition ability. Interaction of two EM waves may result in an overall intensification or cancellation. Intensification is called “constructive interference” while cancellation is called “destructive interference”. Superposition of EM waves is utilized in broadcasting and wireless communication [4].

Undesired electromagnetic interference (EMI) as a result of possible interactions is a serious problem for engineering applications. Interaction of electromagnetic waves transmitted from different sources may cause decrease in the quality and misinterpretation of the transferred data. Information loss due to this interaction can be avoided by the use of appropriate EMI shielding structures and EM wave absorbing materials.

2.2. Applications of Millimeter Wavelength EM Waves

Microwave band is defined as the EM waves between 300 MHz to 300 GHz frequency range. Corresponding wavelengths in the microwave frequency band is from 1 mm to 1 m. Engineering applications of high frequency and low wavelength devices is possible in microwave band.

Electronic systems and devices operating at higher frequencies are needed for higher performance and precision. Many molecular, atomic and nuclear resonance frequencies are involved in the microwave frequencies. This provides a basis for the applications such as remote sensing, medical diagnostics, cooking and materials processing. In defense applications, development of radars operating at higher frequencies is required for detection of structures with low radar cross-section. Moreover, microwaves are not bent by the ionosphere. When compared to conventional low frequency techniques, higher capacity in communication is achieved by application of microwave frequencies [7]. In aerospace applications, communication between orbiting satellites is established by EM waves. Nevertheless, it is practically challenging to manufacture, analyze and design microwave components. Utilization of short wavelengths requires development of electrical components smaller in size.

In many daily applications such as airport traffic control radars, missile tracking radars, fire control radars, weather forecasting radars, long - distance telephone communication and military communication networks benefit from microwaves. According to the types of applications, microwave frequencies are separated into several bands. In Table 2.1., radar band designations according to IEEE 521 -2002 standard and their typical application fields are given.

Table 2.1 Radar frequency bands and corresponding field of application [2]

Radar Frequency Bands and General Usages		
Band Designation	*Frequency Range*	*General Usage*
VHF	50 - 300 MHz	Very Long-Range Surveillance
UHF	300 - 1000 MHz	Very Long-Range Surveillance
L	1 - 2 GHz	Long Range Surveillance Enroute Traffic Control
S	2 - 4 GHz	Moderate Range Surveillance Terminal Traffic Control Long Range Weather
C	4 - 8 GHz	Long Range Tracking Airborne Weather Detection
X	8 - 12 GHz	Short Range Tracking Missile Guidance Mapping, Marine Radar Airborne Intercept
Ku	12 - 18 GHz	High Resolution Mapping Satellite Altimetry
K	18 - 27 GHz	Little Used (Water Vapor Absorption)
Ka	27 - 40 GHz	Very High Resolution Mapping Airport Surveillance
Millimeter	40 - 100+ GHz	Experimental

Eventually, systems and devices operating at microwave frequencies have become common in daily applications. Consequently, electromagnetic interference problems are expected to grow as high frequency applications become more widespread. In order to satisfy requirements of the systems operating at various frequencies, development of shielding and/or absorbing materials effective within broadband frequencies is essential. In the present study, design and characterization EM wave absorbing materials for K band frequencies (18 -27 GHz) is discussed.

2.3. EM Wave - Material Interactions

Electromagnetic waves emitted from electronic sources travel in various media especially in atmospheric air. Power of EM wave is attenuated as it gets farther from power source. Cause of possible attenuation is the EM wave-matter interactions along the pathway. Energy carried by the EM wave is transferred to the constituents involved inside media. Loss of electromagnetic energy is influenced by the electrical and magnetic properties of the medium under consideration. Energy absorbed by the medium (material) is dissipated as heat [2]. Interaction of electromagnetic waves with physical obstacles is due to electrical and magnetic differences between the material and the environment. Structures targeted by the EM waves absorb, reflect or transmit incident electromagnetic power. According to energy conservation principle, sum of fractions of the reflected power, P_R, transmitted power, P_T, and absorbed power, P_A, with respect to the power of the incident wave, P_0, should be unity.

$$1 = \frac{P_R}{P_0} + \frac{P_T}{P_0} + \frac{P_A}{P_0} \tag{2.7}$$

In designing efficient EM wave absorbing materials, the absorbed component of the incident energy should be maximized, while the reflected and the transmitted ones are minimized. Therefore, the lossy character of the materials under consideration should be enhanced based on various possible loss mechanisms.

2.3.1. Electromagnetic Loss Mechanisms

In electromagnetic wave absorbing materials practice, amount of electromagnetic energy carried by EM wave is stored within the target material. According to the atomic structure and atomic bonding characteristics, electromagnetic power is absorbed and reradiated by condensed matter. Energy absorption is processed as polarization of dipoles (dielectric loss), movement of magnetic domains (magnetic loss), flow of free electrons (conductance loss) and/or atomic vibrations [8]. For effective absorption of electromagnetic energy both electric field and magnetic field component of the incident wave should be suppressed simultaneously. Otherwise, according to the postulates of Maxwell's Equations, presence of a changing magnetic field causes generation of a changing electric field and vice versa [4]. In order to improve EM wave absorption capacity of a material, its electrical and magnetic properties should be tailored accordingly.

2.3.1.1. Dielectric Loss

Dielectric materials are identified as mainly ionic insulating materials which are susceptible to polarization in the presence of an electric field [9]. A polarization vector (P) can be defined between positive and negative ionic charges separated by a distance d. [1]. Charge duality is considered as a dipole. Due to application of electric field, electric dipoles inside the dielectric material are aligned in the direction of the applied electric field (Figure 2.4). Moment produced by the electric field is known as dielectric dipole moment, m_e [10]. Molecules having a net dipole moment in the presence of an electric field are known as "polar molecules", while dipoles with no net dipole moment are called "nonpolar molecules." Polarization may take place due to dipole rotation, electronic displacement, ionization and thermal effects [8].

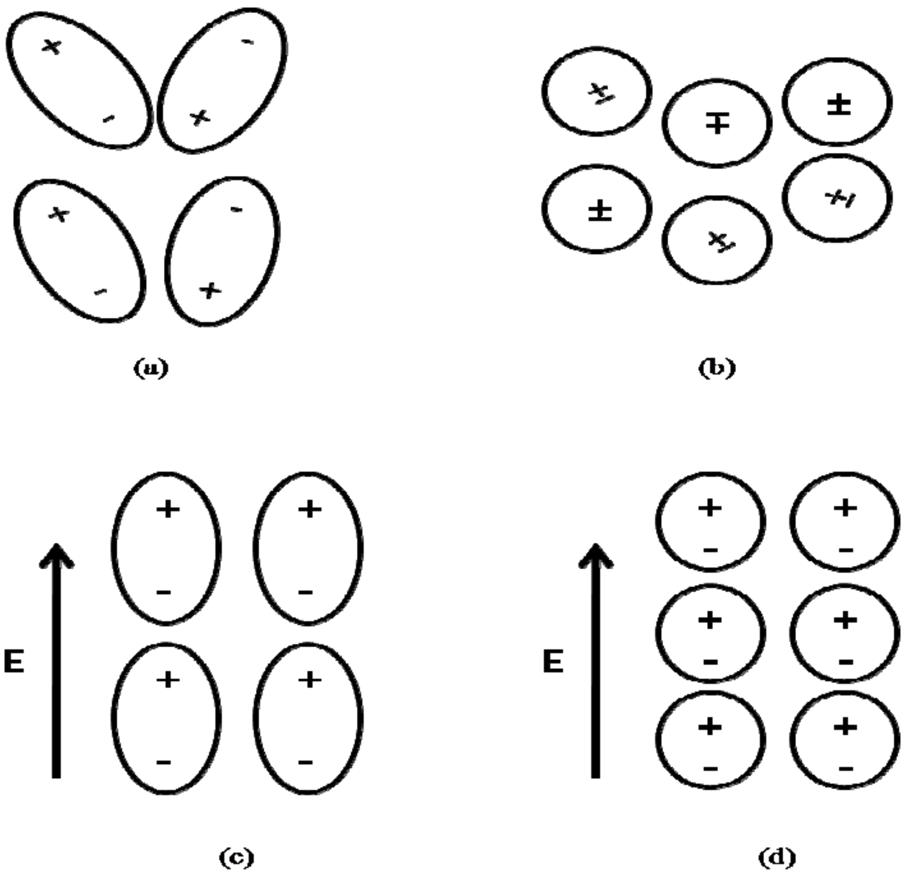

Figure 2.4 Polar dipoles (a), nonpolar dipoles (b) and their polarization in the presence of electric field (c,d) [1].

Permittivity (Є) is defined as the proportionality constant between electric flux density (D) and applied electric field (E) [11]: Permittivity indicates polarization ability of a material due to applied electric field.

$$\mathrm{D} = \epsilon\, \mathrm{E} \qquad (2.8)$$

Relative permittivity (ϵ_r) is expressed as a normalized value with respect to free space quantity (ϵ_0 = 8.854 x 10^{-12} Farads/meter).

$$\epsilon_r = \epsilon / \epsilon_0 \qquad (2.9)$$

When an alternating current is applied to a dielectric, a time dependent relaxation is observed. In homogenous dielectrics, stages of time dependent relaxation include orientation of dipoles and direction reversal due to changing electric field polarity [1]. Relaxation time (τ) for dipoles is being limited by increasing AC frequency. As a result, a frequency dependent opposition against alternating electric field is expressed by complex permittivity.

$$\epsilon = \epsilon' - j\epsilon'' = \epsilon_0(\epsilon_r' - j\epsilon_r'') \quad (2.10)$$

Real part of the complex number (ϵ_r') should extent of energy storage capacity, while imaginary part (ϵ_r'') represents the power loss [12]. Dielectric loss tangent ($tan\delta_\epsilon$) is expressed by the ratio,ϵ''/ϵ', showing the amount of power loss from the stored energy. Change of complex dielectric properties for a hypothetical dielectric is given in Figure 2.5.

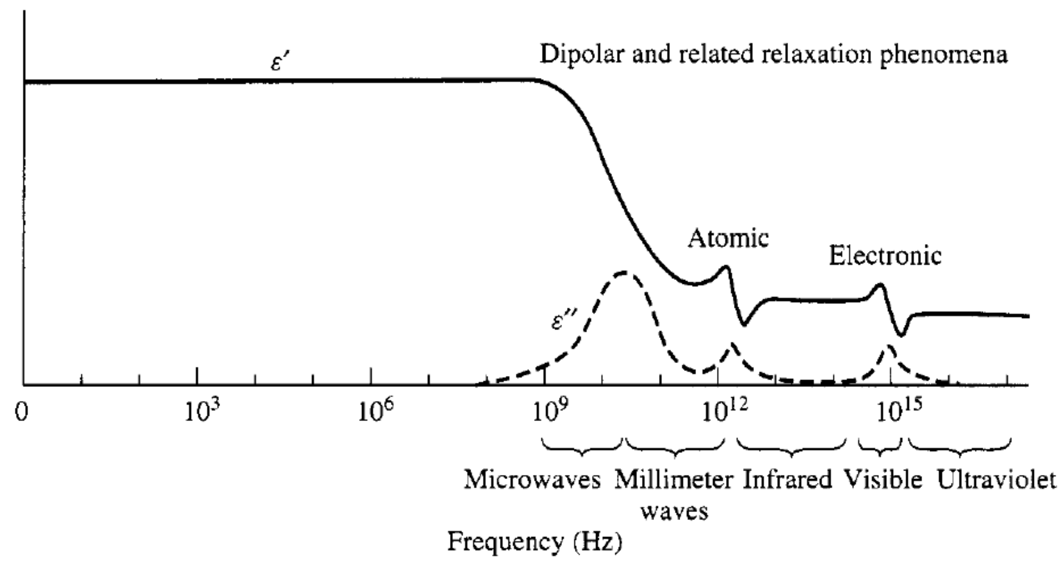

Figure 2.5 Frequency dependence of permittivity of a hypothetical dielectric material [13].

Dielectric loss is constituted by conductance loss, dielectric relaxation loss and resonance loss.

2.3.1.1.1. Conductance Loss

Energy of EM wave may be absorbed due to finite conductivity of materials. In conductive materials, electric field component of the incident EM wave couples with the free electrons present. Dielectric materials have almost no conductivity (less than $10^{-10}\ \Omega^{-1}m^{-1}$) where this coupling is not possible. Resistance of a bulk volume against charge carrier flow is given according to the Equation 2.11.

$$R = \rho \frac{l}{A} \tag{2.11}$$

where ρ is the resistivity, l is the length and A is the cross-sectional area of the object. In the current study, application of conductive surface modification on samples with certain geometry is discussed. In this case, cross-sectional thickness of the conductive thin film applied on the surface is directly proportional to cross - sectional area (A). As the thickness of the surface modification increases, resistance due to surface modification is expected to decrease. As a result, higher conductance loss could be attained by increasing surface modification thickness.

2.3.1.1.2. Dielectric Relaxation Loss

Electromagnetic energy can also be converted to mechanical energy via dipole movement. Time required for electronic displacement is very short when compared to dipole rotation and thermal polarization [8]. As frequency increases dielectric relaxation loss based on dipole rearrangement becomes limited.

2.3.1.1.3. Resonance Loss

Resonance takes place when the frequency of incident EM wave is the same as the natural oscillation frequency of atoms, ions or electrons constituting the material. As the frequency of the incident radiation matches with this natural oscillation frequency effective absorption takes place. Resonance loss is emitted mainly as heat [8].

2.3.1.2. *Magnetic Loss*

EM waves consist of electrical field and magnetic field components. Magnetic component of EM wave interacts with magnetic materials. According to "Pauli Exclusion Principle", unpaired electrons with unbalanced magnetic spin are attracted by magnetic field. This is called "paramagnetism" [14]. Magnetic dipoles available inside paramagnetic materials rotate with the applied external magnetic field and become aligned with the magnetic field direction. In case of "diamagnetism," magnetic dipoles do not exist due to the presence of valance electrons with balanced magnetic spins. Diamagnetic materials oppose applied magnetic field which is represented as magnetic dipole formation opposite to the applied magnetic field (Figure 2.6(a)) [9]. Paramagnetism can be regarded as inertia of non-magnetic material against an applied magnetic field (Figure 2.6(b)).

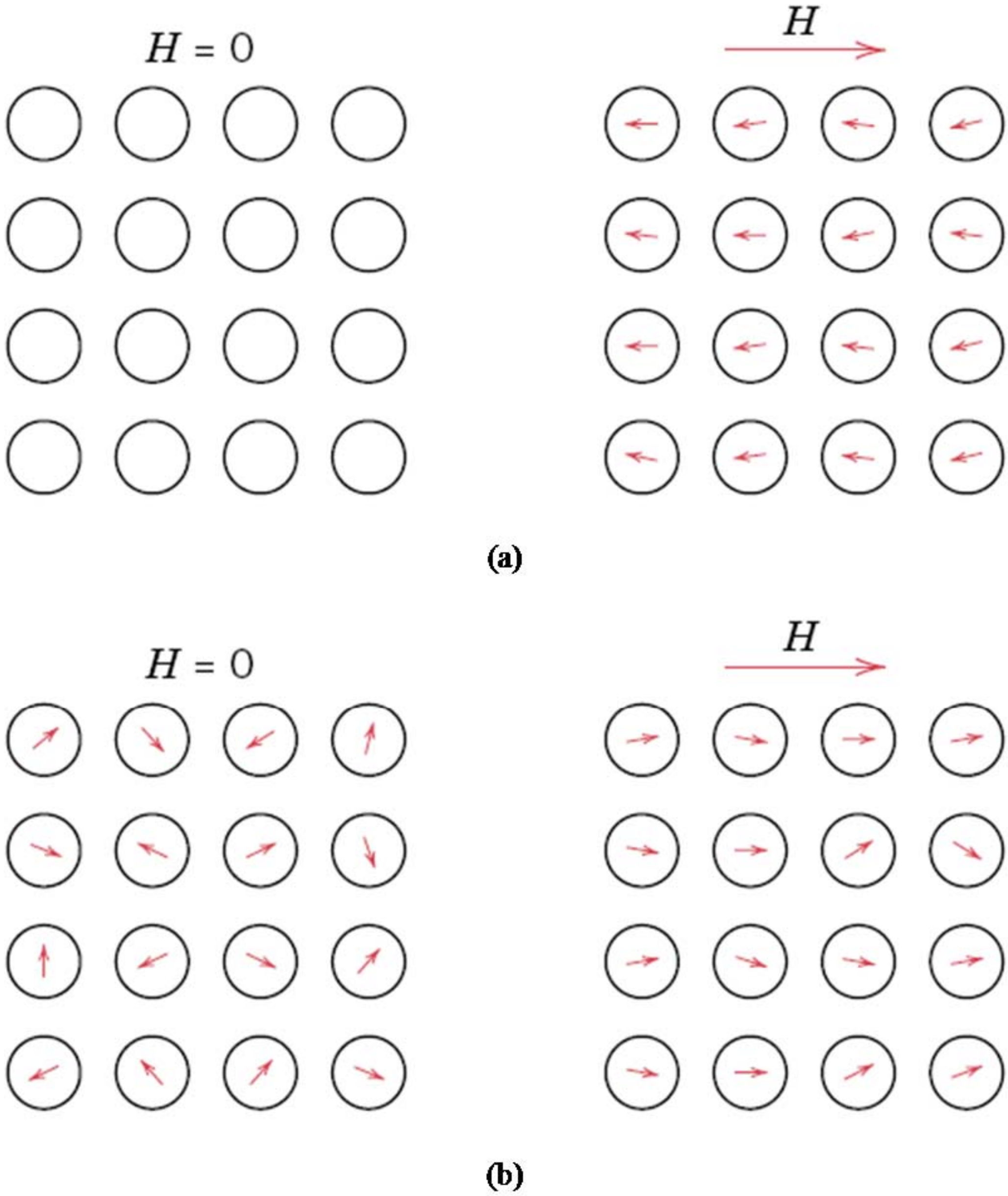

Figure 2.6 Magnetic dipole configuration in the absence / existence of applied magnetic field (H) for diamagnetic materials (a) and paramagnetic materials (b) [9].

Response of magnetic materials against applied magnetic field strength (H) is represented by Equation 2.12.

$$B = \mu H \tag{2.12}$$

where B is the magnetic flux density and μ is the permeability. Relative permeability (μ_r) is expressed as a normalized value with respect to the permeability of free space ($\mu_0 = 4\pi \times 10^{-7}\ Henrys/meter$).

$$\mu_r = \mu / \mu_0 \tag{2.13}$$

Magnetic susceptibility (χ_m) is the ease of magnetization (M) due to magnetic moment alignment which is positive for paramagnetic materials and negative for diamagnetic materials.

$$\chi_m = \mu_r - 1 \tag{2.14}$$

In case of alternating magnetic field strengths, permeability is expressed by frequency dependent complex numbers similar to permittivity.

$$\mu = \mu' - j\mu'' = \mu_0(\mu_r' - j\mu_r'') \tag{2.15}$$

Energy storage due to magnetization is expressed by the real part (μ’) of the complex permeability(μ), where the imaginary part (μ’’) represents power loss [12]. α - Iron (BCC ferrite), cobalt, nickel, gadolinium exhibit ferromagnetism. Ferrimagnets are ceramic structures with properties similar to those of ferromagnets. In ferromagnetic and ferrimagnetic materials, mutual spin alignment regions known as “magnetic domains” exist. Magnetic susceptibility of ferromagnetic materials is high and they can easily be magnetized permanently by a magnetic field. Thus, energy storage capacity of ferromagnetic materials is high. Materials with ferromagnetic or ferrimagnetic properties are widely used in EMI shielding applications [15-19]. In the present study, nickel surface modification is applied to make use of the advantage of ferromagnetic properties. Magnetic loss can be examined in detail by eddy -current loss, magnetic hysteresis loss and residual loss mechanisms.

2.3.1.2.1. Eddy Current Loss

Changing magnetic field applied on a conductive material causes electrical induction. AC current induced on the conductive material gives rise to a changing magnetic field opposing to the magnetic component of the incident EM wave [1]. Simultaneous electrical and magnetic interaction of the EM wave with material leads to attenuation of electromagnetic energy. In ferromagnetic materials, eddy - current loss is also contributed by magnetic storage. Changing magnetic flux on the conductive material generates an eddy-current in opposing electric field direction with respect to the electric field direction within the incident EM wave.

2.3.1.2.2. Magnetic Hysteresis Loss

Loss of electromagnetic energy due to mechanical rotation of magnetic dipoles and movement of magnetic domains is expressed as magnetic hysteresis loss [8].

2.3.1.2.3. Residual Loss

In case of fluctuating magnetic field, time dependent magnetic relaxation takes place. At high frequencies, residual loss due to size, ferromagnetism, domain wall movement and natural resonance is limited. In Figure 2.7 and Table 2.2, effect of frequency on dielectric and magnetic properties of sintered nickel - zinc ferrites is shown. Between 0.1 - 10 GHz, decrease in dielectric and magnetic properties with increasing frequency is represented. At frequencies lower than 0.1 GHz frequency, increase of magnetic permeability is observed to prolonged relaxation time and other secondary loss mechanisms. Optimum EM wave absorption is expected to be observed between 0.1 - 0.5 GHz frequency range where both permittivity and permeability are high.

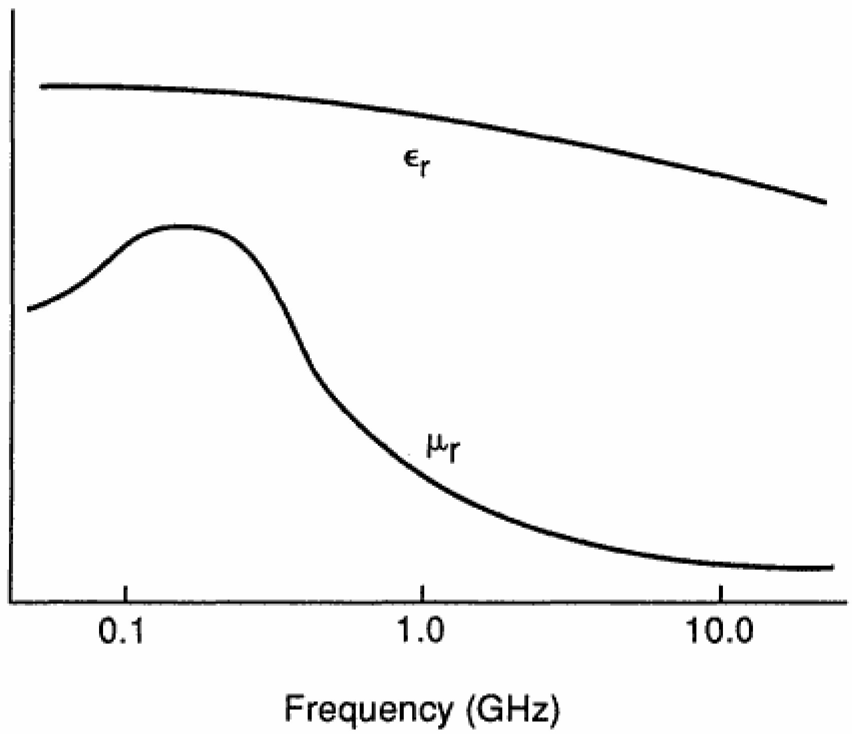

Figure 2.7 Effect of frequency on ferrite permittivity and permeability [2].

Table 2.2 Electrical and magnetic properties of sintered nickel - zinc ferrite [2]

	Frequency (GHz)				
	0.1	0.5	1.0	3.0	10.0
ϵ'_r	27.0	24.0	20.0	18.0	15.0
ϵ''_r	54.0	24.0	9.0	6.3	6.3
μ'_r	15.0	9.0	1.2	0.9	0.1
μ''_r	45.0	45.0	12.0	6.3	0.3
$(\mu_r\epsilon_r)^{1/2}$	53.5	39.5	16.3	11.0	2.3

2.3.2. Electromagnetic Diffraction and Concept of Intrinsic Impedance

Opposition of a circuit component (or medium) against alternating current (AC) transmission is expressed by impedance (Z) [20]. Intrinsic impedance (η) of a medium is the ratio of electric field to magnetic field components of a plane wave [10]. Intrinsic impedance of a medium can also be considered as the square root of the ratio of its permittivity (ϵ) to its permeability (μ) and expressed in ohms (Ω) [7].

$$\eta = \sqrt{\frac{\mu}{\epsilon}} \tag{2.16}$$

When an EM wave propagating through air is incident to an obstacle with different intrinsic impedance than air, propagation velocity of the EM wave changes and it is being refracted. Phase velocity (ν_p) and index of refraction (n) are expressed by Equation 2.17 and Equation 2.18 in terms of speed of light (c) and relative permeability and permittivity;

$$\upsilon_p = \frac{c}{\sqrt{\mu_r\epsilon_r}} \tag{2.17}$$

$$n = \sqrt{\mu_r\epsilon_r} \tag{2.18}$$

As a result of refraction, a part of EM wave power is reflected at the object surface. Rest of the EM wave power is transmitted and/or stored by the material as defined by Equation 2.7.

Transmission coefficient (T) of a medium with finite thickness (d) is expressed by Equation 2.19;

$$\mathrm{T} = \mathrm{e}^{-\gamma \mathrm{d}} \tag{2.19}$$

$$\gamma = \gamma_0 \sqrt{\epsilon_r \mu_r} \tag{2.20}$$

$$\gamma_0 = (j2\pi/\lambda_0) \tag{2.21}$$

where $\gamma_0$is the propagation constant for free space, and $\lambda_0$is the wavelength of the EM wave in free space. It is clearly seen from Equation 2.19 that as thickness increases transmission coefficient decreases. This implies that transmission characteristics of a material can easily be tailored by simple thickness adjustments. Achievement of low reflected component is essential to obtain sufficient electromagnetic energy absorption. Electromagnetic reflectivity coefficient (Γ) at the air - material interface is given by the Equation 2.22 when wave is normally incident;

$$\Gamma = \frac{z-1}{z+1} \tag{2.22}$$

where z is the normalized characteristic impedance of the material [13] and is expressed by Equation 2.23;

$$\mathrm{z} = \sqrt{\frac{\mu_r}{\epsilon_r}} \tag{2.23}$$

From Equations 2.22 and 2.23, it can be inferred that zero reflectivity coefficient can be obtained when normalized characteristic impedance equals unity. That is, intrinsic impedance difference between free - space and the material under consideration should be minimized. This can be idealized when $\mu_r = \epsilon_r$. Practically, for non-magnetic materials μ_r is taken as 1. In literature, available magnetic materials are reported to have higher relative permittivities than their relative permeabilities [2]. Considering this fact, magnetic materials with convenient electrical properties can be selected for electromagnetic energy absorption purposes. Applications of ferromagnetic and ferrimagnetic powders as lossy materials is frequently discussed in literature within this context [18, 19, 21, 22].

Penetration distance of an EM wave into a material or interaction range at the surface is expressed as skin depth (δ_s). Skin depth is the distance from the material surface where the amplitude of the fields decay to an amount of 1/e of the incident wave [7]. Skin depth is expressed by the Equation 2.24.

$$\delta_s = \sqrt{\frac{2}{\omega\mu\sigma}} \tag{2.24}$$

$$\omega = 2\pi f \tag{2.25}$$

where ω is the angular frequency. It should be noted that skin depth is dependent on frequency, and it is defined for materials with finite conductivity (σ).

Skin depths of metallic materials are in the order of few nanometers. Power loss in conductive materials is mainly due to reflection loss, if absorption loss is assumed to be zero for bulk conductive materials. In terms of complex permittivity, rather than conductivity, this condition is equivalent to $\epsilon'' \gg \epsilon'$ [7]. In practice, conductive materials are accepted to be reflective to EM waves. In this study, conductive surface modifications smaller than 100 nm thickness, which is comparable to skin depth, are applied. By the controlled conductive surface modification, tailoring of reflection power loss is aimed.

2.4. Characterization Methods for EM Wave Absorbing Materials

Investigation of interactions between electromagnetic waves and materials (electromagnetic properties) requires characterization of electrical and magnetic properties such as electrical conductivity as well as dielectric and magnetic properties. Electromagnetic properties of materials can be tailored by modifications on electronic and magnetic structure of materials. Characterization of EM wave absorption properties can be done by various methods according to thickness, homogeneity and type of material under consideration.

Present study aims to investigate the effect of surface modification applied on fiber glass woven fabric layers on their electromagnetic properties. In this case, observation of property differences within modified and unmodified surfaces is essential. Electromagnetic property differences between front and back surfaces of the fabric layers should be evaluated by transmission - reflection methods. Coaxial air line method, hollow metallic waveguide method, surface waveguide method and free - space method are possible methods for the measurement of EM wave reflection and transmission of materials [13].

In this study, free - space method is selected as the most convenient characterization method among others when heterogeneity and multilayered structure of the reciprocal target material is considered.

2.4.1. Free -Space Method

Free-space method is a technique to characterize complex electromagnetic properties and EM wave reflection and transmission behavior of a medium with certain thickness. Main advantage of free-space method is its applicability on inhomogeneous and/or anisotropic media [13]. Figure 2.8 schematically illustrates the free-space setup used in the current study.

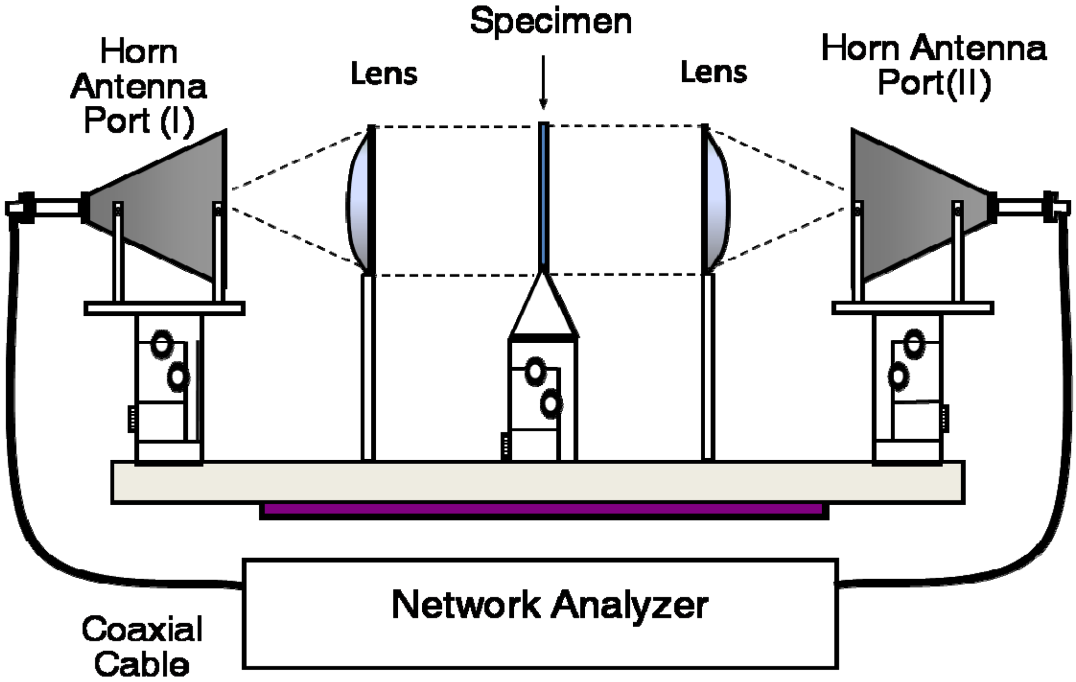

Figure 2.8 Schematic of the free-space measurement setup.

Typically a free-space measurement system consists of two oppositely positioned horn antennas and optionally lenses attached to each of these, if collimation of the incident EM wave is required. Power generated by the network analyzer is transferred via coaxial cables, and power waves are emitted by the antennas. In the present study, condensing lenses were used to focus emitted waves to the specimen surface. Reflected and transmitted waves resulting from the interaction of the incident wave with the specimen are collected and evaluated by the network analyzer. In free-space method, electromagnetic properties of the specimen are characterized on the basis of electromagnetic wave theory between defined aperture with certain thickness.Essentially, impedance/admittance against EM wave transmission is measured through introduced spacing. Reflection and transmission characteristics of the EM wave are observed from various EM wave incidence directions and expressed by matrix notation. Complex dielectric and magnetic properties of the material under investigation can also be determined by the free-space method if a vector network analyzer is employed [23].

Free-space method is regarded as an effective method for electromagnetic characterization of inhomogeneous materials such as ceramic and composite materials. Moreover, free-space method is advantageous in characterizing irregularly shaped and delicate specimens as it is an contactless and non-destructive method [13].

2.4.1.1. Through - Reflect - Line (TRL) Calibration

Free-space measurement technique requires isolation of measurement aperture from environmental effects. In order to maintain measurement accuracy, power losses due to electronic devices and transmission cables should be eliminated by through - reflect - line (TRL) calibration [13]. In this calibration method, initially aperture to be measured is introduced to the network analyzer for complete transmission and reflection conditions. In through calibration system is calibrated for direct EM wave passage. In reflection calibration two reflective faces of a metallic calibration block with certain thickness is introduced. Line calibration requires setting aperture value to the quarter wavelength of the central frequency of the frequency band to be tested and application of a through calibration [13]. Free – space method may exhibit error in measurement due to the inevitable reasons related to measurement setup [24]. These error can be minimized by proper TRL calibration.

2.4.1.2. Impedance and Admittance Matrices

Material with a finite thickness can be considered as a two – port network to represent EM characteristic of it. In this representation electromagnetic flux is expressed in “port” quantities such as voltage (V) and current (I). Impedance and admittance of a circuit is a matrix description to relate port parameters [7]. Impedance matrix [Z] can be regarded as resistivity of a circuit against EM wave transmission. On the other hand, admittance matrix [Y] of a system can be expressed as reciprocal of impedance matrix.

$$[V] = [Z][I] \tag{2.26}$$

$$[I] = [Y][V] \tag{2.27}$$

$$[Y] = [Z]^{-1} \tag{2.28}$$

An arbitrary microwave network of two ports (2-port) is illustrated in Figure 2.9. Corresponding impedance matrix for such a system can be given using Equation 2.29.

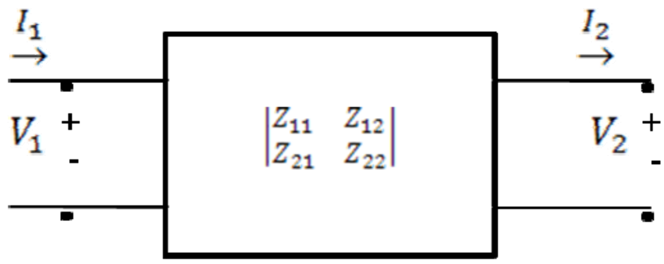

Figure 2.9 An arbitrary 2-port microwave network [7].

$$\begin{vmatrix} V_1 \\ V_2 \end{vmatrix} = \begin{vmatrix} Z_{11} & Z_{12} \\ Z_{21} & Z_{22} \end{vmatrix} \begin{vmatrix} I_1 \\ I_2 \end{vmatrix} \tag{2.29}$$

Impedance matrix for reciprocal network is symmetric. That is, $Z_{21} = Z_{12}$ for free-space setup [7]. Impedance matrix is expressed in complex numbers and can be correlated to complex dielectric and complex magnetic properties of materials. Impedance matrix can also be expressed by scattering matrix (S-parameters) or transmission matrix (ABCD parameters). A conversion between impedance, admittance, scattering and transmission matrices can be done as shown in Table 2.3.

Table 2.3 Port parameter conversion Table [7].

	S	Z	Y	$ABCD$
S_{11}	S_{11}	$\frac{(Z_{11}-Z_0)(Z_{22}+Z_0)-Z_{12}Z_{21}}{\Delta Z}$	$\frac{(Y_0-Y_{11})(Y_0+Y_{11})+Y_{12}Y_{21}}{\Delta Y}$	$\frac{A+B/Z_0-CZ_0-D}{A+B/Z_0+CZ_0+D}$
S_{12}	S_{12}	$\frac{2Z_{12}Z_0}{\Delta Z}$	$\frac{-2Y_{12}Y_0}{\Delta Y}$	$\frac{2(AD-BC)}{A+B/Z_0+CZ_0+D}$
S_{21}	S_{21}	$\frac{2Z_{21}Z_0}{\Delta Z}$	$\frac{-2Y_{21}Y_0}{\Delta Y}$	$\frac{2}{A+B/Z_0+CZ_0+D}$
S_{22}	S_{22}	$\frac{(Z_{11}+Z_0)(Z_{22}-Z_0)-Z_{12}Z_{21}}{\Delta Z}$	$\frac{(Y_0+Y_{11})(Y_0-Y_{22})+Y_{12}Y_{21}}{\Delta Y}$	$\frac{-A+B/Z_0-CZ_0+D}{A+B/Z_0+CZ_0+D}$
Z_{11}	$Z_0\frac{(1+S_{11})(1-S_{22})+S_{12}S_{21}}{(1-S_{11})(1-S_{22})-S_{12}S_{21}}$	Z_{11}	$\frac{Y_{22}}{\lvert Y\rvert}$	$\frac{A}{C}$
Z_{12}	$Z_0\frac{2S_{12}}{(1-S_{11})(1-S_{22})-S_{12}S_{21}}$	Z_{12}	$\frac{-Y_{12}}{\lvert Y\rvert}$	$\frac{AD-BC}{C}$
Z_{21}	$Z_0\frac{2S_{21}}{(1-S_{11})(1-S_{22})-S_{12}S_{21}}$	Z_{21}	$\frac{-Y_{21}}{\lvert Y\rvert}$	$\frac{1}{C}$
Z_{22}	$Z_0\frac{(1-S_{11})(1+S_{22})+S_{12}S_{21}}{(1-S_{11})(1-S_{22})-S_{12}S_{21}}$	Z_{22}	$\frac{Y_{11}}{\lvert Y\rvert}$	$\frac{D}{C}$
Y_{11}	$Y_0\frac{(1-S_{11})(1+S_{22})+S_{12}S_{21}}{(1+S_{11})(1+S_{22})-S_{12}S_{21}}$	$\frac{Z_{22}}{\lvert Z\rvert}$	Y_{11}	$\frac{D}{B}$
Y_{12}	$Y_0\frac{-2S_{12}}{(1+S_{11})(1+S_{22})-S_{12}S_{21}}$	$\frac{-Z_{12}}{\lvert Z\rvert}$	Y_{12}	$\frac{BC-AD}{B}$
Y_{21}	$Y_0\frac{-2S_{21}}{(1+S_{11})(1+S_{22})-S_{12}S_{21}}$	$\frac{-Z_{21}}{\lvert Z\rvert}$	Y_{21}	$\frac{-1}{B}$
Y_{22}	$Y_0\frac{(1+S_{11})(1-S_{22})+S_{12}S_{21}}{(1+S_{11})(1+S_{22})-S_{12}S_{21}}$	$\frac{Z_{11}}{\lvert Z\rvert}$	Y_{22}	$\frac{A}{B}$
A	$\frac{(1+S_{11})(1-S_{22})+S_{12}S_{21}}{2S_{21}}$	$\frac{Z_{11}}{Z_{21}}$	$\frac{-Y_{22}}{Y_{21}}$	A
B	$Z_0\frac{(1+S_{11})(1+S_{22})-S_{12}S_{21}}{2S_{21}}$	$\frac{\lvert Z\rvert}{Z_{21}}$	$\frac{-1}{Y_{21}}$	B
C	$\frac{1}{Z_0}\frac{(1-S_{11})(1-S_{22})-S_{12}S_{21}}{2S_{21}}$	$\frac{1}{Z_{21}}$	$\frac{-\lvert Y\rvert}{Y_{21}}$	C
D	$\frac{(1-S_{11})(1+S_{22})-S_{12}S_{21}}{2S_{21}}$	$\frac{Z_{22}}{Z_{21}}$	$\frac{-Y_{11}}{Y_{21}}$	D

$|Z| = Z_{11}Z_{22} - Z_{12}Z_{21}$; $|Y| = Y_{11}Y_{22} - Y_{12}Y_{21}$; $\Delta Y = (Y_{11}+Y_0)(Y_{22}+Y_0) - Y_{12}Y_{21}$; $\Delta Z = (Z_{11}+Z_0)(Z_{22}+Z_0) - Z_{12}Z_{21}$; $Y_0 = 1/Z_0$

2.4.1.3. Scattering Matrix

In high frequency applications impedance matrix of a two port network is represented by "scattering matrix" or by "S-parameters". Reflection loss related to the EM waves emitted from port 1 and reflected back to port 1 is expressed as S11. Transmission loss related to the EM waves emitted from port 1 and transmitted to port 2 is expressed as S21. Reflection and transmission losses for the emission based on port 2 are called S22 and S12, respectively. Reflection coefficient (Γ) and transmission coefficient (T) of air / material interface is correlated to corresponding S-parameters by the Equations 2.30 to 2.32;

$$K = \frac{S_{11}^2 - S_{21}^2 + 1}{2S_{11}} \tag{2.30}$$

$$\Gamma = K \pm \sqrt{K^2 - 1} \tag{2.31}$$

$$T = \left(\frac{S_{11} + S_{21} - \Gamma}{1 - (S_{11} + S_{21})\Gamma}\right) \tag{2.32}$$

Reflection loss (R_{dB}) and transmission loss (T_{dB}) are logarithmic expressions of the ratio of the power reflected (P_R) or power transmitted (P_T) to total power supplied by the system (P_0), respectively, given in decibels (dB). Neither reflected nor transmitted portion of the incident EM energy is said to be absorbed by the sample.

$$R_{dB} = 10 \log \left|\frac{P_R}{P_0}\right| \tag{2.33}$$

$$T_{dB} = 10 \log \left|\frac{P_T}{P_0}\right| \tag{2.34}$$

2.4.1.4. Transmission (ABCD) Matrix

In practice, many microwave networks are composed of cascade connection of two or more-port networks [7]. Electromagnetic response of such a network can be determined by multiplication of ABCD parameters. Figure 2.10, shows cascade connection of two port networks.

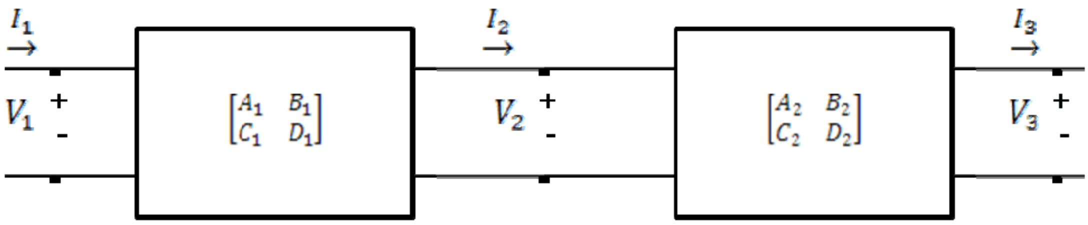

Figure 2.10 Cascade connection of two-port networks [7].

Transmission matrix for cascaded structure can be computed by Equation 2.35.

$$\begin{bmatrix} V_1 \\ I_1 \end{bmatrix} = \begin{bmatrix} A_1 & B_1 \\ C_1 & D_1 \end{bmatrix} \begin{bmatrix} A_2 & B_2 \\ C_2 & D_2 \end{bmatrix} \begin{bmatrix} V_3 \\ I_3 \end{bmatrix} \quad (2.35)$$

In the current study, electromagnetic properties of multilayered structures of glass woven fabrics have also been studied. When individual layers of surface modified glass fiber woven fabric samples are treated as a two-port network, EM wave absorption characteristics of the multilayered structure can be computed. This approach can be utilized in designing EM wave absorbing multilayered composite structures. Computation methods composed of mathematical correlations between ABCD parameters can be used as an effective tool in predicting EM wave absorption potential of multi-component, complex structures. In this study, application of such a computation method on multilayered arrangements of nickel surface-modified glass fiber woven fabrics is presented.

2.5. Electromagnetic Wave Absorbing Materials

In the past, application of electromagnetic wave absorbing materials was limited to reducing radar cross sections of vehicles for military purposes [2]. Development of EM wave absorbing materials effective at a specific frequency was followed by the development of multi-frequency radar absorbing and jammer systems. With the advance in technology, widespread utilization of systems based on EM wave radiation has increased in daily applications. As a result, development of effective broadband EM wave absorbers has become an obligation. Earlier solutions like multilayered Jaumann absorbers provided disadvantages such as increased thickness resulting in extra weight [12]. The key to the solution of such problems mainly includes modification of intrinsic properties for structural materials. In this scope, EM wave absorbers are classified according to the electromagnetic loss mechanism used[1].

2.5.1. Salisbury Screens and Dallenbach Layers

The Salisbury screen consists of a resistive film placed quarter wavelength ($\lambda/4$) distance away from a metallic sheet or surface to absorb the specific EM wave with wavelength λ (Figure 2.11). There is $\lambda/2$ phase difference between the reflected EM waves from resistive film and metallic backing. As a result, "destructive interference" of reflected EM waves occurs. Reflection is completely cancelled (no reflection loss) at frequency corresponding to wavelength λ. There is also no transmission (zero transmission loss) through the system due to metallic back plate. Thus, high level of EM wave absorption would be attained at a certain frequency.

Dallenbach layers differ from Salisbury screens in that the spacing between resistive film and metallic backing is filled with a lossy dielectric medium. In Dallenbach layers, thickness of the separation between resistive film and metallic backing, and hence the frequency to be absorbed is dependent on the propagation constant of the lossy medium.

In Figure 2.12, reflection loss of Dallenbach layers with magnetic media ($\epsilon = 1 + 0j$) and dielectric media ($\mu = 1 + 0j$) are illustrated with respect to ratio of separation thickness (t) to wavelength in free-space (λ_0).

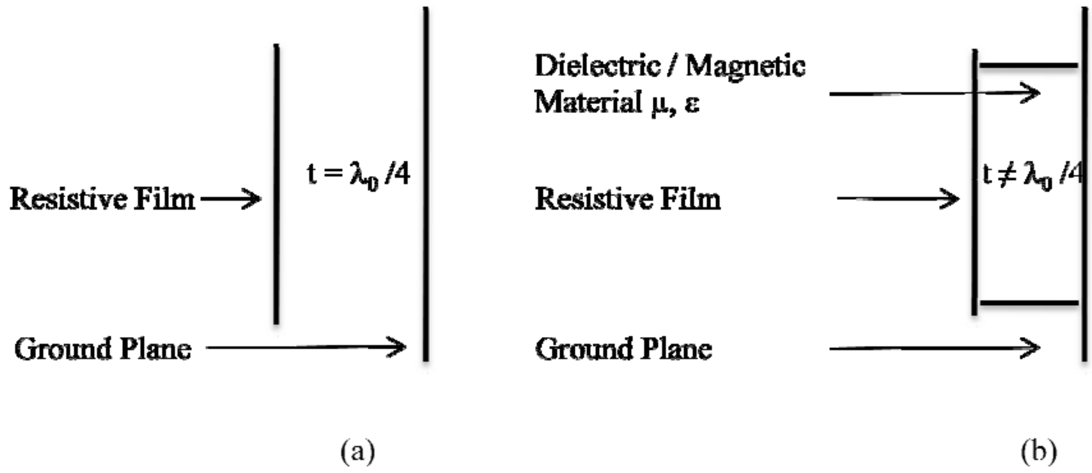

Figure 2.11 Schematic representation of Salisbury screen (a) and Dallenbach layer (b) [12].

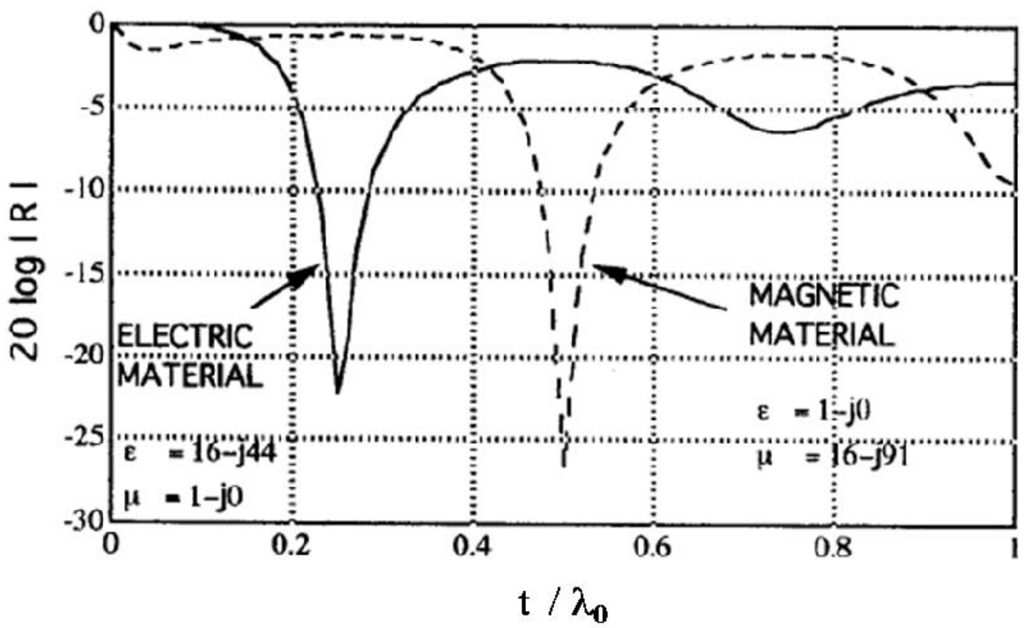

Figure 2.12 Effect of complex material properties on Dallenbach layer thickness [2].

Unlike Salisbury screens, Dallenbach layers are very convenient to be applied in sandwich type composite structures due to the geometry control based on the lossy medium used. On the other hand, both Salisbury screens and Dallenbach layers represent inadequate broadband effectiveness.

2.5.2. Jaumann Absorbers

Jaumann absorbers have been developed to improve broadband performance of EM wave absorbing structures based on Salisbury screen or Dallenbach layer approaches [12]. Jaumann absorbers are multilayered structures in which resistive layers are cascaded in the order of decreasing resistivity towards the metallic backing plate [2]. Separation between adjacent layers is set to quarter wavelength of the central frequency of the frequency range under consideration. Effect of layer number on reflection loss is shown in Figure 2.13.

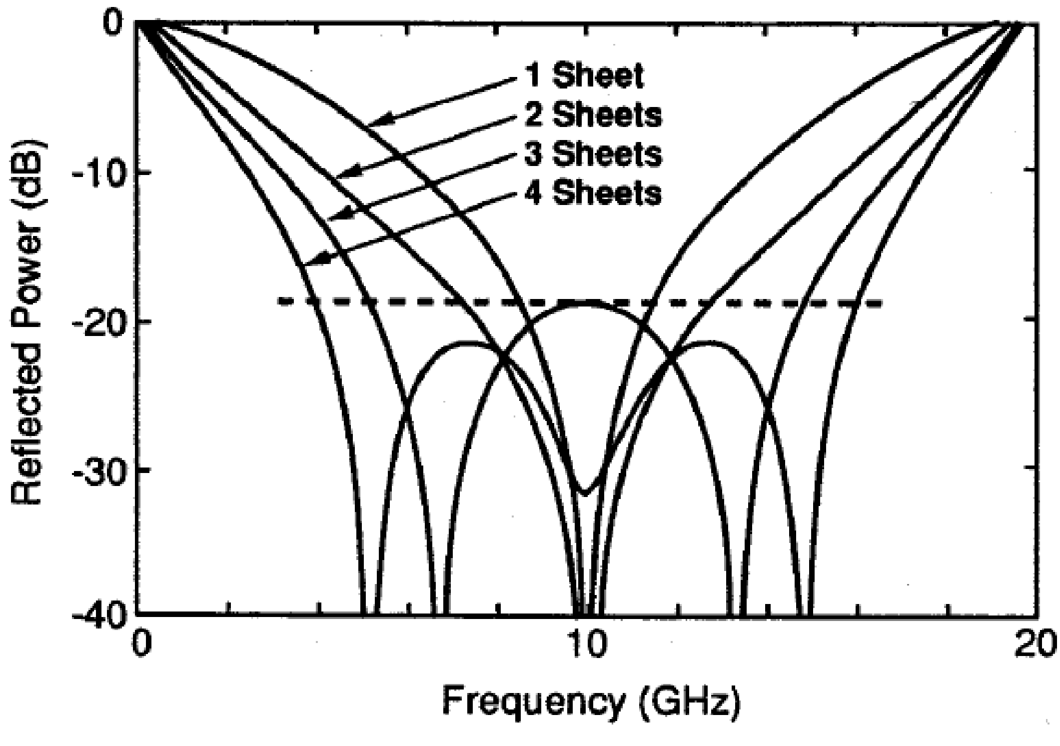

Figure 2.13 Predicted performance of multilayered Jaumann absorbers [2].

Broadening of reflection loss peak by the increased layer number is clear from Figure 2.13. As number of resistive layers increases interaction of EM waves reflected by multiple layers results in decreased reflection loss at frequencies different than the central frequency. Although reflection loss seems to be increasing for a specific frequency, broadband EM wave absorption stability is attained by increased number of layers. Despite the advantages obtained, main limitations encountered in Jaumann absorbers are related to thickness and weight considerations.

2.5.3. Graded Absorbers

Graded absorbers are used in order to obtain a tapered lossy transmission line. Dielectric and/or magnetic dipole density of graded absorbers varies within material structure. Gradual intrinsic impedance difference between air-material interface is set to eliminate strong reflection loss from material surface. Phase velocity of the incident wave is decelerated systematically, and thus strong refraction is also eliminated. Pyramidal geometries filled with lossy dielectrics [2] and tapered line absorbers [1] are typical design approaches available for graded absorber manufacturing. Graded dielectric arrangement is also often applied in multilayer applications such as Jaumann absorbers.

2.5.4. Magnetic Absorbers

Utilization of magnetic loss mechanisms can be intended for EM wave absorption. Especially application of magnetic ceramics is common in literature. Lossy ferrite particles dispersed in a matrix is widely used in tailoring electromagnetic properties of polymers or polymer composites [17, 19, 24]. Such ceramics are also suitable for fabrication of 3D magnetic absorbers such as ferrite grids and ferrite fins [1]. Ferromagnetic materials can also be utilized for EM wave absorption in a similar sense. Magnetic susceptibility and permanent magnetization presented by the ferromagnetic particles such as carbonyl iron, cobalt and nickel are utilized in EM wave absorption [16, 18, 25]. Diamagnetic carbon black powder has also been studied as a lossy constituent in microwave absorption applications of composite materials [26, 27].

2.5.5. Circuit Analog Geometries

Geometrical repetitive structures are also being utilized in EM wave absorption. Metallic textures such as strips, grids, hollow squares, loops, crosses etc. are applied for filtration of certain frequencies [2]. Counteraction of EM wave induced magnetism and/or electricity generated on looped Figures against each other also contributes to the attenuation of electromagnetic energy. Rather than being an individual absorber, circuit analog geometries are being used as contributors to EM wave absorption achieved by other methods.

2.5.6. Hybrid Absorbers

Hybrid absorbers are engineered materials in order to maintain maximized EM wave absorption throughout broadband frequencies. In hybrid absorber design, utilization of multiple EM wave absorption mechanisms is aimed. Mainly, simultaneous interaction with electric and magnetic components of the EM wave is desired to provide low reflection loss and transmission loss. Impedance matching of the overall structure is provided. Design and fabrication of hybrid absorber requires unifying different materials and processes used in fabrication.

In the present study, EM wave absorption efficiency of the surface modified glass fiber woven fabrics has been focused to achieve broadband EM wave absorption in the millimeter wavelength range by multilayer application. Intrinsic electromagnetic properties of fiber woven fabric layers have been controlled via surface modifications. Graded structure is attained by ordered arrangement of successive surface modified layers with decreasing resistivity. Impedance difference between adjacent layers is minimized in order to minimize multiple reflections due to interaction of EM waves. Surface modification is applied via thin film deposition techniques. Being ferromagnetic, nickel was selected as the surface modification target. Textured surface of glass fiber woven fabrics is expected to contribute to EM wave absorption characteristics. Present study has mainly focused on optimization of EM wave absorption characteristics of the glass fiber reinforcements to be used in glass fiber reinforced plastic (GFRP) composite materials. Combination of surface modified reinforcement layers incorporated to a lossy matrix can be applied for further maximization of EM wave absorption potential achieved. Physical and mechanical properties of the resulting composites should also be considered in order to obtain hybrid GFRP absorbers with superior electromagnetic absorption function and adequate structural properties.

2.6. EM Wave Absorption Potential of GFRP Composite Materials

Polymeric materials are widely used in engineering applications where lightweight structural solutions are fundamentally required. In order to satisfy certain physical needs, polymeric materials are engineered via composite materials' manufacturing techniques. Typical applications of GFRP composites include aerospace, automotive, sporting goods, marine applications, consumer goods, construction and various civil applications. Fiber reinforcement is the most widely used technique for development of mechanical performance in terms of specific strength, toughness and damping capacity [28]. Glass fibers are widely used in polymer matrix composites (PMC) as reinforcement. When compared to other reinforcements glass fibers have advantages in terms of handling and price [29]. In conventional techniques, glass fibers used in GFRP production can be in discontinuous form as chopped - strand fibers or in continuous form as glass fiber woven fabrics [30]. Glass fiber woven fabric plies are used in multilayered GFRP composite manufacturing. Mechanical properties of multilayered GFRP composites are anisotropic, where directional mechanical properties of multilayered structures can be tailored by weaving texture, fiber direction and/or load carrying fiber density. Examples of glass fiber woven fabric texturing are shown in Figure 2.14.

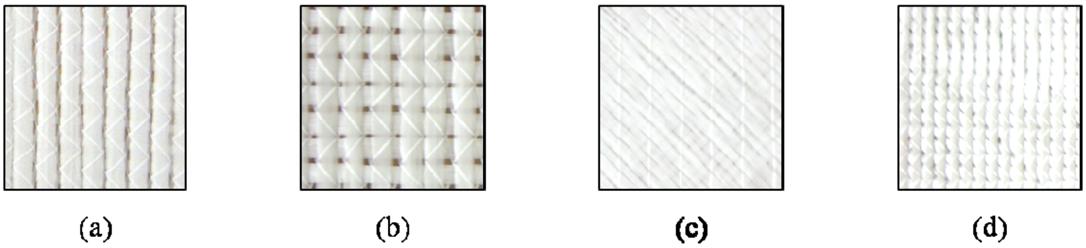

Figure 2.14 Uniaxial (a), ± 90 biaxial (b), ±45 biaxial (c) and quadriaxial (d) weaving textures in glass fiber woven fabrics.

Types of glass fiber reinforcements can also be classified according to the physical properties of the glass composition used in fiber production. According to ASTM standard glass fibers with varying chemical compositions are classified into six groups in terms of their typical characteristics as presented in Table 2.4.

Table 2.4 Glass fiber types and designations [31].

Letter Designation	Property or Characteristic
E, electrical	Low electrical conductivity
S, strength	High strength
C, chemical	High chemical durability
M, modulus	High stiffness
A, alkali	High alkali or soda lime glass
D, dielectric	Low dielectric constant

Electromagnetic wave absorption can be introduced to PMC composite materials by electrical and magnetic modifications on both polymer matrix and/or glass fiber reinforcements. In literature, typical applications are directed towards incorporation of electromagnetic lossy particles into lossy matrix, lossy wire additions to reinforcing fabrics or nanoscale modifications on reinforcements via thin films or heat treatment [8, 15, 17-19, 21, 22, 24-26, 32-35]. In the current study, effect of nanoscale surface modification on the electromagnetic properties of glass fiber woven fabric reinforcements has been investigated.

Surface modified glass fiber reinforcement layers have also been cascaded in terms of increasing intrinsic impedance. A similar approach has been suggested by Huo et. al. based on three multilayer group arrangements for optimum EM wave absorption. (Figure 2.15).

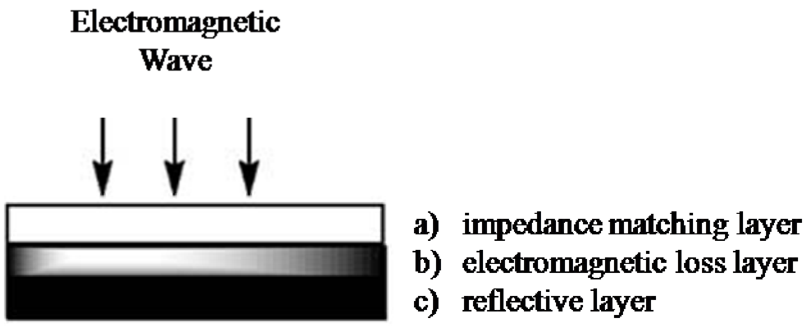

Figure 2.15 Three layer group arrangement in effective EM wave absorption [8].

In this arrangement the first layer (layer a Figure 2.15) provides impedance matching at the material-air interface. By the use of such layers reflection loss from material surface is minimized. These receiving layers should reveal low reflection loss along with impedance matching they provide. Power of the incident EM wave should be transformed into absorption loss by the second stage layers (layer b in Figure 2.15). Effect of reflection loss from these layers should be optimized by impedance adjustments with the first layer. Last stage layers in the multilayered structure should provide strong reflection in order to eliminate transmission loss. Reflection generated by reflection layers (layer c in Figure 2.15) is expected to be reabsorbed by the lossy layers on the reflection pathway.

Suggested method can be utilized in cascading of surface modified fiber woven fabric reinforcement layers to be used in GFRP composite material manufacturing. Obtained multilayered structure with high EM wave absorption can be incorporated into a pristine or lossy polymeric matrix in order to enhance EM wave absorption capacity of the resulting GFRP composite material.

CHAPTER 3

EXPERIMENTAL PROCEDURE

3.1. Materials, Sample Geometry and Treatments

Quadriaxial type (0° / ±45° / 90° reinforcement angles) woven glass fabrics (METYX®, Telateks Textile Products, Co., Ltd., Istanbul, Turkey) were used in this study [36]. Quadriaxial fabrics are woven in 0 / 45 /45 / 90 reinforcement angles in order to supply reinforcement against loading within these directions. Schematic view of quadriaxial layers are given in Figure 3.1.

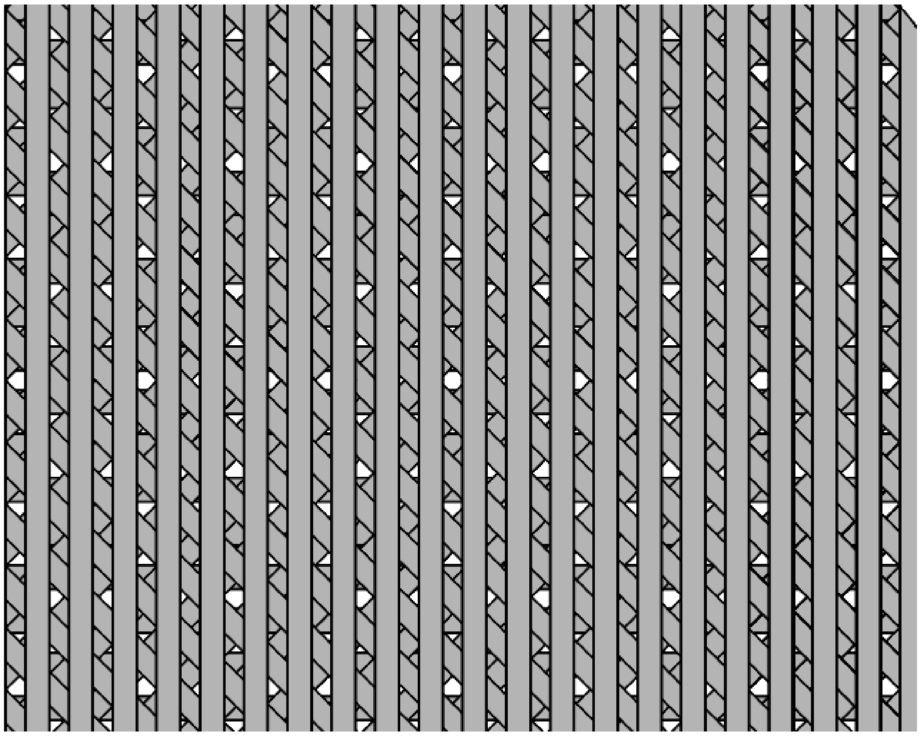

Figure 3.1 Fiber directions in METYX Q625 fiber glass woven fabric.

Commercially, varying bundle thicknesses are used in different fabrics for different purposes. Reinforcement layers are classified as their weight per unit area. In the current study, Q625 quadriaxial fiber glass woven fabrics with area density 625 g/m^2 were used. Fabric type used was selected as a representative reinforcement type for typical applied in numerous structural applications. Technical specifications related to Q625 fiber glass woven fabric reinforcements is given in Table 3.1.

Table 3.1 Technical specification for Q625 quadriaxial woven fiber glass fabrics [35].

METYX Quadriaxial Woven Fiber glass	
METYX Product Name	Q625
Reinforcement Directions	0 / 45 / 90 / -45
Weave Type	Quadriaxial / Linear
Area Weight	625 gr /m²
Fiber Diameter	9.5 μm
Bundle Width	1.70 mm
Stitch Length	3.00 mm
Overall Thickness	0.40 mm
Glass Content	52 %
Moisture Content	Max. 0.20 % by weight
Resin Compatibility	Polyester, Vinyl Ester, Epoxy Resins
Tensile Strength	208 MPa
Young's Modulus	14.5 GPa
Elongation	3 %

Having very long fiber length when compared to fiber diameter, fiber glass woven fabrics are classified as continuous fibers. Mechanical properties of GFRP composite materials can be computed by basic rule of mixtures. Having anisotropic mechanical properties due to angular fiber orientation, layer orientations should be designed to meet loading requirements. In multilayered structures, relative positions of fiber glass woven fabric plies should also be considered in mechanical calculations. For this reason, orientation angles of fiber bundles were set as an independent variable in this study.

As it was stated, the principle of superposition applies to EM waves. Interaction of electromagnetic waves reflected from parallel reflection planes may cause destructive or constructive interference. Such interferences are taking place depending on the spacing between reflective planes and the wavelength of the incident wave. In multilayered EM wave absorbing GFRP composite material application, spacing between woven fabric surfaces embedded in the polymer matrix is expected to be the thickness of the fiber glass woven ply thickness. However, in the current study, measurements were initially conducted on free standing 0.4 mm thick fabrics only, where they were fixed on 0.8 mm thick cardboard frames to provide rigidity to fiber glass woven samples for easier handling and alignment. Details on overall sample geometry for single layered and multilayered structures used in this study are illustrated in Figure 3.2 and Figure 3.3.

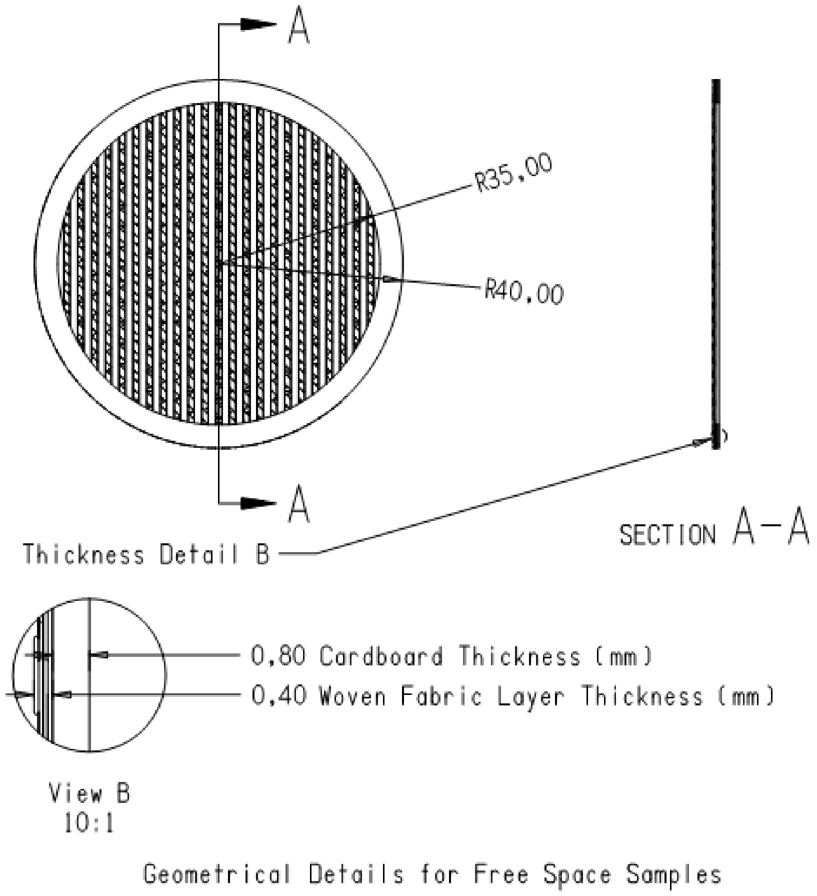

Figure 3.2 Technical drawing for single layer sample geometry composed of one layer woven fabric affixed on a circular cardboard frame.

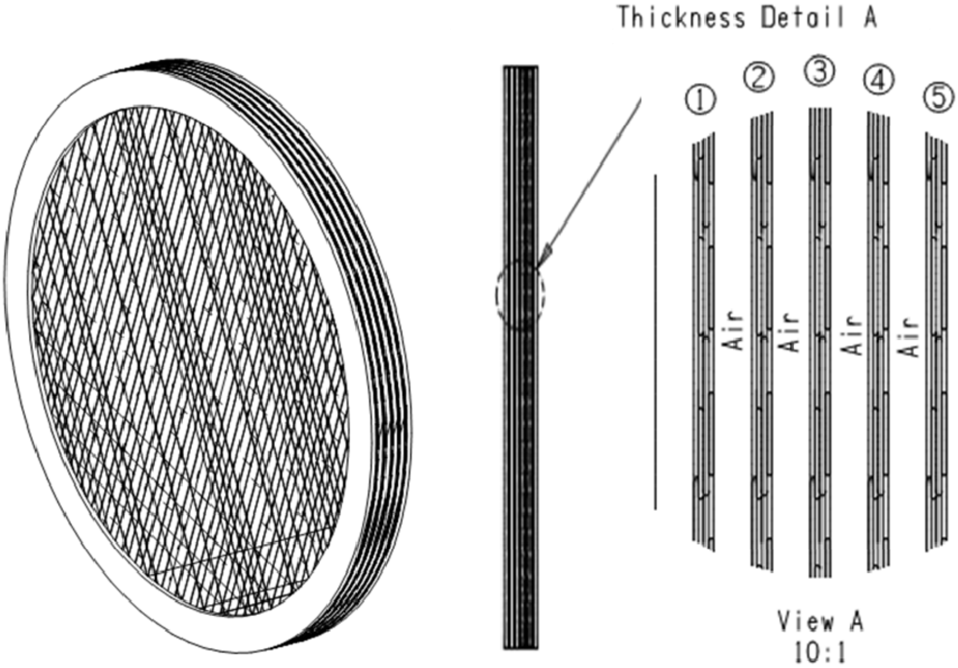

Figure 3.3 Schematic representation of multilayer geometry composed of cascaded layers illustrated in Figure 3.2 spaced by air.

Q625 layers are known to be transparent to EM waves in as-received state. In order to provide electromagnetic loss surface of as-received Q625 layers were modified by nickel coating of varying thickness 25, 35, 50, 75 and 100 nm and also by gold coating of thicknesses 25, 50, 75 and 100 nm (Figure 3.4).

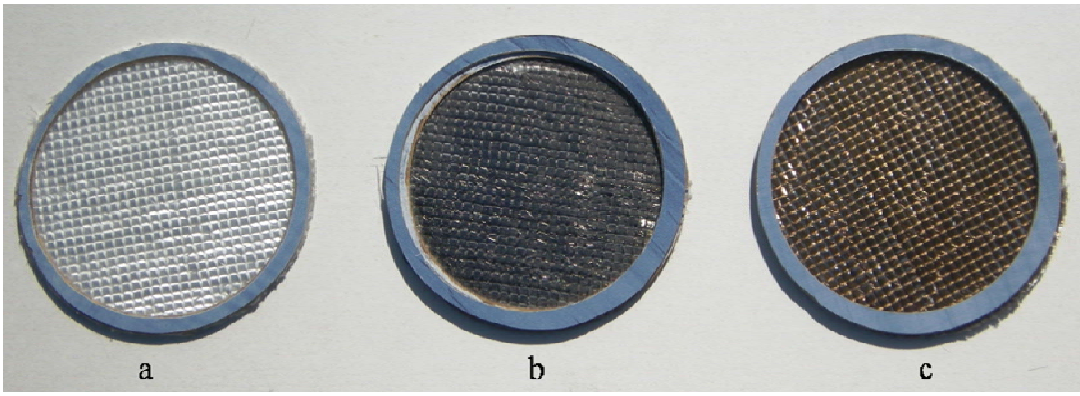

Figure 3.4 Representative samples of as - received (a), nickel coated (b) and gold coated (c) fiber glass woven fabrics used in this study.

Being a conductive and ferromagnetic material, nickel coating was expected to suppress electric and magnetic component of the incident EM wave simultaneously. Surface modification by nickel was conducted by RF sputter deposition technique. A 99.999% purity nickel foil was used as the target for sputter deposition. Under vacuum, an alternating electric field was applied in the presence of argon gas inside the chamber. Thickness of the nickel coating was continuously controlled and displayed by a quartz crystal during deposition.

Surface modification by gold coating was applied as an alternative to nickel surface modification. Being a good conductor, gold was expected to cause efficient ohmic loss of EM energy. Furthermore, oxidation of gold is not expected in ambient conditions. By gold surface modification, layers with durable electromagnetic properties were aimed. Diamagnetic characteristic of gold is not as effective as bismuth, graphite or silver. As a result, suppression of magnetic component of the incident EM wave was not expected. Gold modification on as-received Q625 layers was applied by electron beam (e–beam) evaporation method. Electrons accelerated by a high voltage source are used to bombard a piece of gold placed inside a crucible causing it to evaporate. Subsequently, gold vapor is condensed on Q625 substrates. Thickness of gold coating was controlled and displayed by quartz crystal during the process.

3.2. Characterization of EM Wave-Glass Woven Fabric Interaction by Free-Space Method

Selected technique for characterization of electromagnetic reflection, transmission, and hence absorption properties of as-received as well as surface-modified fiber glass woven fabric is free-space method. The method was chosen considering the advantages such as easier and accurate applicability on inhomogeneous and/or anisotropic media [37] as described in the preceding chapter. Key features of the free-space system used were introduced in section 2.4.1, and photo of the free-space measurement setup ,designed and built in METU Electrical and Electronics Engineering Department laboratories, based on the setup proposed in the literature is shown in Figure 3.5 schematically [37].

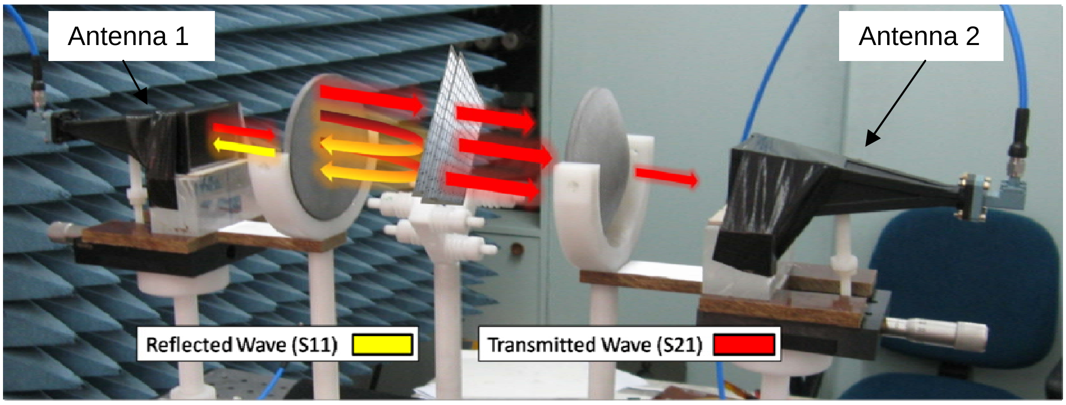

Figure 3.5 Free-space measurement setup designed and built in METU Electrical and Electronics Engineering Department Laboratories operating in 18 - 27 GHz frequency range.

Reflected and transmitted waves are both collected and evaluated by E8361A PNA Vector Network Analyzer within IEEE K-Band where the incident wave was generated by the same equipment. Transmission loss (dB), reflection loss (dB) and corresponding phase angles (degree) at different frequencies were recorded for different sample sets. Reflection loss related to the EM waves emitted from horn1 and reflected back to horn1 is expressed as S11. Transmission loss related to the

EM waves emitted from horn1 and transmitted to horn2 is expressed as S21. Reflection and transmission loss originating from the second port is recorded as S22 and S12, respectively.

EM wave absorption percentage from port 1 to port 2 can be calculated from Equation 3.1 based on the principle of conservation of energy;

$$\%\text{EM Wave Absorption} = (1 - 10^{S11/10} - 10^{S21/10}) \times 100 \quad (3.1)$$

Similar determination for EM wave absorption from port 2 to port 1 can also be conducted. Since samples measured in the free-space system were not symmetrical, a remarkable difference between the EM wave absorptions of the first port and second port was expected.

During this study, TRL calibration of the system was done prior to every free-space measurement session. Following calibration, samples were placed into measurement opening of the sample holder at the center of the two horn antennas. Port parameters (S11, S22, S21, S12) and phase angles of reflecting/transmitting EM waves were evaluated in order to monitor EM wave absorption potential of surface-modified fiber glass woven fabrics and their multilayered arrangements.

3.3. Surface Modification by Metal Coating

Nickel and gold coating surface modifications were applied on Q625 fiber glass woven fabrics. Nickel surface modification was applied by radio frequency (RF) sputter deposition technique. Gold surface modification was applied by “e-beam deposition” technique. Thickness control was achieved by deposition time control under identical process parameters. Because of fibrous and hence rough substrate surface, thickness measurement calibration was initially conducted on reference slide glass substrates applying the deposition parameters and durations to be applied. Calibrated coating thicknesses were found to be compatible with those determined by the quartz thickness monitor used in the coating systems.

3.4. Mathematical Modeling for Multiple Layer Cascading

As discussed earlier in the scope of transmission matrix explanation, equivalent S parameters for cascaded structures can be found by the matrix product of related ABCD parameters. Conversion methodology between scattering matrix and transmission matrix was given by Table 2.3. In a similar context, mathematical transformations on scattering matrix can be utilized to predict EM wave absorption characteristics of multilayered structures of fiber glass woven fabrics with numerous combinations depending on the surface modification applied to each layer along with the layer number used.

Determination of ABCD parameters from S parameters can be done using Equations 3.2 -3.5.

$$A = \frac{(1+S_{11})(1-S_{22})+S_{12}S_{21}}{2S_{21}} \tag{3.2}$$

$$B = Z_0\frac{(1+S_{11})(1+S_{22})-S_{12}S_{21}}{2S_{21}} \tag{3.3}$$

$$C = \frac{1}{Z_0}\frac{(1-S_{11})(1-S_{22})-S_{12}S_{21}}{2S_{21}} \tag{3.4}$$

$$D = \frac{1}{Z_0}\frac{(1-S_{11})(1+S_{22})+S_{12}S_{21}}{2S_{21}} \tag{3.5}$$

ABCD matrices for multilayers composed of two or more individual layers can be calculated. Matrix product of transmission matrices provides the transmission matrix of the multilayer under consideration. ABCD parameters can be converted into S parameters and S parameters of multilayers can be determined accordingly.

$$S_{11} = \frac{A + B/Z_0 - CZ_0 - D}{A + B/Z_0 + CZ_0 + D} \tag{3.6}$$

$$S_{21} = \frac{2}{A + B/Z_0 + CZ_0 + D} \tag{3.7}$$

$$S_{22} = \frac{-A + B/Z_0 - CZ_0 + D}{A + B/Z_0 + CZ_0 + D} \tag{3.8}$$

$$S_{12} = \frac{2\,(AD - BC)}{A + B/Z_0 + CZ_0 + D} \tag{3.9}$$

In the present study, EM wave reflection and transmission properties of multilayer structures were predicted by circuit cascading method. Predicted reflection and transmission losses were compared with the experimental results obtained by free-space measurements.

CHAPTER 4

RESULTS AND DISCUSSION

This chapter includes “free-space” measurement results for single and multilayered structures consisting of surface-modified woven fiber glass fabrics. EM wave reflection, transmission, and hence absorption properties of as-received woven fiber glass fabrics were examined. The effect of surface modification was demonstrated on surface-modified single layers. EM wave absorption potential of multilayered structures composed of nickel and gold coating surface-modified layers in various arrangement combinations were investigated. Finally, a computer aided computation method for estimation of overall EM response of multilayered reinforcement structure was introduced. Following sections present results and pertaining discussion about these investigations.

4.1. Interaction of As-Received Fiber Glass Woven Fabrics with Electromagnetic Radiation

Q625 type fiber woven fabric consists of glass (52%), polymeric silane coating, moisture and air gaps. With this structure in ambient conditions, as-received fiber glass woven fabrics are expected to be transparent to EM waves. Being a non-magnetic insulator, fiber glass is not expected to be reflective against EM waves. However, a certain amount of transmission loss is expected due to the operation of some dielectric loss mechanisms. Because of the limited dielectric characteristic of glass content, a remarkable impedance difference can be observed between ambient air and the woven fabrics. In Figure 4.1, EM wave reflection characteristic of the as-received Q625 is compared with reflection loss of ambient air.

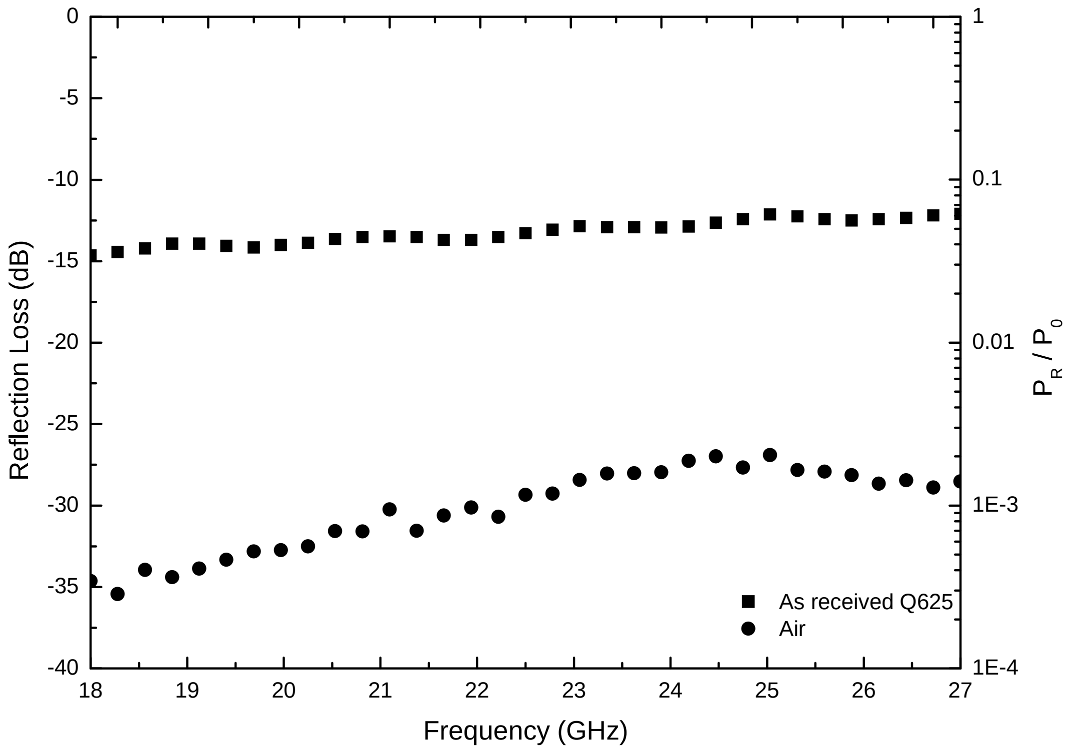

Figure 4.1 EM wave reflection difference between air and Q625 fiber glass woven fabric.

Contribution of dielectric loss is seen on reflection loss curve. Due to dielectric loss EM wave reflection up to 3% is observed. Reflection of ambient air is seen to be about 0%.

Transmission loss of ambient air is zero pointing out to perfect transmission through air. Transmission loss for Q625 fiber glass woven fabric is given in Figure 4.2. which is seen to be slightly lower than that of ambient air. Approximately 95% of the incident EM wave is transmitted through Q625 single layer. Approximately 2% of the incident EM energy is absorbed by the as-received Q625 layer.

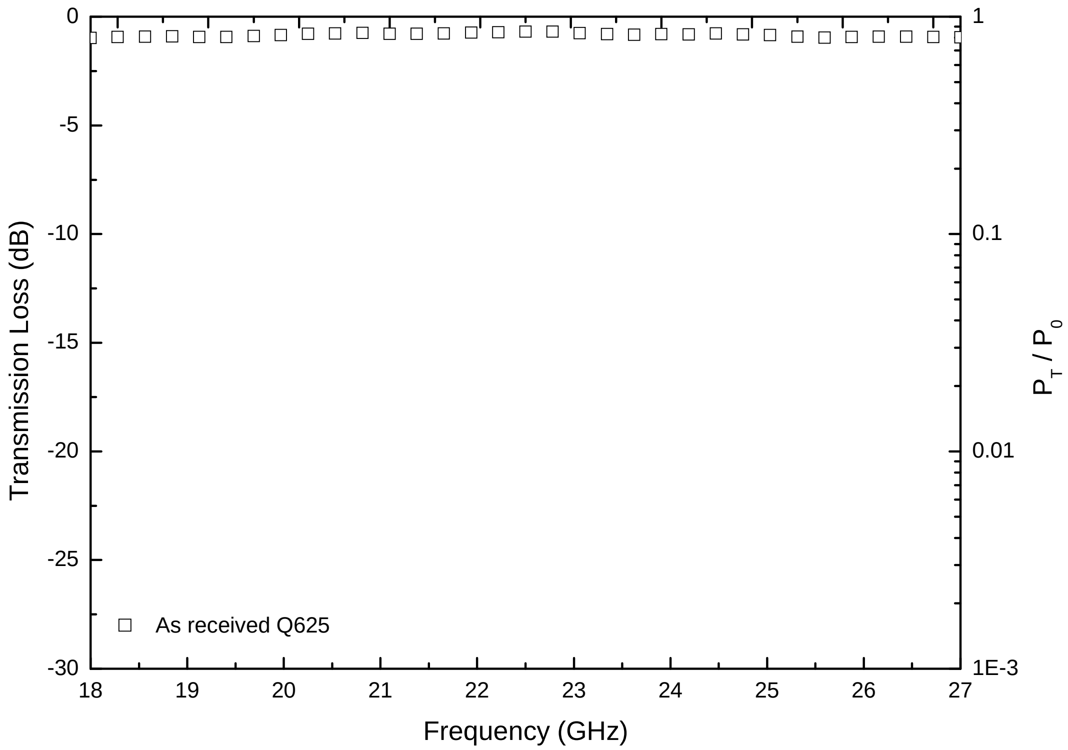

Figure 4.2 Transmission of as-received single layer Q625 fiber glass woven fabric.

In applications using EM waves, fiber glass woven fabrics have moderate reflection properties when compared to widely used Kevlar, alumina and carbon fiber woven reinforcements. Comparison of EM wave reflection properties of the possible reinforcement materials used in polymer matrix composites along with that of the neat epoxy is shown in Figure 4.3.

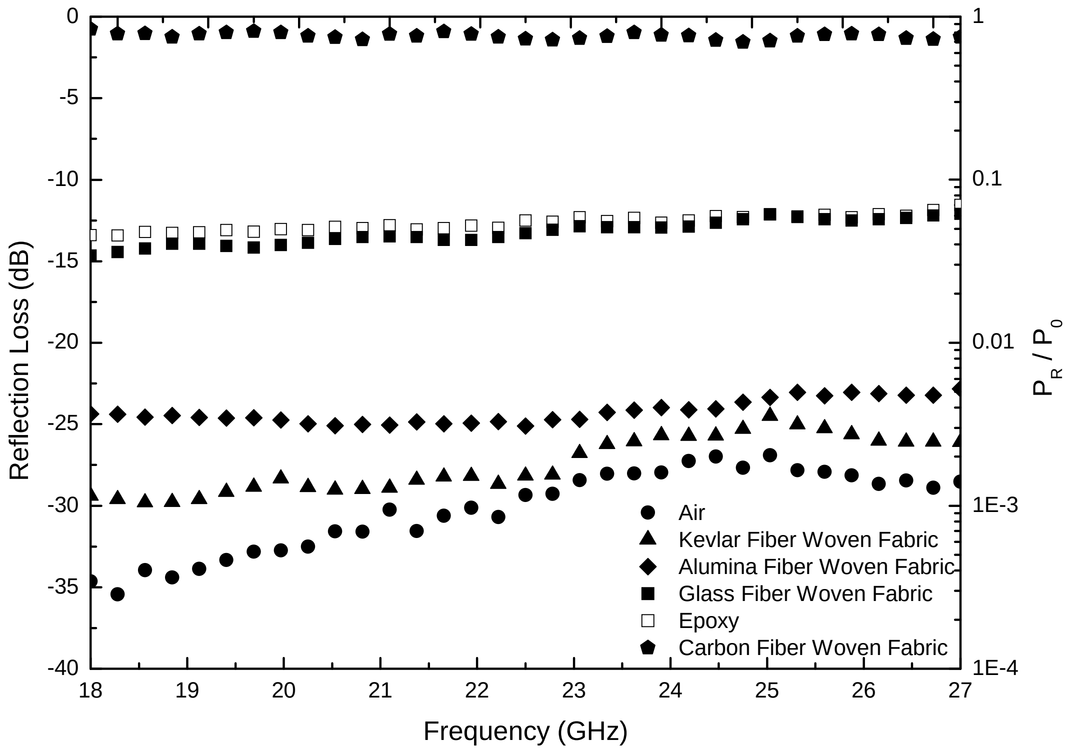

Figure 4.3 Reflection loss of different woven fabric reinforcements and epoxy matrix

Among the possible reinforcement types, Kevlar and alumina has the greatest potential in terms of minimized reflection loss. Intrinsic impedances of Kevlar and alumina fibers are observed to be more compatible with that of ambient air. Carbon fiber reinforcements are strong reflectors of EM wave due to electrical conductivity of carbon. In applications where minimal reflection loss is required carbon fiber woven fabric reinforcement usage should be avoided.

4.2. Effect of Surface Modification on the Electromagnetic Properties of Single Layer Fiber Glass Woven Fabrics

Application of thin metallic coating on intrinsically EM wave transmissive substrates causes EM reflection to increase while leading to EM wave transmission to be reduced. Application of conductive surface modification causes ohmic loss mechanism to become operative.

As it was stated in earlier chapters, effective absorption of EM waves can be achieved by simultaneous interaction of the material with the electric and magnetic field components of incident EM wave. For this reason, materials with suitable electrical and magnetic property sets should be selected for effective EM wave absorption. Conductive and ferroelectric coatings such as iron, nickel, cobalt and gadolinium can provide ohmic and magnetic loss simultaneously. As a result, further dissipation of electromagnetic energy is achieved.

Reflection loss can be controlled by the thickness of the applied surface modification. For better control of electromagnetic properties, target materials with low skin depth and electrical conductivity should be selected. In the present study, nickel and gold coating was applied on fiber glass woven fabrics. From their bulk material properties skin depth of pure gold and nickel was predicted. Skin depth of pure gold was found to be between 590 and 530 nm in 17 – 26.5 GHz range. Being a ferromagnetic and conductive material, skin depth of pure nickel was found to be between 40 and 50 nm in the same frequency range. Adjusting the deposition density of the deposition method applied, critical coating thickness can be extended. In addition, electrical conductivity of nickel is lower when compared to gold. As a result of this, samples with nickel surface modification are expected represent higher EM wave absorption when compared to gold samples with the less pronounced reflection they should reveal. In this study, effect of surface modification up to 100 nm coating thickness has been examined.

4.2.1. Effect of Surface Modification by Gold Coating on the Electromagnetic Properties of Single Layer Fiber Glass Woven Fabrics

In order to investigate the effect of surface modification by gold coating on the EM Wave reflection and transmission characteristics of fiber glass woven fabrics within 17-26.5 GHz frequency range, reflection and transmission loss of as received and gold coatedQ625 fiber glass woven fabrics are presented in Figure 4.4 and Figure 4.5, respectively.

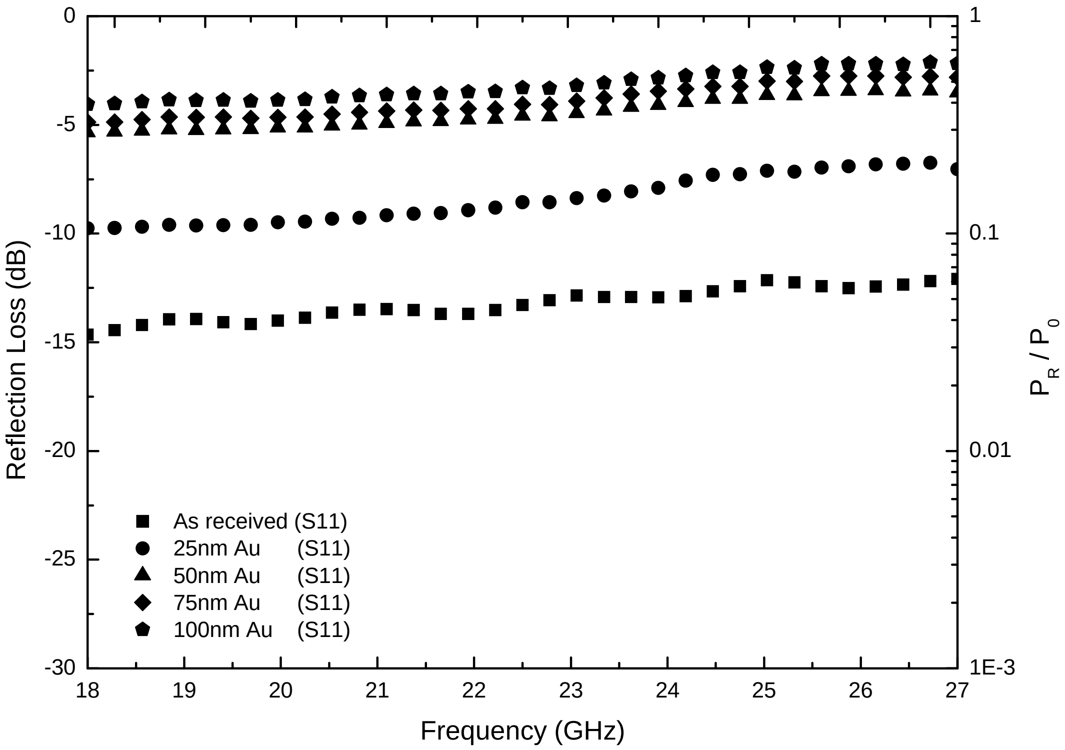

Figure 4.4 Effect of surface modification by gold coating with varying thickness on the EM wave reflection properties of Q625 fiber glass woven fabrics.

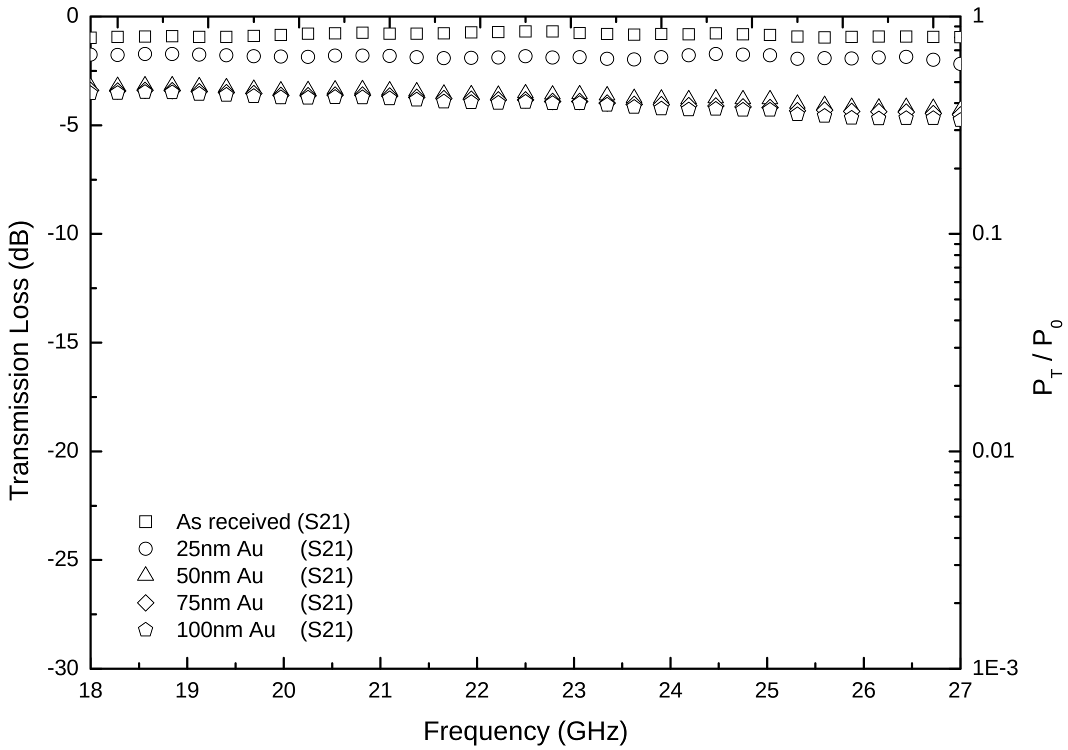

Figure 4.5 Effect of surface modification by gold coating with varying thickness on the EM wave transmission properties of Q625 fiber glass woven fabrics.

As coating thickness of the applied gold layer increases, reflection loss of the surface-modified samples are observed to increased, which points out that by the application of a thicker conductive layer glass woven fabrics become more reflective against EM wave. Similarly, increasing coating thickness caused reduction in transmission loss showing that the transmissive nature of the glass woven fabrics is suppressed by the conductive coating application. Observed changes in the electromagnetic properties by the application of the surface modification seem to be very sensitive to coating thickness up to 50 nm. Reflection difference between as-received along with 25 and 50 nm thick gold surface-modified woven fabrics can clearly be seen in Figure 4.5. Comparison of reflection loss and transmission loss for single layered surface-modified Q625 samples show transmissive to reflective transition of electromagnetic characteristic with increasing modification thickness. Another result observed from the examination of 100 nm thick gold modified Q625 sample is the balanced reflection and transmission loss in the vicinity of -4 dB corresponding to 20% EM wave absorption.

4.2.2. Effect of Surface Modification by Nickel Coating on the Electromagnetic Properties of Single Layer Fiber Glass Woven Fabrics

In 18–27 GHz frequency range, EM wave absorption and transmission characteristics of nickel surface-modified fiber glass woven fabrics were measured by free-space method, and effect of nickel surface modification on electromagnetic reflection/transmission characteristic was investigated. Change in the reflection loss of the fiber woven fabrics due to nickel surface modification is shown in Figure 4.6.

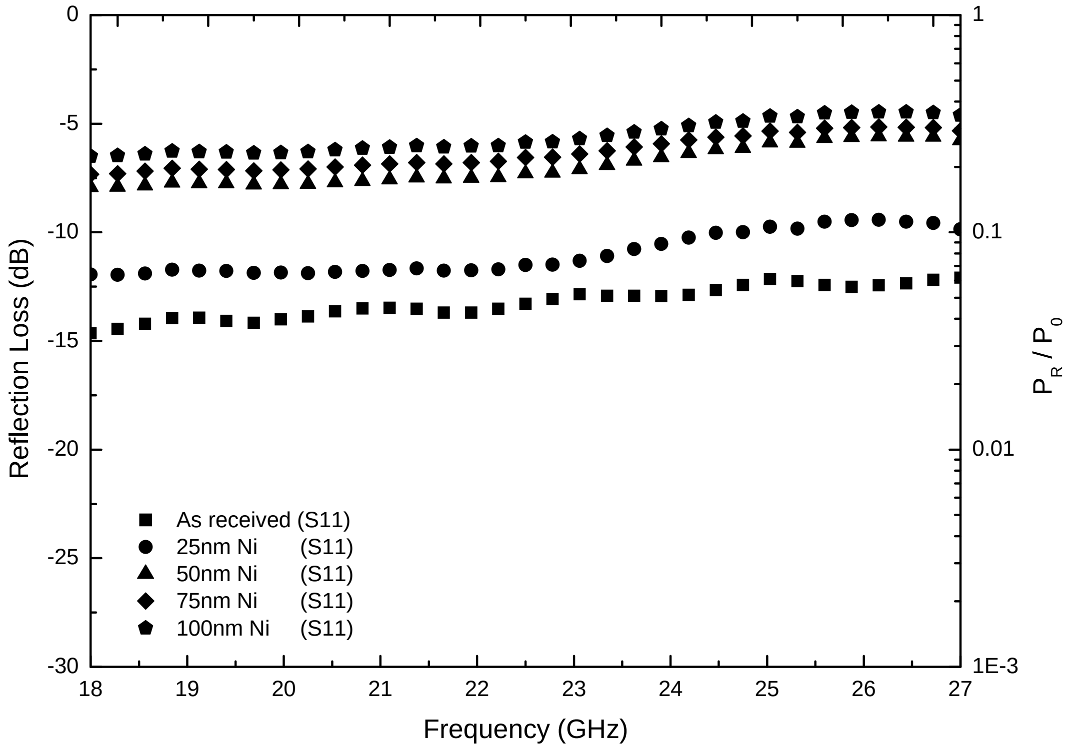

Figure 4.6 Effect of surface modification by nickel coating with varying thickness on the EM wave reflection properties of Q625 fiber glass woven fabrics.

As it is seen in Figure 4.6, reflection loss increases as surface modification thickness is increased. Since the electrical conductivity of nickel is moderate, difference of reflection loss due to surface modification is more controllable by thickness when compared to target materials with higher conductivities like gold. In fact, when compared to gold surface-modified fiber glass woven fabric layers (Figure 4.4) more gradual transition to reflective character is observed. Reflection differences between 25 and 50 nm thick nickel surface-modified woven fabrics compared to as -received Q625 layers are remarkable. Reflection losses of 50, 75 and 100 nm thick nickel surface-modified layers are slightly different. As coating thickness approaches to skin depth, effectiveness of surface modification starts to become less pronounced.

Due to ferromagnetic nature of nickel, magnetic loss mechanisms are also available in the case of this surface modification. In order to determine absorption loss due to ohmic and magnetic loss, transmission loss of nickel surface-modified Q625 layers should also be examined. Transmission loss of nickel modified and as-received Q625 layers are shown in Figure 4.7.

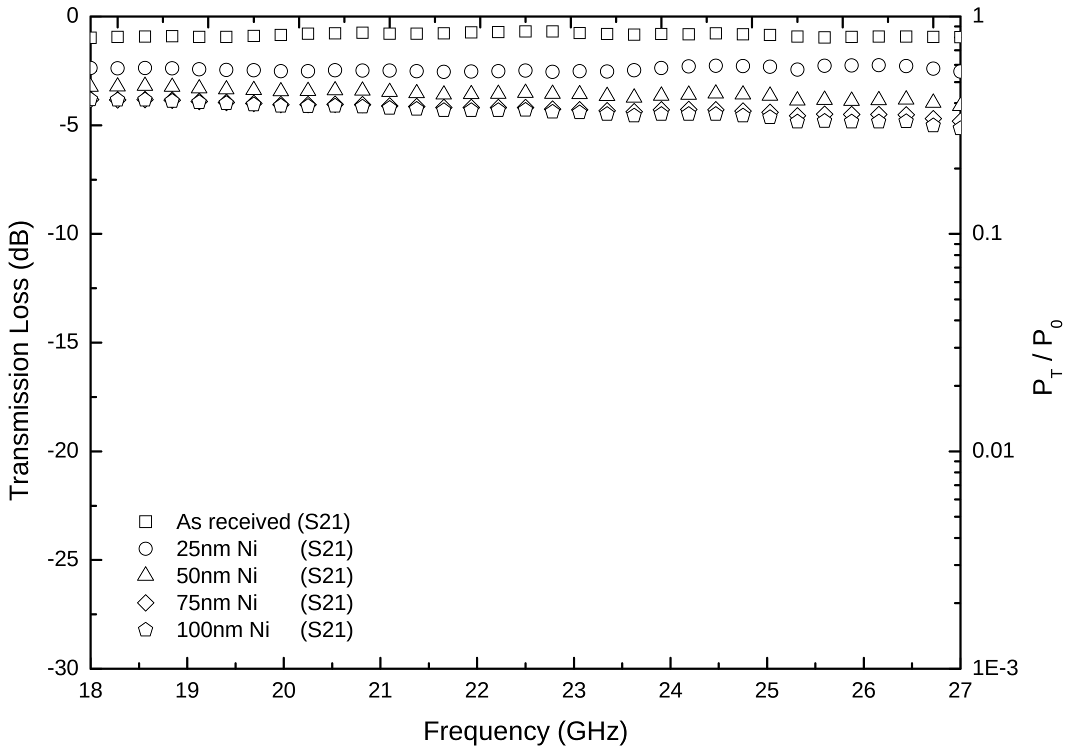

Figure 4.7 Effect of surface modification by nickel coating with varying thickness on the EM wave transmission properties of Q625 fiber glass woven fabrics.

Transmission losses of nickel surface-modified Q625 layers decrease as modification thickness increases. 100 nm thick nickel surface-modified Q625 layer revealed an average transmission loss of. 5 dB while reflection loss was found to be 6 dB for this layer. Thus, approximately 40% EM wave absorption has been attained by 100 nm thick nickel surface modification.

Comparison of EM wave absorption percentages for 100 nm thick gold and nickel coated Q625 layers show the additional effect of magnetic loss by ferromagnetic nickel surface modification. Approximately 20% higher EM wave absorption of EM waves was achieved in nickel surface-modified Q625 layers. Despite its higher electrical conductivity when compared to nickel, gold surface modification showed less EM wave absorption due to lack of magnetic loss. In nickel surface-modified samples, simultaneous suppression of electric and magnetic fields of the incident EM wave resulted in more effective absorption of EM energy. As a result, absorption effectiveness of nickel surface modification was found to be higher than that of gold surface modification.

4.3. Electromagnetic Properties of Multilayered Reinforcement Structures Composed of Surface-Modified Fiber Glass Woven Fabrics

Multilayered arrangement of EM wave reflecting and/or absorbing layers provides additional EM wave absorption mechanisms to be operative due to interaction of EM waves reflected from different layers once it enters into the structure. Although limited, improvement of broadband absorption efficiency can be attained by multilayered structures such as Jaumann absorbers. In multilayered structures, distribution of electrical power on a higher number of lossy layers can also be employed to improve overall EM energy loss gained. Design principles for lossy layer cascading were given in Chapter 2. According to graded absorber design principles, surface-modified layers can be cascaded from the EM wave receiving surface according to increasing electromagnetic interaction characteristics, i.e. higher reflective yet less transmissive nature should be maintained towards the back layer.

In Figure 4.8, reflection loss of double layered structure composed of back to back standing 25 nm Ni and 50 nm Ni surface-modified woven fabrics is given in comparison to those of the surface-modified individual layers forming this double layer structure.

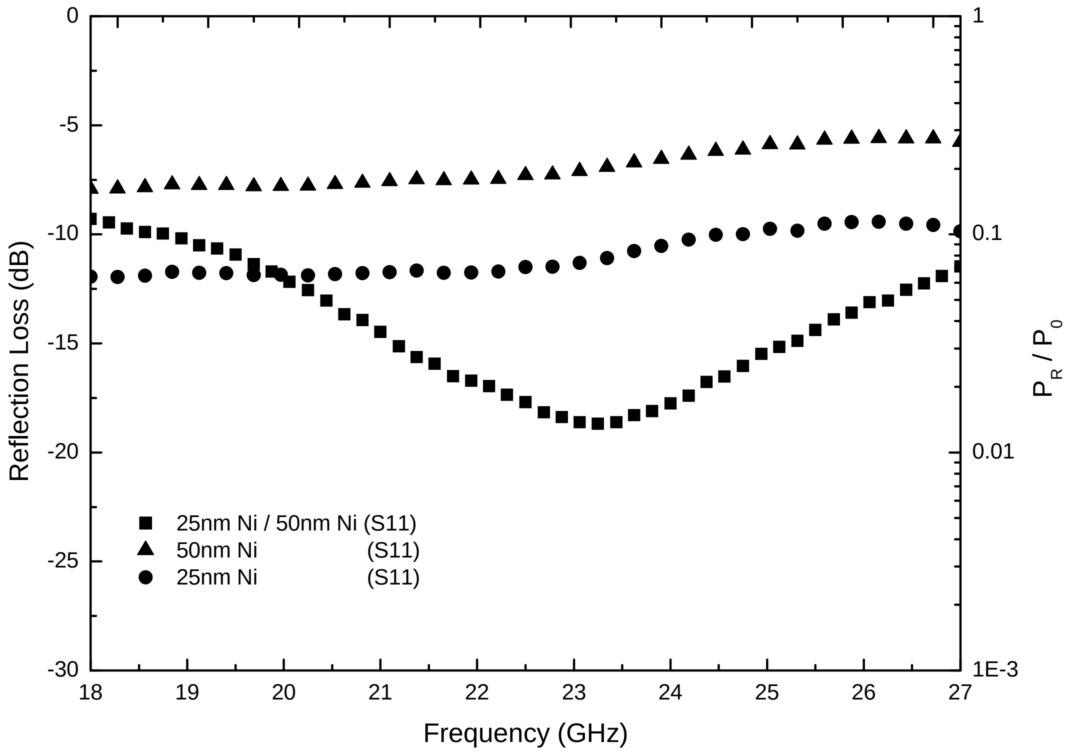

Figure 4.8 Reflection loss of 25 nm Ni / 50 nm Ni double layered structure along with those of the individual layers.

Reflection loss of double layered structure is lower when compared to those of individual single layers forming the double layered structure above 20 GHz. Around 23 GHz frequency, an effective decrease in reflection loss is observed. This reflection drop is due to interference of the EM waves reflected from first and second layers. Distance between the first and second surface modification layer is filled with inhomogeneous fiber glass woven fabric and air. Impedance difference at the sample-air interface also causes refraction of the incident EM wave. As a result, additional reflection loss due to double layered structure was observed.

In double layered structure, power emitted by the network analyzer is received by two lossy layers simultaneously. This is possible only if the frontal (receiving) layer reveals a lower reflection loss than the successive layer so that a higher portion of the incident wave can penetrate into the structure. Power distributed in the double layered structure is attenuated by surface-modified lossy layers, and thus overall weakened reflection power is observed in the double layered structure. In order to determine EM wave absorption potential, evaluation of transmission loss is also required. In Figure 4.9, transmission loss of 25nm Ni and 50nm Ni surface-modified double layered structure is given in comparison to those of the 25 nm Ni and 50 nm nickel surface-modified single layers.

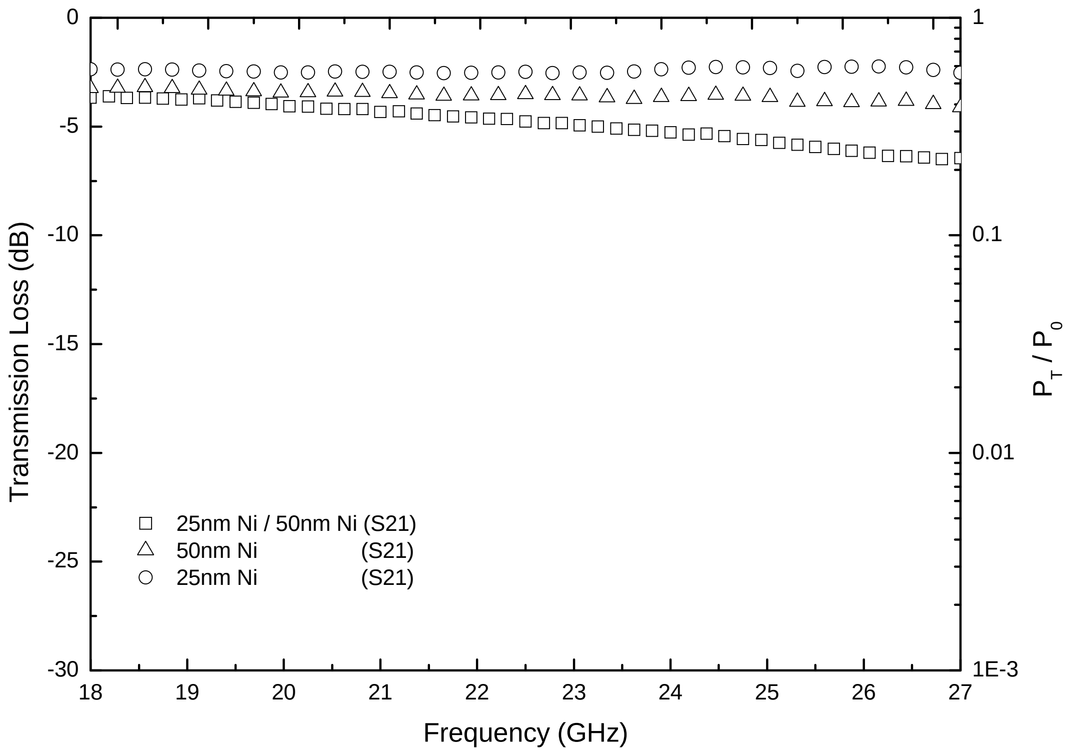

Figure 4.9 Transmission loss of 25 nm Ni / 50 nm Ni double layered structure along with those of the individual layers.

S21 parameter decreases in the case of the double layered structure when compared to 25 nm and 50 nm surface-modified single layers. As the number of layers increases, transmission of EM wave is hindered by the reflective layers. Transmission power is attenuated and transmission loss is observed to decrease.

Consequently, transmission loss of EM wave absorbing structure can be controlled by increasing number of surface-modified layers. In order to achieve high level of EM wave absorption, reflection loss of multilayered structures should be minimized within broadband range. In Figure 4.10, EM wave absorption percentage of 25 nm Ni / 50 nm Ni double layered structure is given with that of the 25 nm thick Ni coated single woven fabric layer.

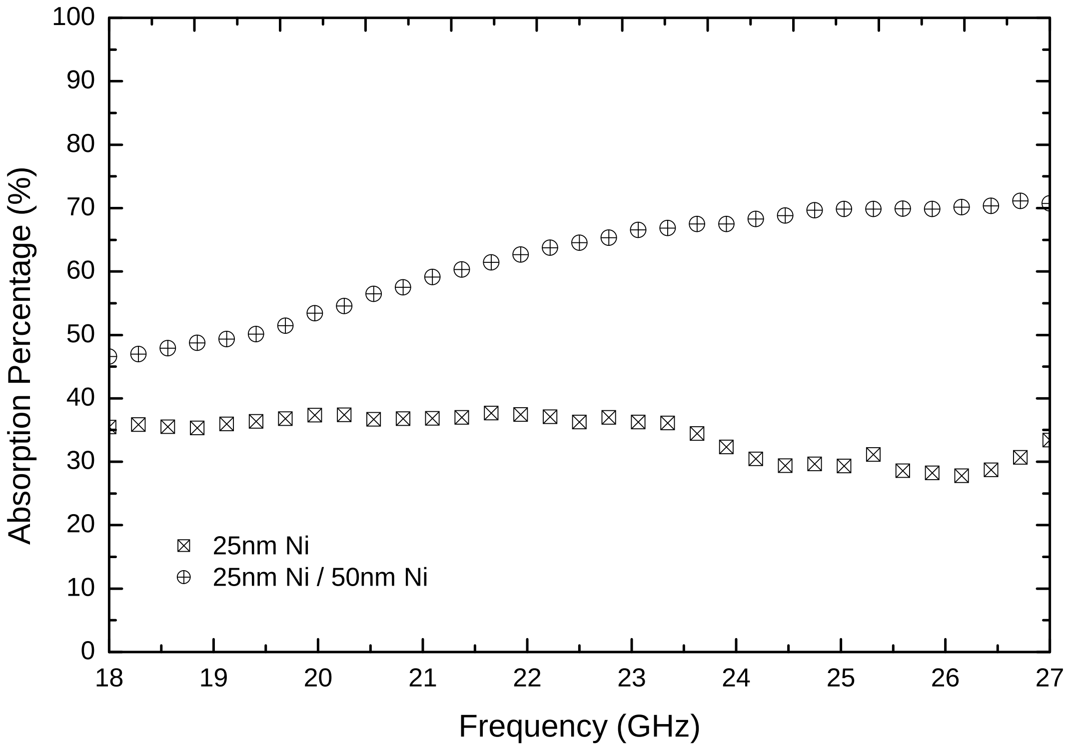

Figure 4.10 EM wave absorption of 25 nm Ni / 50 nm Ni double layered structure in comparison to that of 25 nm Ni single layer

EM wave absorption characteristic of double layered structure is improved when compared to EM wave absorption percentage of 25 nm nickel surface-modified layer. EM wave absorption of 25 nm nickel surface-modified layer is found to be changing between 30 and 40% within 18-27 GHz frequency range. Due to reduced reflection loss and transmission loss simultaneously, EM wave absorption potential of the double layered structure is expected to be higher. As it is expected, on average EM wave absorption of 25 nm Ni / 50nm Ni surface-modified structure is improved to 60% level within IEEE K band which reaches up to 70% around 23 GHz region. Free-space measurements of double layered structures have demonstrated the increasing EM wave absorption potential as the number of surface-modified layers increases.

4.3.1. Electromagnetic Interaction Behavior of Three Layered Structures

Evaluation of Figure 4.9 shows insufficient transmission loss of the double layered structure which is around 5 dB. Majority of the achieved EM wave absorption shown in Figure 4.10 is due to reduced reflection loss. Improvement of transmission loss can be provided by application of additional surface-modified layers. Free space measurement results of 25 nm Ni / 50 nm Ni / 75 nm Ni surface-modified layers are given in Figure 4.11 and Figure 4.12.

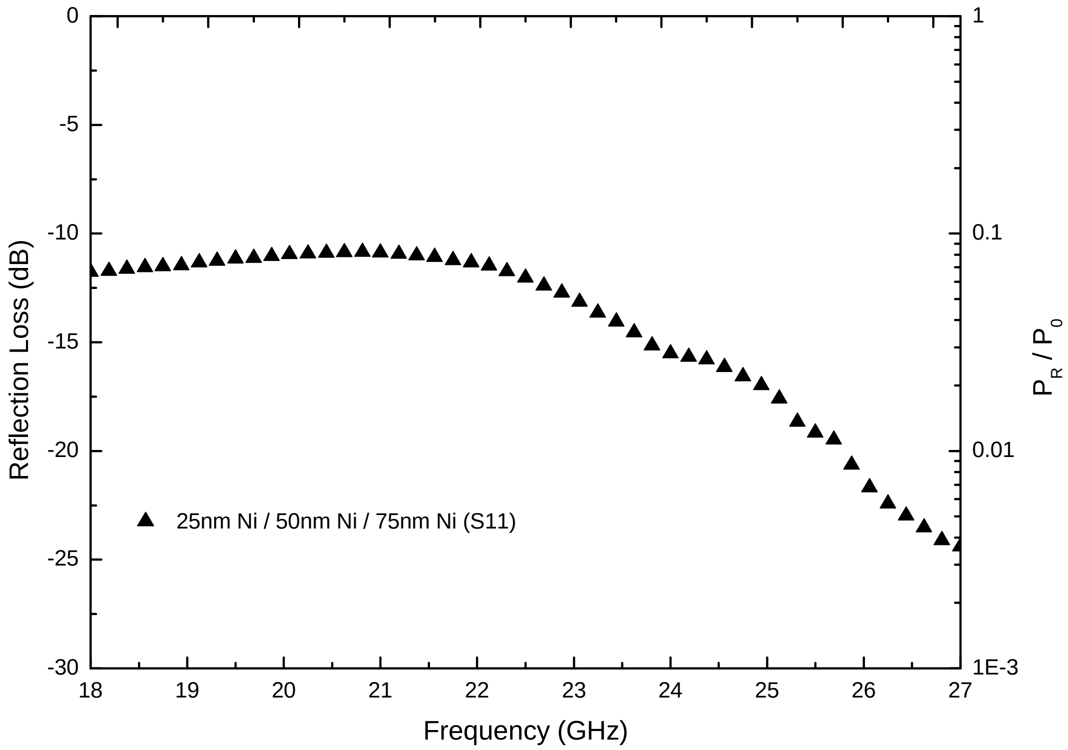

Figure 4.11 Reflection loss of 25 nm Ni / 50 nm Ni /75 nm Ni triple layered structure.

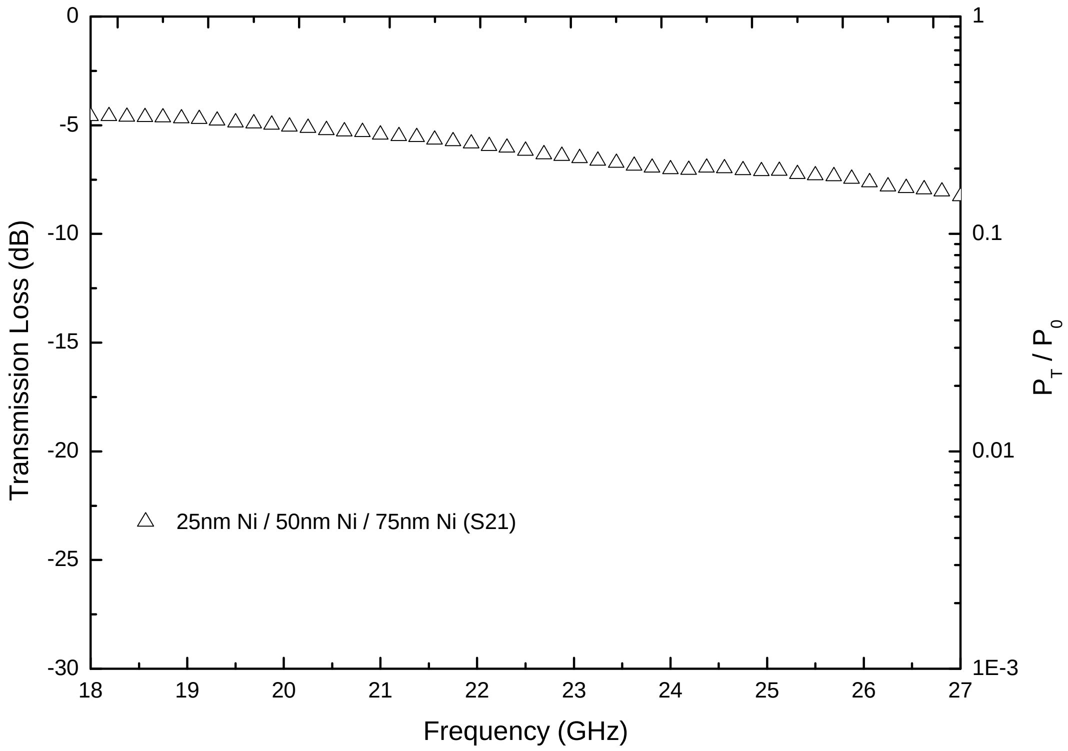

Figure 4.12 Transmission loss of 25 nm Ni / 50 nm Ni /75 nm Ni triple layered structure.

Decrease in transmission loss accompanied by reduced reflection loss due to application of an additional surface-modified layer is observed in 25 nm Ni / 50 nm Ni / 75 nm Ni surface-modified triple layered multilayer structure. In 22-27 GHz range two sharp reflection drops are observed. Reflection drop in 25-27 GHz range is due to extension of reflection drop observed in 25 nm Ni / 50 nm Ni double layer. (Figure 4.8). Extension of reflection drops is typical in multilayered Jaumann absorbers (Figure 2.14). Transmission loss of the three layered structure is lower than 5 dB. When compared to 25 nm Ni / 50 nm Ni double layered structure reduction in transmission coefficient is evident. However, sufficient transmission loss does not seem to be achieved. By the application of an additional fourth layer with high reflection loss an overall decrease in the transmission loss of the whole multilayer structure can be attained.

As a result of decrease in reflection loss and transmission loss, improvement in EM wave absorption is expected. In Figure 4.13, EM wave absorption percentage of 25nm Ni / 50nm Ni / 75nm Ni surface-modified structure is given.

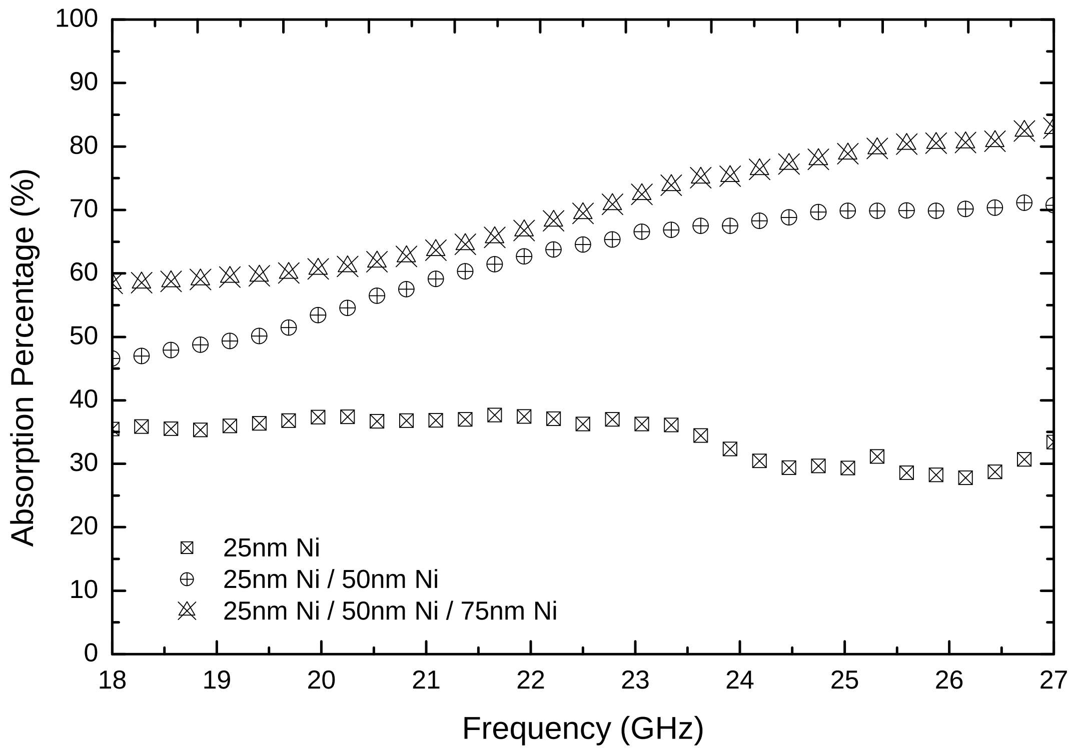

Figure 4.13 EM wave absorption of 25 nm Ni / 50 nm Ni /75 nm Ni triple layered structure in comparison to those of the single and double layers.

As expected, EM wave absorption percentage is improved with the addition of the third layer (Figure 4.13). Especially in 22-27 GHz range higher EM wave absorption due to pronounced reflection drop is observed. EM wave absorption reaching up to 80% has been achieved. In 18-27 GHz frequency range, EM wave absorption characteristic has been changed slightly compared to the double layered structure.

4.3.2. Electromagnetic Interaction Behavior of Four Layered Structures

Free-space measurement on double and three layered structures have shown the possibility of achieving broadband effectiveness in terms of EM wave absorption by using surface-modified glass woven fabrics in a multilayer form. Transmission loss for three layered 25 nm Ni / 50 nm Ni / 75 nm Ni structure is above 10 dB where reflection loss is lower than 10 dB. Application of an additional layer is expected to further decrease both transmission loss and reflection loss due to increased EM wave power distribution within the structure. Furthermore, incorporation of a 100 nm thick Ni-modified fourth layer is expected to minimize overall transmission by reflecting most of the EM wave transmitted through the first three layers. On the reflection path, EM wave energy would be attenuated an additional time. As a result, improved EM wave absorption characteristic is expected. Free-space measurement results of 25 nm Ni / 50 nm Ni/ 75 nm Ni/ 100 nm Ni four layered structure is given in Figure 4.14 - 4.16.

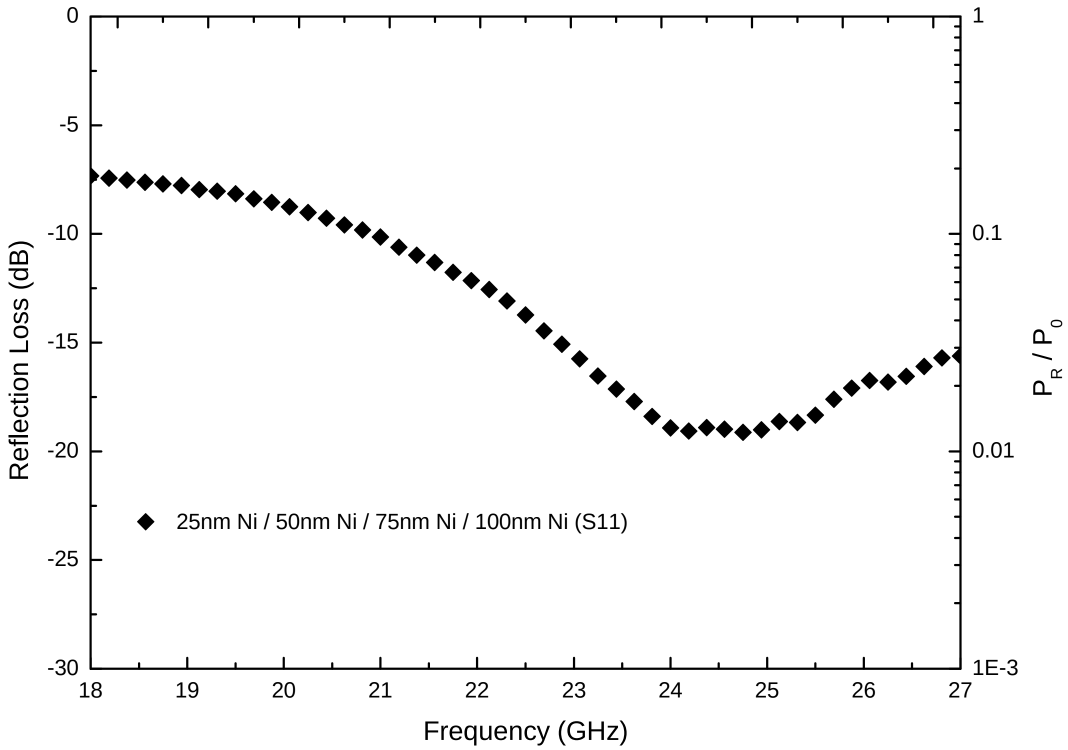

Figure 4.14 Reflection loss of 25 nm Ni / 50 nm Ni /75 nm Ni / 100 nm Ni four layered structure.

Decrease in reflection loss due to increased number of surface-modified Q625 layer can be observed in Figure 4.14. Effectiveness is increased as in the case of Jaumann absorbers due to gradual decrease in the electrical resistivity of the multilayer structure towards the last layer. Reflection loss is below 10 dB within a broad frequency band. Especially in 22-27 GHz frequency range, reflection loss lower than 15 dB reaching to 20 dB is observed. Power distributed among four successive lossy layers provided a four layered structure with weak reflection power. Despite the insertion of an additional layer with a thicker metallic coating occurrence of a lower reflection response of the whole structure can be explained by the gradual intrinsic impedance change through surface-modified layers. Slight impedance difference between ambient air and graded medium prevented strong EM wave reflections from multilayered structure. In graded type absorbers, symmetry of electromagnetic properties from two opposite receiving surface of the material cannot be attained. With the reverse order of surface-modified layers, or on S22 reflection, high reflection loss due to sharp impedance difference is observed. Comparison of S11 (reflection on Port I side with thinnest surface coating) and S22 (reflection on Port II side with thickest surface coating) reflection for 25 nm Ni / 50 nm Ni / 75 nm Ni / 100 nm Ni four layered structure is given in Figure 4.15.

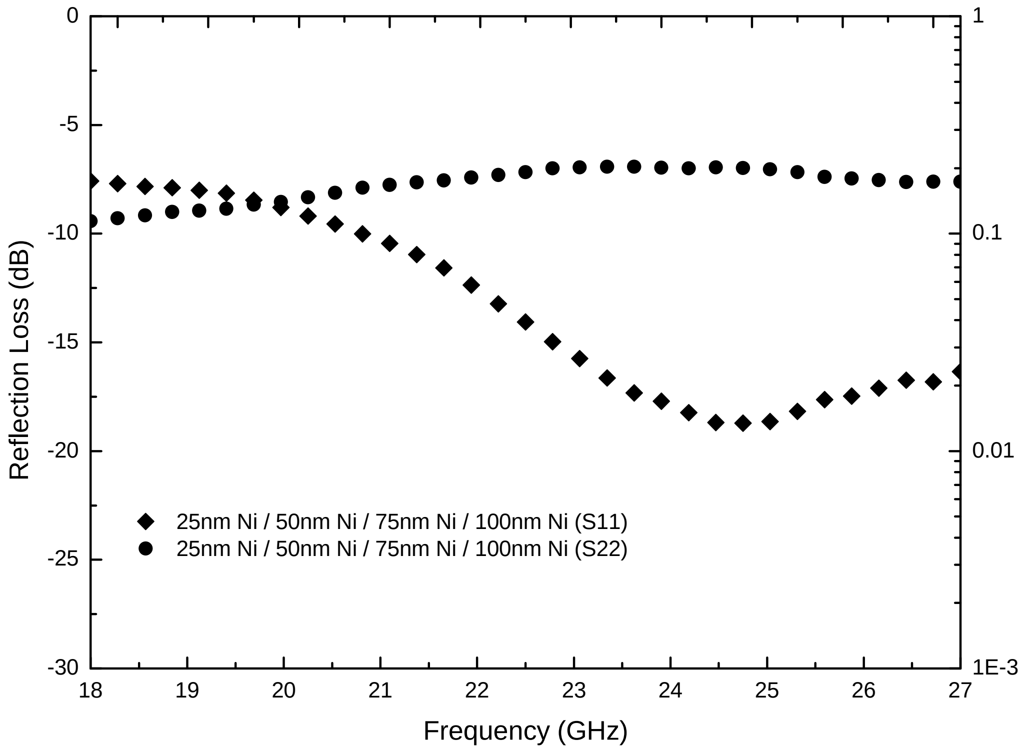

Figure 4.15 Difference between S11 and S22 reflection loss of 25 nm Ni / 50 nm Ni / 75 nm Ni / 100nm Ni four layered structure.

Difference between front face reflection and back face reflection can be used as an advantage in applications where EM wave isolation is aimed such as anechoic chambers. Symmetry in the reflection properties can be attained by mirror image arrangement of the layers on the two faces of the multilayered structure. Main disadvantage of this method is the doubling number of surface-modified layers, and hence doubled thickness and weight of the overall material. Problems related to thickness constraints may be solved by applying different type glass fiber or other alternative woven fabric selections for fiber-reinforced composite material manufacturing.

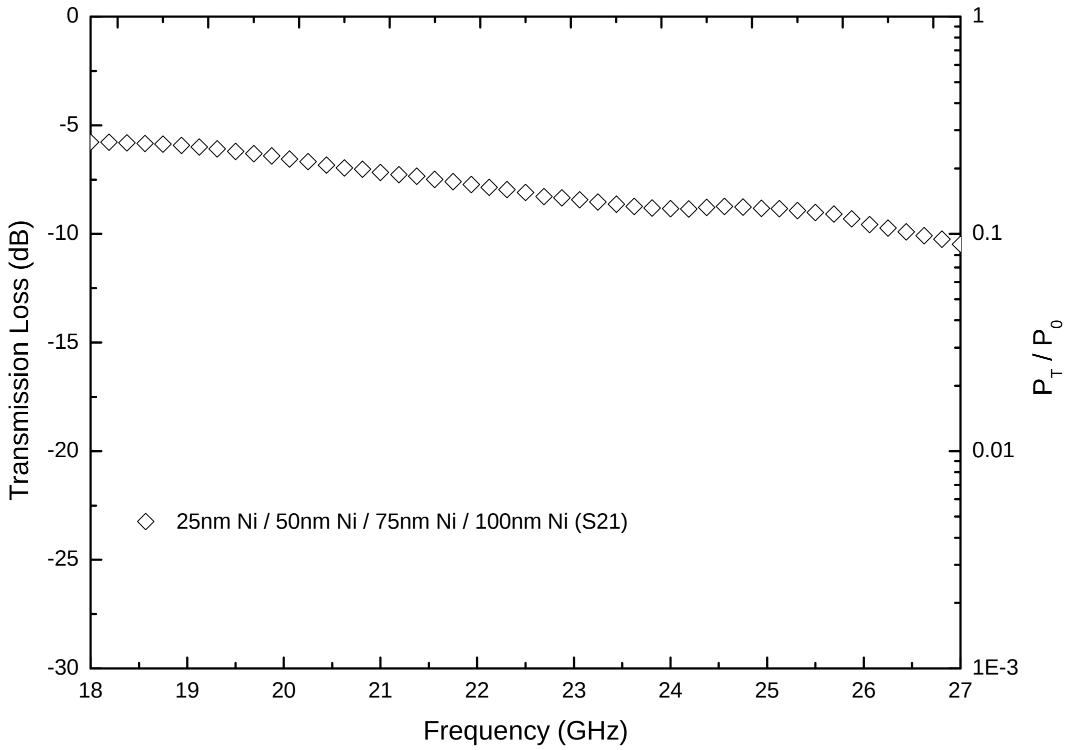

Figure 4.16 Transmission loss of 25 nm Ni / 50 nm Ni /75 nm Ni / 100 nm Ni four layered structure.

Transmission loss of four layered structure is lower compared to that of the three layer structure, as expected. Due to slight reflection difference between 75 nm Ni and 100 nm Ni surface-modified layers, transmission loss of four layered structure did not decreased remarkably. At the point of application, after certain transmission loss is achieved by the addition of extra layers, modified layers with high reflection coefficient can be incorporated to suppress overall reflection response. EM waves strongly reflected from the back layer are expected to re-attenuate on the multiple reflection paths, and thus more effective transmission and reflection reduction can be attained. This can also be done by mirror image arrangement of the used layers to provide EM wave response symmetry. By this method EM wave absorption properties of multilayered structures can be maximized.

As a hybrid application of Jaumann and graded type absorbers 25 nm Ni / 50 nm Ni / 75 nm Ni / 100 nm Ni four layered structure is expected to provide high EM wave absorption characteristic. EM wave absorption potential of the four layered structure and its comparison with those of the single, double and three layered structures is given in Figure 4.17.

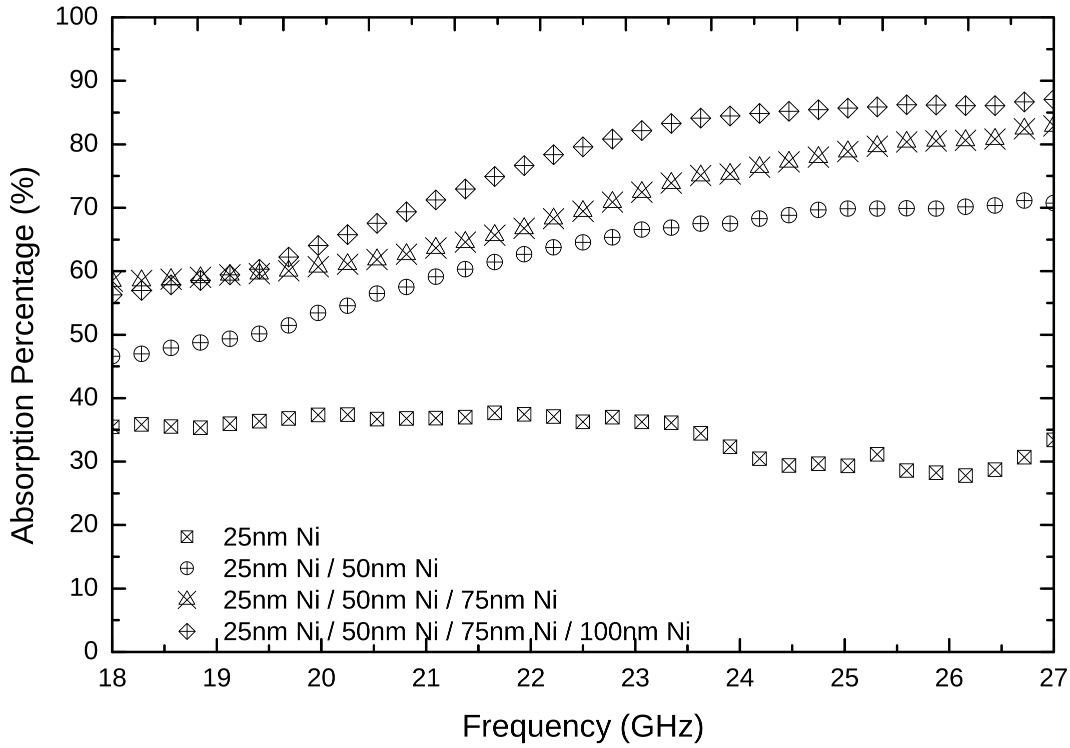

Figure 4.17 EM wave absorption of 25 nm Ni / 50 nm Ni / 75 nm Ni / 100 nm Ni four layered structure along with those of the single, double and triple layers.

Among all, highest EM wave absorption capability of the four layered multilayer structure within a broadband can clearly be seen. By the formation of the 25 nm Ni / 50 nm Ni / 75 nm Ni/ 100nm Ni four layered structure EM wave absorption reaching up to 85% was achieved.

4.4. Computation of Electromagnetic Absorption Properties for Surface-Modified Multilayered Structures

In order to achieve multilayered structures with well-tailored and optimized EM wave absorption, experimental determination of the electromagnetic properties of modeled structure is essential. However, in advance prediction of EM wave absorption properties for some potential structures with some certainty may provide basis for better and more rapid development of EM wave absorbing multilayered materials.

Computer aided computation of EM wave interaction properties of multilayered EM wave absorbing structures can be done by cascading the complex EM wave parameters of individual layers. Methods suggested for cascading include arithmetic operations on transmission parameters. Details of these operations were discussed in Chapter 3.4. Software codes written for cascading of EM wave port parameters is expected provide transmission–reflection, and hence absorption data for multilayered structures. In the current study, EM wave data harvesting software AWR (AWR Corporation, CA, USA) has been utilized for computation of cascaded structures.

4.4.1. Computation of Nickel Coating Modified Multilayered Structures

Surface-modified single layer fiber glass woven fabrics and multilayered structures consisting of modified layers were characterized by free-space method. S parameters obtained by the measurements on single layers were used as input in the construction of cascaded structure computation. In order to test the success of the applied computation method, prediction technique was applied to nickel coating modified multilayered EM wave absorbing structures up to four layers, and achieved results were compared with the already presented experimental measurement results.

Computation of multilayered sample geometry is based on the assumption that the spacing between adjacent layers is zero meaning that the single layers are arranged back to back in contact with each other. This order can also be taken as a representative situation for the woven fabric reinforcement layers incorporated in a GFRP composite material where there is a very thin matrix layer separating individual layers. In the case of the experimentally treated multilayer geometry, 800 μm thick air gap exists between adjacent layers. This gap is filled by ambient atmospheric air the transmission loss of which was calibrated to zero during TRL calibration within free-space measurement aperture. That is, free-space method focuses on electromagnetic characterization of the condensed matter content placed into calibrated thickness. For this reason, cascaded computation of surface-modified layers placed in contact with each other is rather acceptable. However, interactions of multiple reflected waves due to 800 μm spacing may not be estimated properly by simple cascading method. In such a case, additional computation methods based on refraction models can be utilized and integrated to cascaded circuit approach [2]. Basically, as a first approximation, estimation of electromagnetic reflection and transmission of the multilayered structures can be done by transmission parameter cascading method. In the current study, computer aided computation of reflection and transmission loss for cascaded multilayered structures have been investigated. Computation results were compared with free-space measurement results of multilayered structures considered in the scope of this study.

4.4.1.1. Computation of EM Wave Transmission / Reflection / Absorption Characteristics of the Double Layered Structure

In Figure 4.18, simulated and experimentally determined S11 parameters of the 25nm Ni / 50nm Ni surface-modified double layered structure is shown.

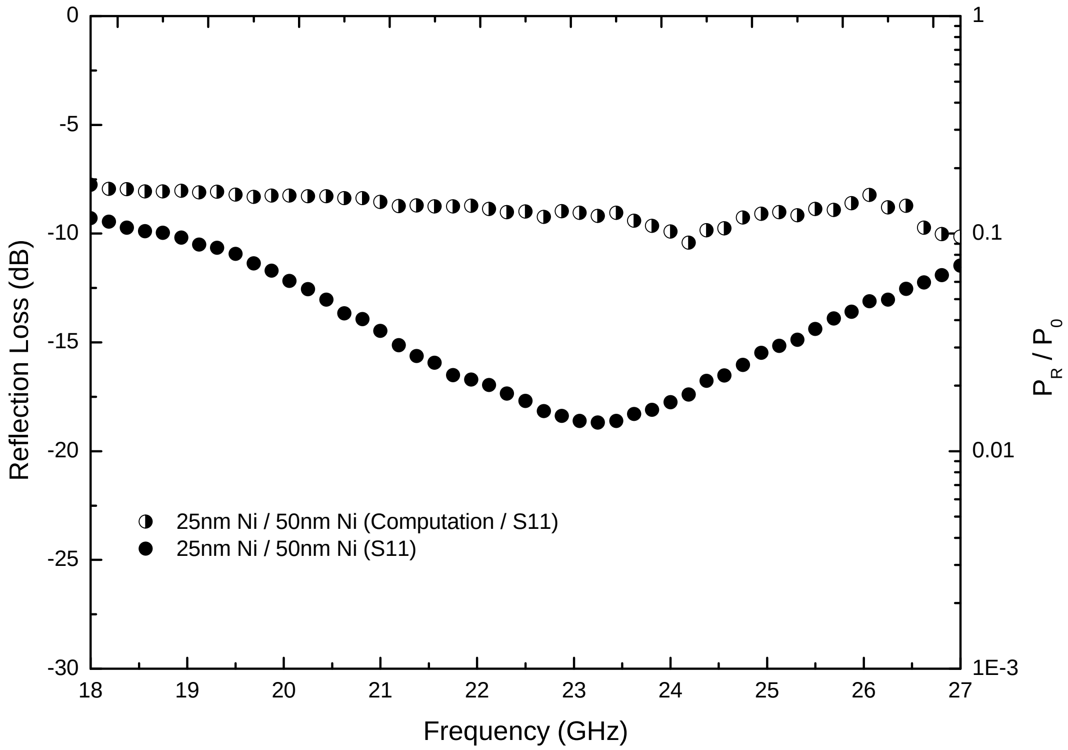

Figure 4.18 Computation of reflection loss for 25 nm Ni / 50 nm Ni double layered structure in comparison to the experimental data.

According to experimental results, throughout the IEEE K band range 25 nm Ni / 50 nm Ni surface-modified double layered structure presents reflection loss values changing around 10 dB. Within 20-23 GHz frequency range a reflection drop is observed. This reflection drop is considered to be due to reflection loss difference between 25 and 50 nm thick Ni surface-modified layers which could not be properly incorporated to the computations.

On average computation result is observed to fit fairly well with the general trend line of the measurement result at around 10 dB. However, reflection loss between

20-23 GHz could not be predicted well by the computation. Multiple reflection observed on the real samples provided a lowered reflection than the estimated value.

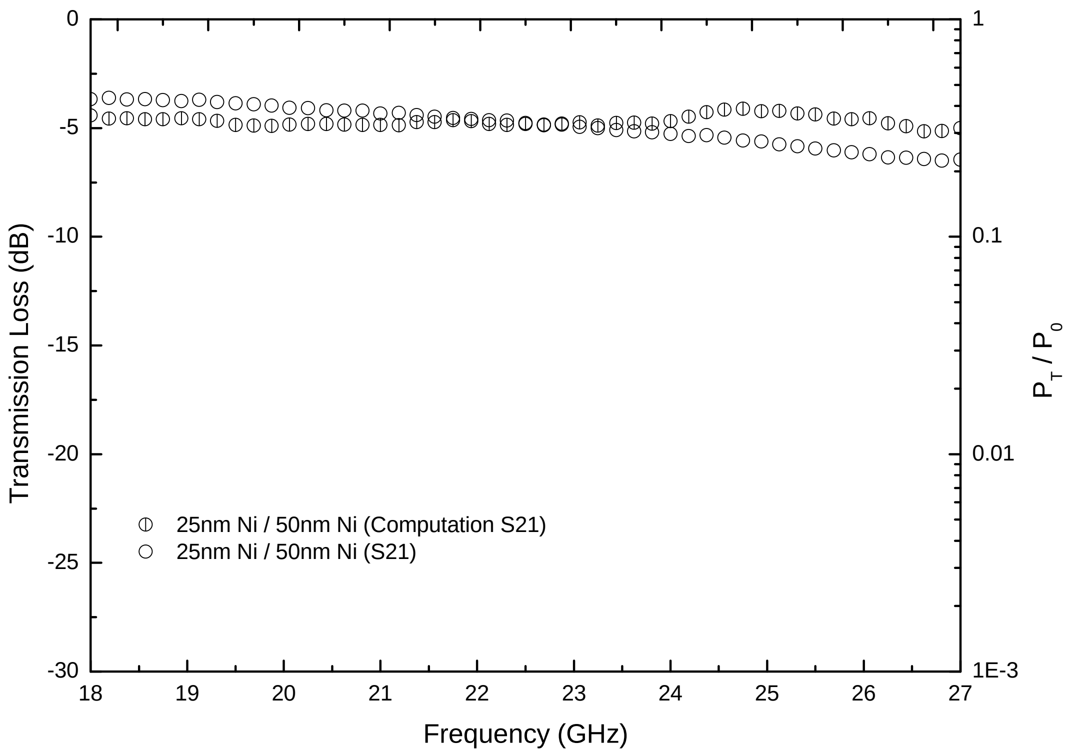

Figure 4.19 Computation of transmission loss for 25 nm Ni / 50 nm Ni double layered structure in comparison to the experimental data.

In Figure 4.19, simulated and experimentally determined transmission loss of 25 nm Ni / 50 nm Ni surface-modified double layered structure is given. S21 values from free-space measurement and computation are compatible. Estimation of EM wave transmission characteristic was done effectively by computation, since EM wave transmission characteristic is not affected by multiple interactions as in the case of the reflection. Computer aided computation provided reasonable results in the estimation of transmission loss of double layered structure.

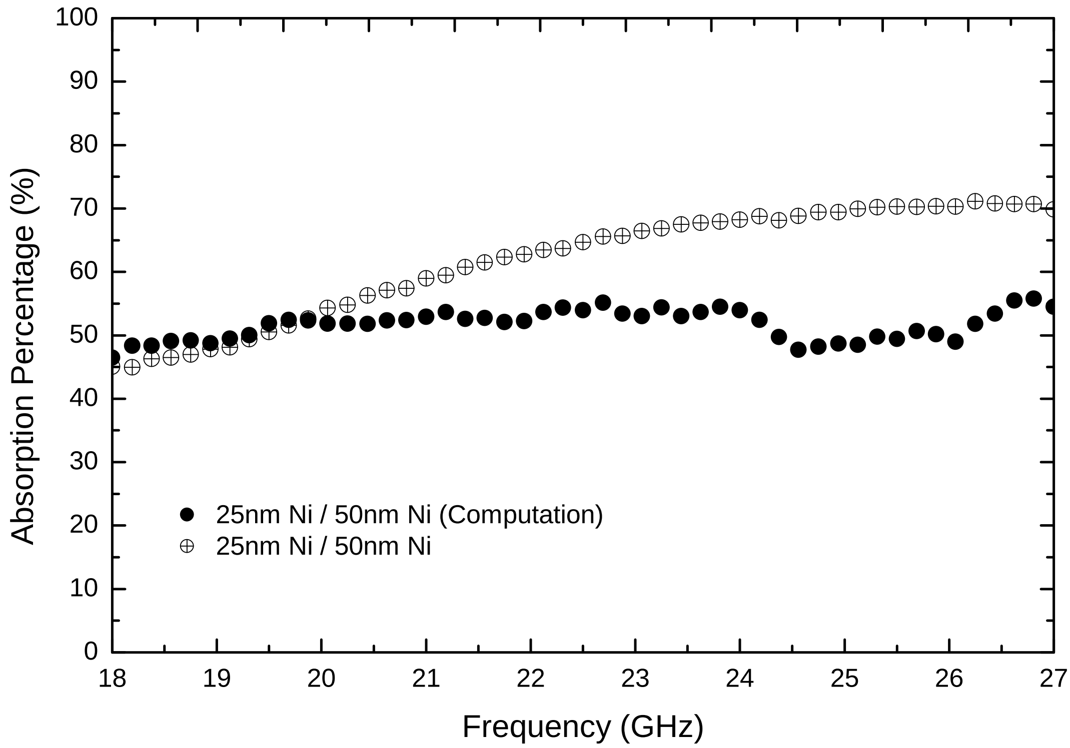

Figure 4.20 Computation of EM wave absorption for 25 nm Ni / 50 nm Ni double layered structure in comparison to the experimental data.

Estimation of EM wave absorption loss can also be done (Figure 4.20) using the transmission and reflection results obtained by the computation. Due to overestimated reflection loss, absorption level is expected to be underestimated. As a result, utilization of computation method for the determination of general reflection and transmission characteristics is reasonable for double layered structure, as a lower bound for the absorption behavior of the multilayer structure can obtained.

4.4.1.2. Computation of EM Wave Transmission / Reflection / Absorption Characteristics of the Triple Layered Structure

In Figure 4.21, reflection loss for 25 nm Ni / 50 nm Ni / 75 nm Ni surface-modified triple layered structure is given in comparison to the experimental data.

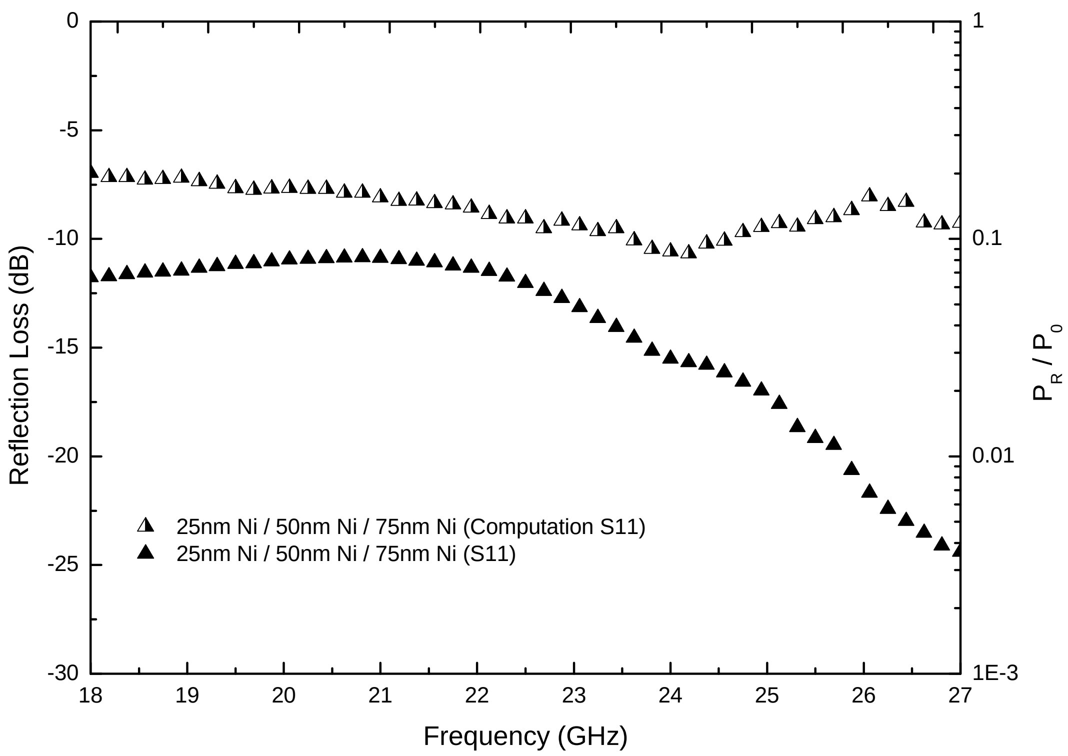

Figure 4.21 Computation of reflection loss for 25 nm Ni / 50 nm Ni / 75 nm Ni triple layered structure in comparison to the experimental data.

Within 18-27 GHz frequency range triple layered structure presents reflection loss on average 10 dB according to the computation results. On the other hand, experimental measurements revealed a reflection drop in 24-27 GHz frequency range where it reaches up to -30 dB at around 27 GHz, while computation result have shown a straight trend line around -10 dB. When compared to free-space measurements, computation provided higher reflection loss. Reflection drop at 24-27 GHz frequency range could not be predicted by the computation. For triple layered EM wave absorbing structure, on average computation provided fairly matching results with the measurement in predicting the EM wave reflection properties.

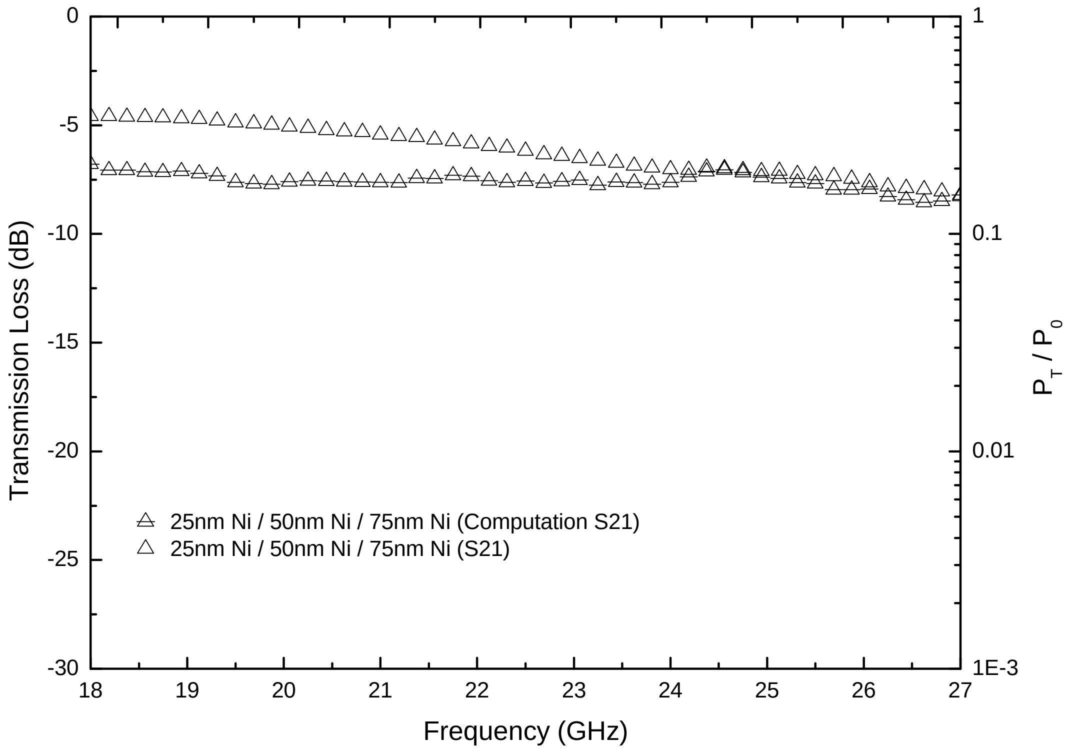

Figure 4.22 Computation of transmission loss for 25 nm Ni / 50 nm Ni / 75 nm Ni triple layered structure in comparison to the experimental data.

In Figure 4.22, simulated S21 transmission loss for 25 nm Ni / 50 nm Ni / 75 nm Ni surface-modified triple layered structure is represented in comparison to the experimental data. Simulated S21 values based on Port I parameters of free-space measurement are observed to be around -5 dB which matches well with the measurement result.

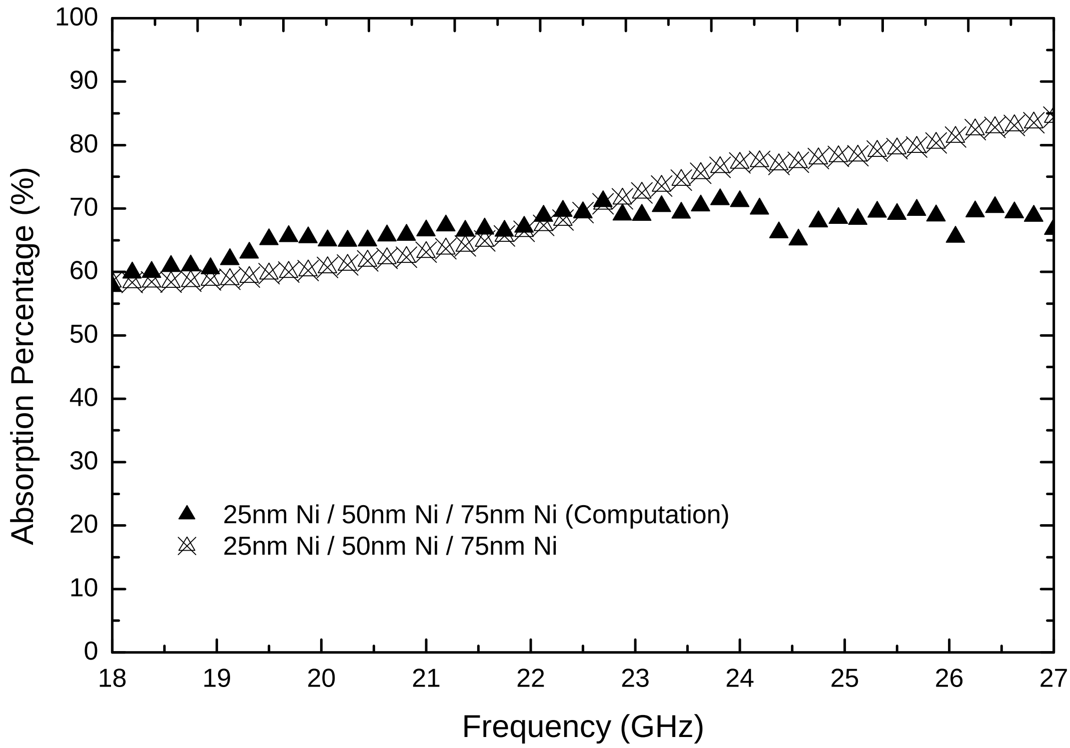

Figure 4.23 Computation of EM wave absorption for 25 nm Ni / 50 nm Ni / 75 nm Ni triple layered structure in comparison to the experimental data.

In Figure 4.23 estimated EM wave absorption potential of 25 nm Ni / 50 nm Ni / 75 nm Ni triple layered structure is shown in comparison to the experimental data. Estimated EM wave absorption is compatible with free-space measurement results. Especially in 24-27 GHz frequency range higher EM wave absorption was observed compared to prediction due to reflection drop that cannot be simulated properly. However, as a first approximation prediction method seems to be useful to determine EM wave absorption characteristic of triple layered structure.

4.4.1.3. Computation of EM Wave Transmission / Reflection / Absorption Characteristics of the Four Layered Structure

In Figure 4.24, estimated reflection loss for 25 nm Ni / 50 nm Ni / 75 nm Ni / 100 nm Ni surface-modified four layered structure is given in comparison to the experimental data..

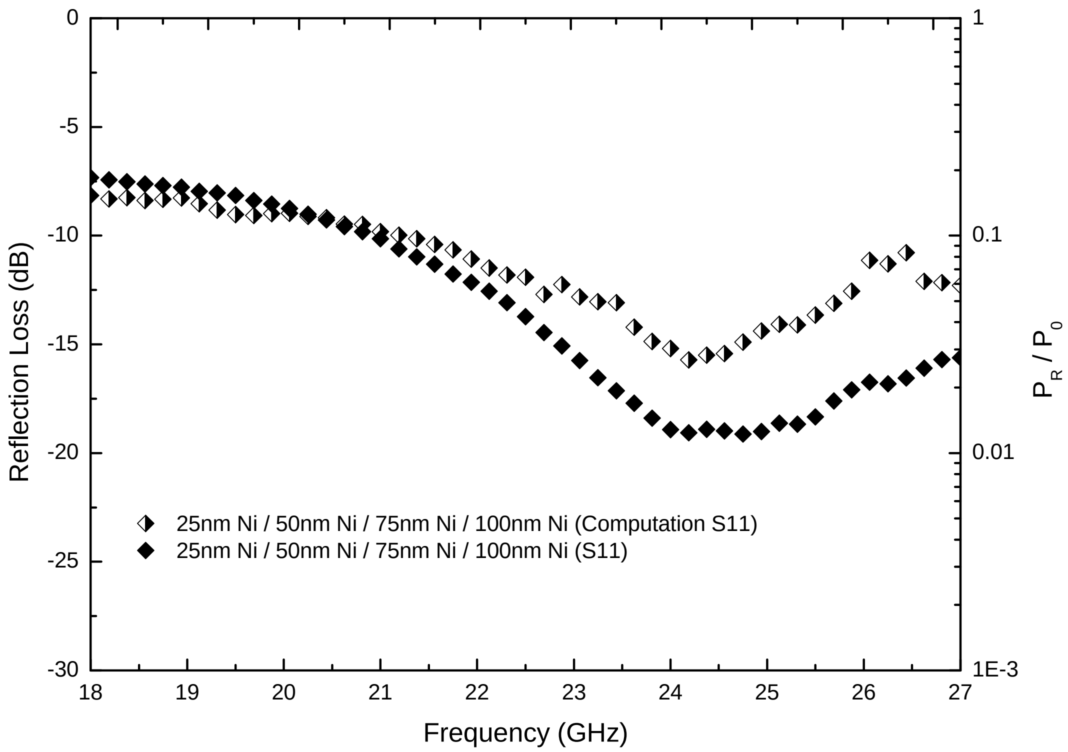

Figure 4.24 Computation of reflection loss for 25 nm Ni / 50 nm Ni / 75 nm Ni / 100 nm Ni four layered structure in comparison to the experimental data.

In 21-27 GHz frequency range a reflection drop is observed in both simulated and experimentally determined results. In addition, due to distribution of electromagnetic power between adjacent layers amplitude of the reflection drop decreased when compared to double and three layered samples. Computation provided quite matching results with free-space measurement results of the four layered structure. Reflection drop at 24-27 GHz frequency range could fairly be predicted by computation. Prediction efficiency of computation in terms of reflection loss has risen by increasing number of surface-modified layers compared to the earlier cases. In order to completely assess effectiveness of computer aided computation consideration of transmission loss is also required.

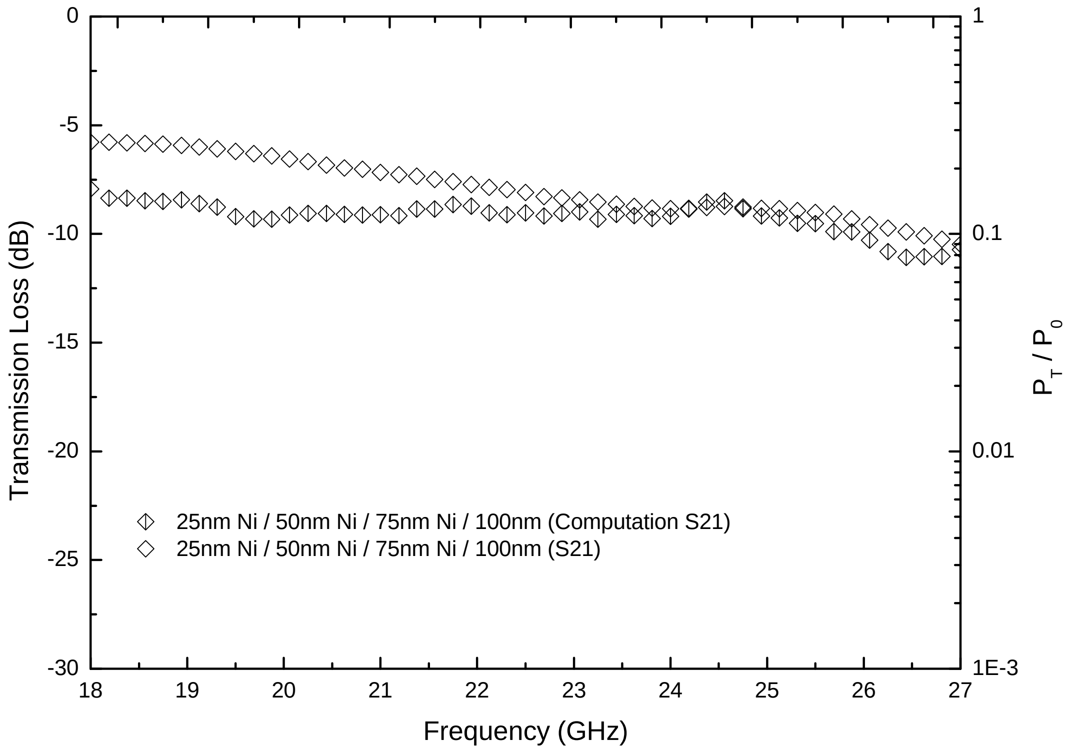

Figure 4.25 Computation of transmission loss for 25 nm Ni / 50 nm Ni / 75 nm Ni / 100 nm Ni four layered structure in comparison to the experimental data.

In Figure 4.25, simulated S21 transmission loss for 25 nm Ni / 50 nm Ni / 75 nm Ni / 100 nm Ni surface-modified four layered structure is represented in comparison to the experimental data. On average simulated S21 response based on Port I parameters of free-space measurement is observed to be below -5 dB. Computation provided compatible results with the free-space measurement.

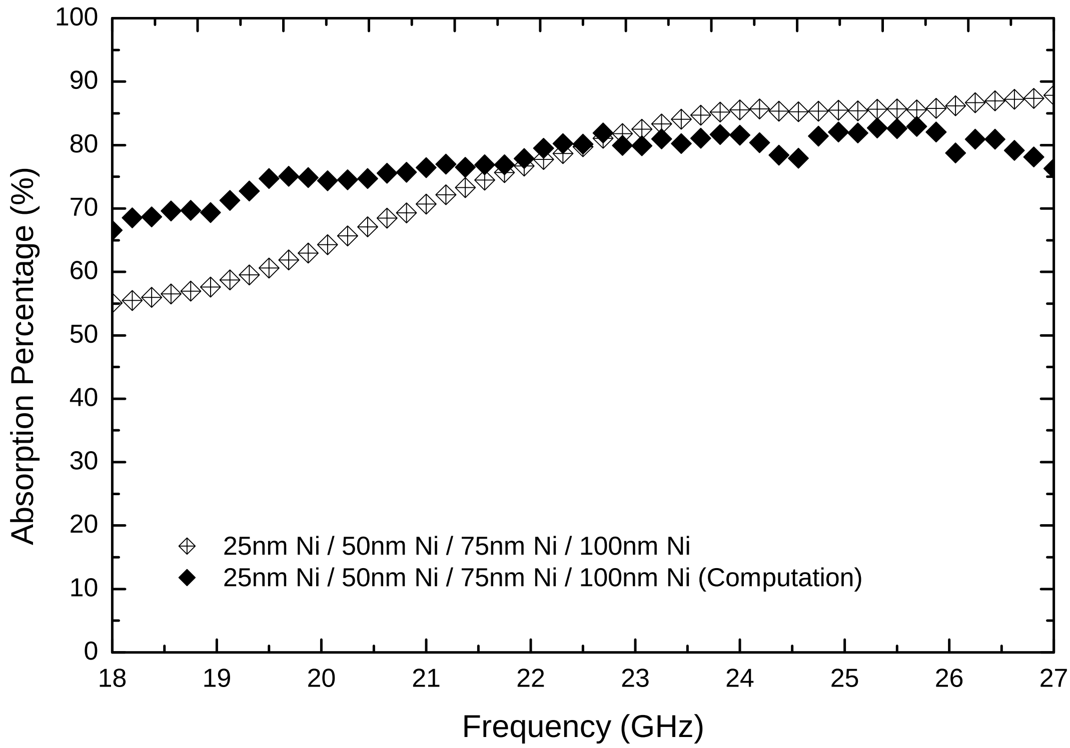

Figure 4.26 Computation of EM wave absorption for 25 nm Ni / 50 nm Ni / 75 nm Ni / 100 nm Ni four layered structure in comparison to the experimental data.

EM wave absorption potential of 25 nm Ni / 50 nm Ni / 75 nm Ni / 100 nm Ni surface-modified multilayer structure is shown in Figure 4.26 in comparison to the experimental data. EM wave absorption properties are successfully predicted by the computation. Consequently, application of multilayered structure is expected to present higher EM wave absorption performance than predicted. Utilization of computation method seems to be advantageous in predicting EM wave absorption potential of multilayered structures with especially four or more layers when S-parameters of individual constituent layers are known.

4.4.2. Computation of Gold Coating Surface-Modified Multilayered Structures

When compared to nickel, gold surface modification has provided lower improvement in EM wave absorption performance of the glass fiber woven fabrics. In K band, skin depth of gold is calculated to be ~500 nm where it is about 50 nm for nickel. In addition, electrical conductivity of gold is considerably high that reflection loss is easily affected by increasing surface modification thickness. Magnetic loss is also not available in gold modified surfaces. As a consequence, gold is not expected to provide a high level of electromagnetic absorption to glass fiber woven fabrics. In Figure 4.27, reflection loss of 25 nm Au / 50 nm Au / 75 nm Au / 100 nm Au four layered structure is given in comparison to the experimental data.

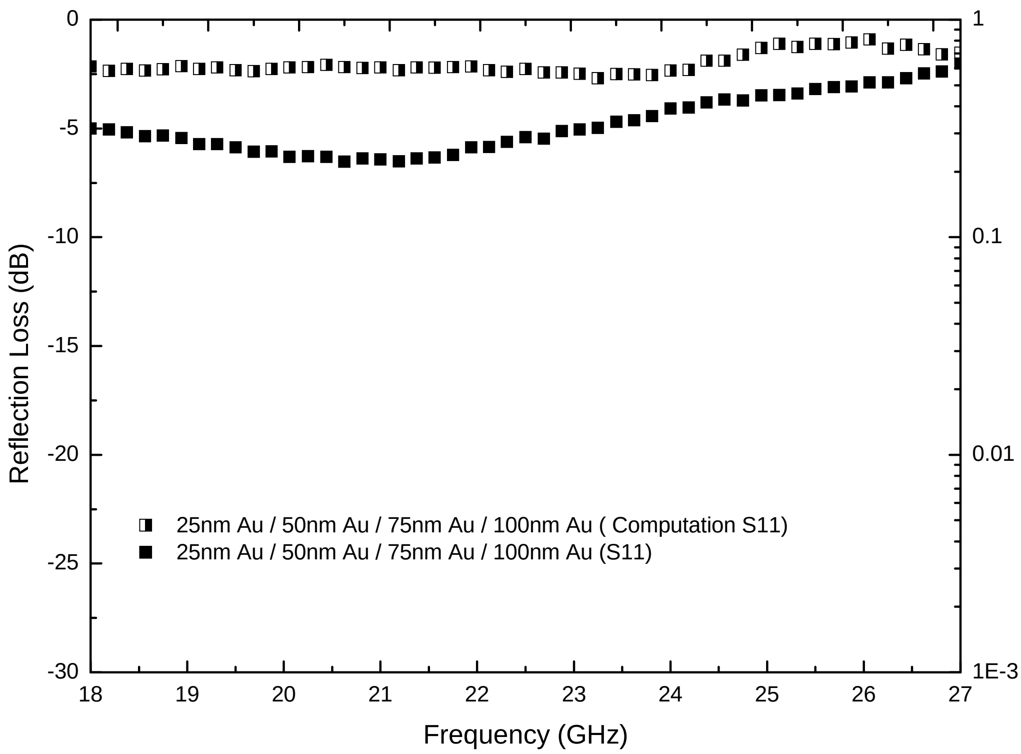

Figure 4.27 Computation of reflection loss of 25 nm Au / 50 nm Au / 75 nm Au / 100 nm Au four layered structure in comparison to the experimental data.

By computation EM wave reflection is predicted to be slightly higher compared to the measurement. Due to multilayered structure in which multiple reflections are taking place measured reflection loss was found to be slightly lower. Reflection loss of around 5 dB corresponds to about 40% reflection. When compared to nickel surface-modified four layered structure (Figure 4.24), reflection loss was found to be considerably higher.

Due to the high reflection level, transmission loss is expected to be rather moderate as most of the incident radiation reflects back from the sample surface. In Figure 4.28 transmission loss for 25 nm Au / 50 nm Au / 75 nm Au / 100 nm Au four layered structure is given in comparison to the experimental data.

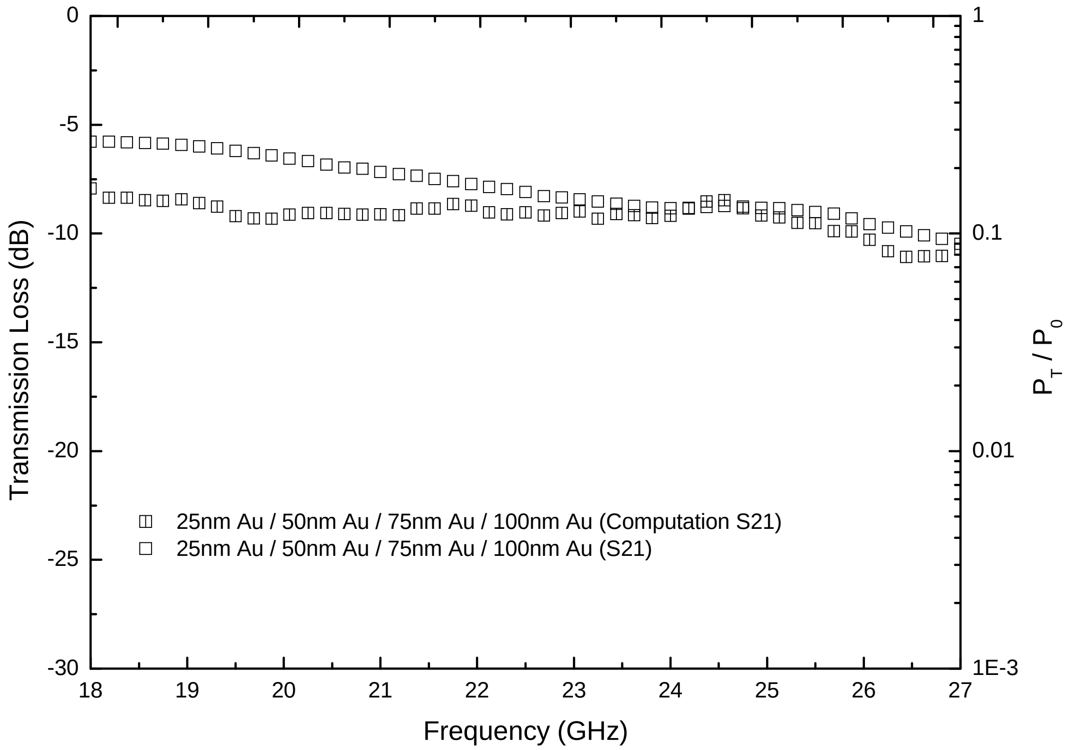

Figure 4.28 Computation of transmission loss of 25 nm Au / 50 nm Au / 75 nm Au / 100 nm Au four layered structure in comparison to the experimental data.

Transmission loss for four the layered structure is changing between 5 and 10 dB corresponding to a transmitted power of 10-20% of the incident wave power. Experimentally determined EM wave absorption for 25 nm Au / 50 nm Au / 75 nm Au / 100 nm Au four layered structure is shown on Figure 4.29.

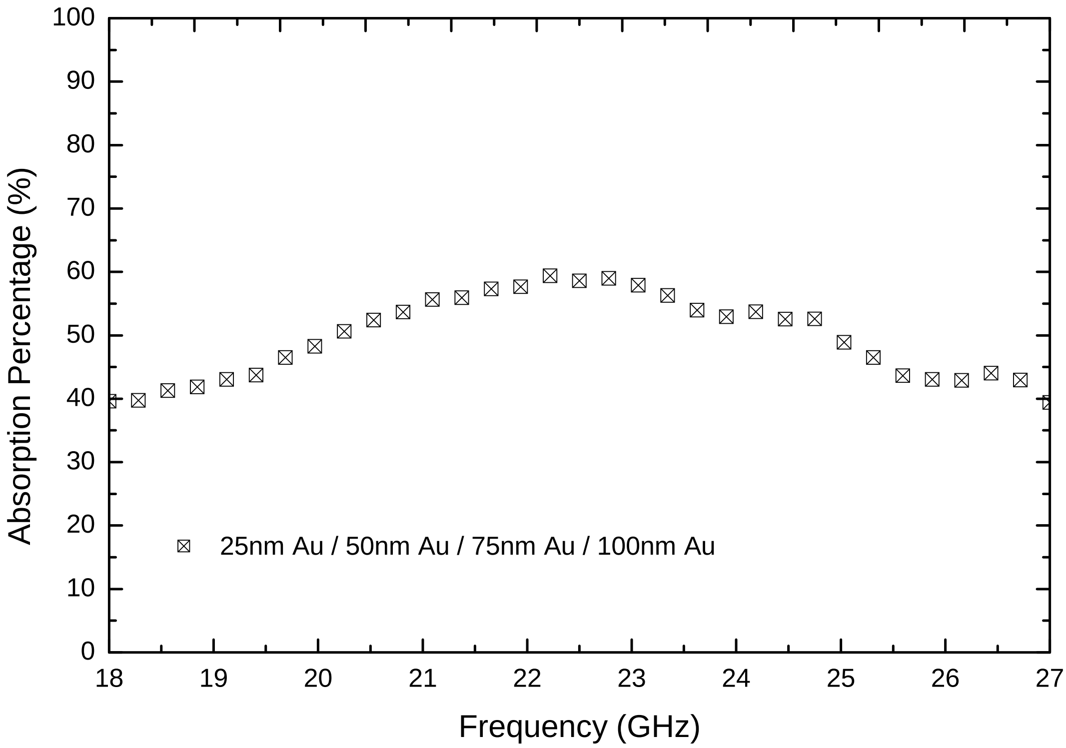

Figure 4.29 EM wave absorption of 25 nm Au / 50 nm Au / 75 nm Au / 100 nm Au four layered structure.

Due to high reflection loss and moderate transmission loss EM wave absorption is insufficient as expected. When compared to four layered combination of nickel surface-modified structure, gold surface-modified multilayer provided 30% less EM wave absorption. In hybrid structures, gold modified layers should be applied as reflective layers in order to increase transmission loss (suppress transmission). Improvement of EM wave absorption level can be attained by a decrease in transmission loss if sufficient reflection loss is supplied by the frontal impedance matching and electromagnetic loss layers.

4.5. Estimation of Theoretical Composite Material Properties and Reinforcement Layer Design for EM Wave Absorbing GFRP Composite Materials

In the current study, computer aided computation results for multilayered structures were compared with free-space measurements. Compatibility between the results has shown the ability of the computational method in predicting EM wave absorption potential of multilayered structures. By the application of computation method and usage of the determined design principles, EM wave absorbing multilayered structures with improved performance can be achieved.

4.5.1. Tailoring of EM Wave Absorption Properties of Nickel Coating Modified Multilayered Structures by Computer Aided Design

In this study, EM wave absorption characteristics of nickel coating surface-modified structures have been discussed. Multilayered structures up to four layers were investigated in terms of S11 and S21 parameters and their compatibility with the computer aided computation results have been verified. Based on the S parameters, it has been determined that EM wave absorption up to 85% can be achieved in multilayered structures formed by metallic coating surface-modified fiber glass woven fabrics.

Investigation of S11 parameter from free-space characterization of 25 nm Ni / 50 nm Ni / 75 nm Ni / 100 nm Ni surface-modified four layered structure revealed that obtained structure has considerable reflection loss between 21-27 GHz (Figure 4.26). In 18-21 GHz frequency range reflection loss higher than 10 dB has been observed. Besides, investigation of S21 parameters has shown that transmission loss of four layered structure is slightly lower than 5 dB. Especially in 18-21 GHz frequency range, EM wave absorption percentage seems to be insufficient.

In order to improve EM wave absorption, understanding EM wave absorption characteristic is essentially required. At this point, evaluation of single layers forming multilayered EM wave absorbing structure is crucial. A solution to the improvement of the EM wave absorption problem may be offered by comparing reflection loss characteristics of individual layers. As it was stated in earlier chapters, problems related to reflection loss is of higher priority. Problems related to transmission loss can easily be solved by the usage of extra surface-modified layers if thickness constraints are not predetermined.

Investigation of S11 parameters for individual 25 nm Ni, 50 nm Ni, 75 nm Ni and 100 nm Ni layers revealed that problems related to reflection loss might be due to reflection loss difference between 25 nm nickel surface-modified fiber glass woven layer and 50nm nickel surface-modified fiber glass woven layer. Refraction of incident EM wave occurs due to impedance difference between adjacent layers. As a result, higher reflection values are observed. At this point, application of an extra surface-modified layer with moderate reflection loss can be used as an effective solution. By this way, impedance difference between adjacent layers can be normalized. Additional layers with moderate reflection loss can be provided by application of surface modification between 25 nm Ni and 50 nm Ni. A 35 nm nickel surface-modified fiber glass woven layer is manufactured and characterized by free-space method. S11 reflection loss of 35 nm Ni surface-modified fiber glass woven fabric and its comparison with those of 25, and 50 nm thick surface-modified fiber glass woven layers are presented in Figure 4.30.

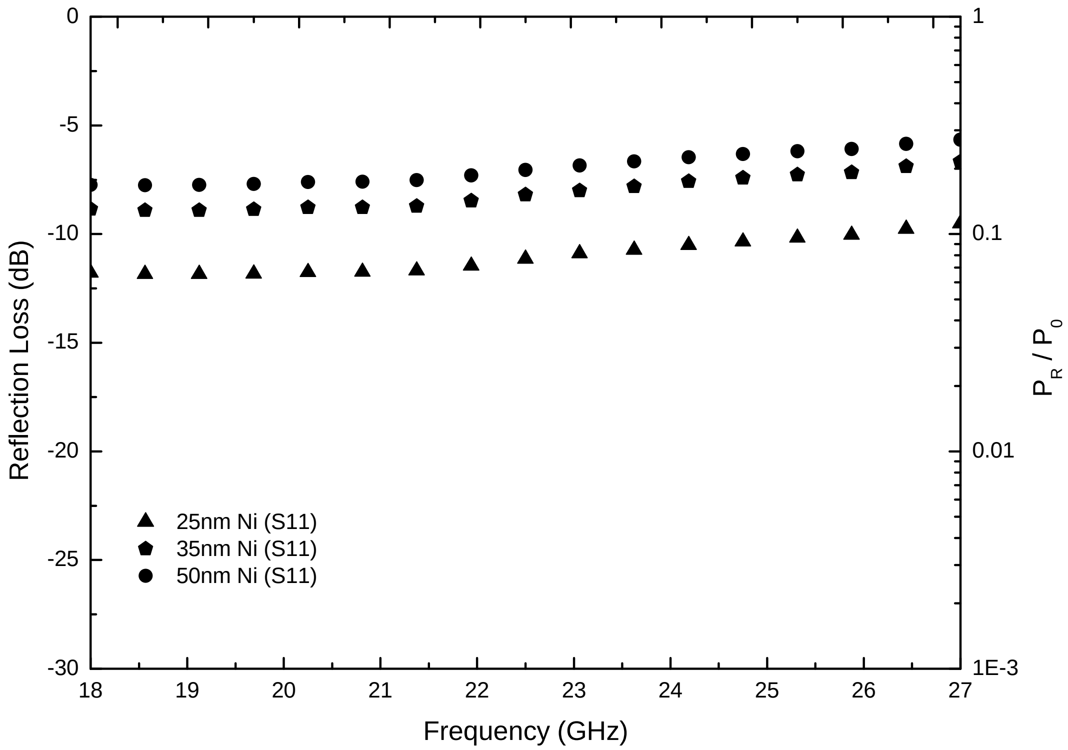

Figure 4.30 Reflection loss of 35 nm Ni surface-modified woven fabric layer in comparison to those of 25 and 50 nm thick Ni surface-modified fiber glass woven fabric layers.

As it is expected, 35 nm nickel surface-modified structure provided an intermediate reflection loss between those of 25 and 50 nm Ni surface-modified fiber glass woven fabric layers. Consequently, by the usage of an extra layer, impedance difference between adjacent layers is expected to be normalized.

In order to investigate differences in EM wave absorption characteristics after the insertion of 35 nm surface-modified fiber glass woven fabric layer, computation for four and five layered multilayer structures were compared. In Figure 4.31, S11 reflection loss for 25 nm Ni / 50 nm Ni / 75 nm Ni / 100 nm Ni four layered structure and 25 nm Ni / 35nm Ni/ 50nm Ni / 75nm Ni /100 nm Ni five layered structure is shown.

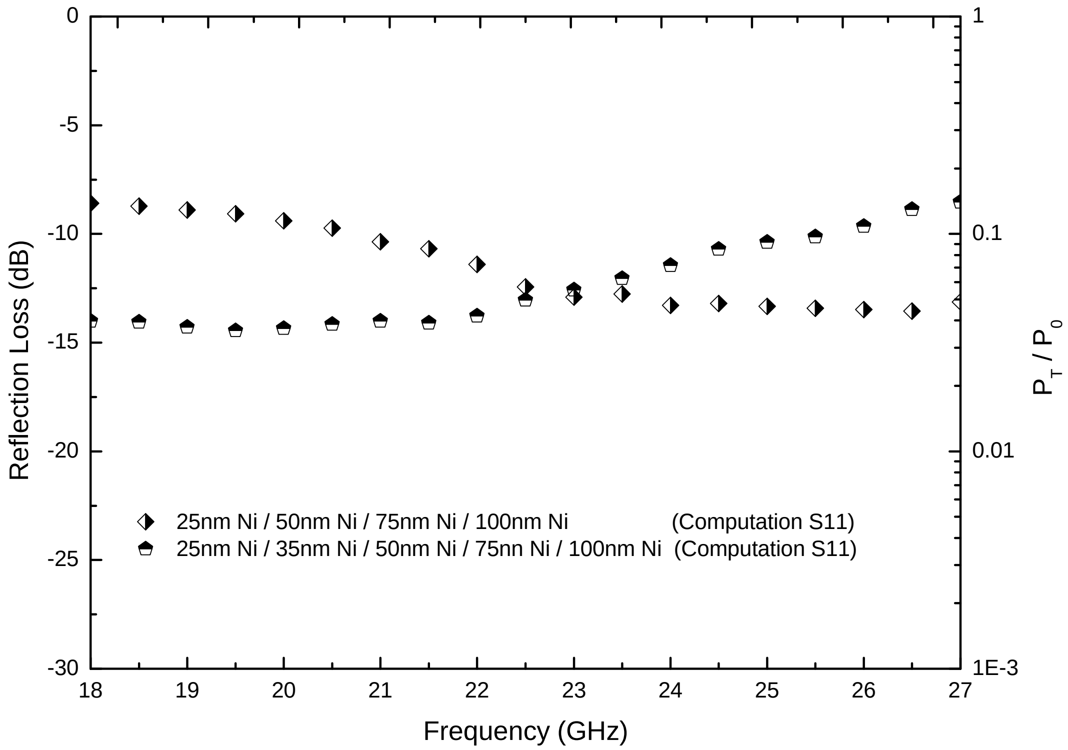

Figure 4.31 Estimated reflection loss for 25 nm Ni / 35 nm Ni / 50 nm Ni / 75 nm Ni / 100 nm Ni five layered structure and its comparison with 25 nm Ni / 50 nm Ni / 75 nm Ni / 100 nm Ni four layered structure

Improvement in reflection loss is clearly seen in Figure 4.31. Especially in 18-21 GHz range considerable decrease in reflection loss is estimated. Reflection loss predicted for five layered structure is estimated to be below 10 dB within 18-27 GHz frequency range. Broadband efficiency of reflection loss is improved by the application of extra surface-modified layer. In order to predict overall EM wave absorption characteristics, comparison of transmission loss behavior of four layered and five layered structure is required as well. In Figure 4.32, transmission loss of 25 nm Ni / 50 nm Ni / 75 nm Ni / 100 nm Ni four layered structure and 25 nm Ni / 35 nm Ni/ 50 nm Ni / 75 nm Ni /100 nm Ni five layered structure is given.

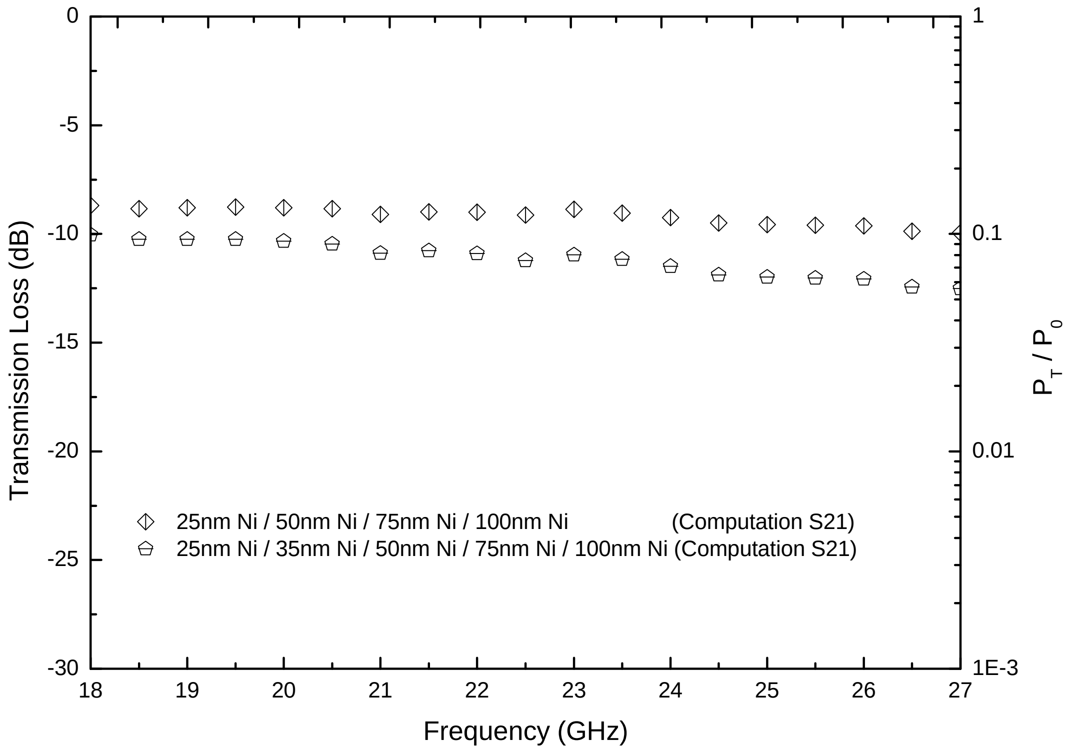

Figure 4.32 Estimated transmission loss of 25 nm Ni / 35 nm Ni / 50 nm Ni / 75 nm Ni / 100 nm Ni five layered structure along with that of 25 nm Ni / 50 nm Ni / 75 nm Ni / 100 nm Ni four layered structure.

Transmission loss is predicted to be decreasing due to increased number of surface-modified layers. By the addition of an extra layer, transmission loss is expected to decrease to around 10 dB level. According to computation results remarkable increase in EM wave absorption potential seems achievable.

In order to verify differences in EM wave interaction characteristics and to make a comparison with the performed computer aided computations, free-space measurements were conducted on 25 nm Ni / 50 nm Ni / 75 nm Ni / 100 nm Ni four layered and 25 nm Ni / 35 nm Ni/ 50 nm Ni / 75 nm Ni /100 nm Ni five layered multilayered reinforcement structures. In Figure 4.33, comparison of S11 reflection characteristics of these two multilayered structures in terms of measurement results is given.

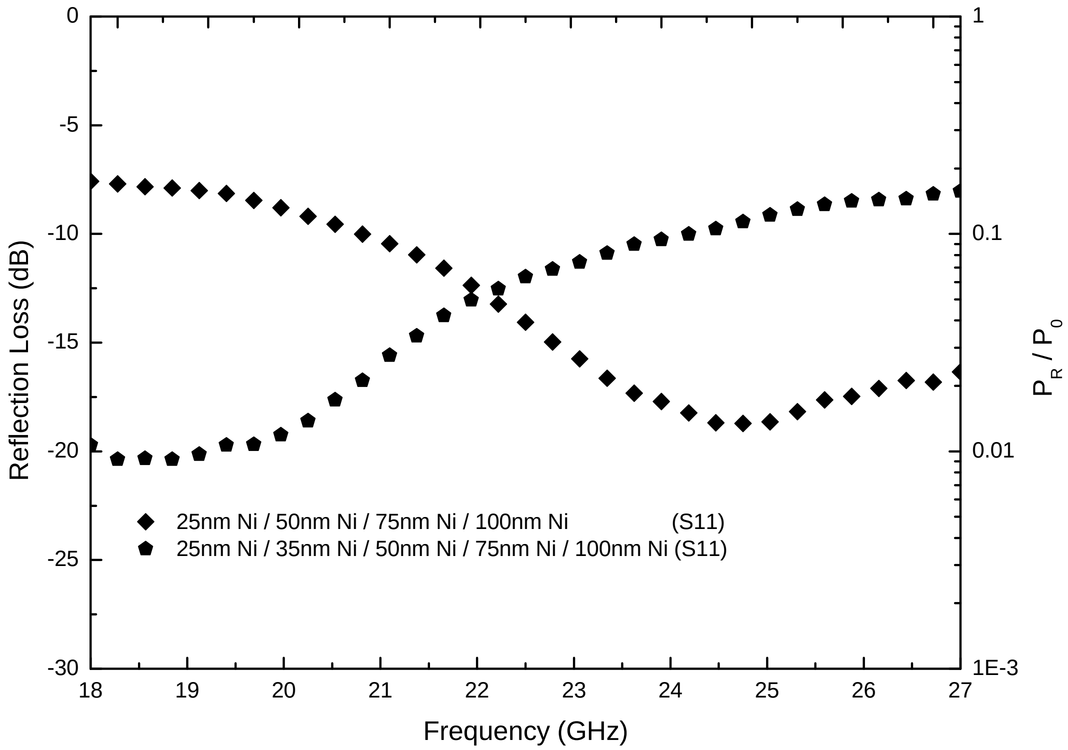

Figure 4.33 Reflection loss of 25 nm Ni / 35 nm Ni / 50 nm Ni / 75 nm Ni / 100nm Ni five layered structure and its comparison with that of 25 nm Ni / 50 nm Ni / 75 nm Ni / 100 nm Ni four layered structure.

Following the insights obtained by the computations, addition of surface-modified extra layer helped reflection loss decrease within 18-27 GHz frequency range. After application of extra surface-modified layer reflection loss decreased below 10 dB. Although it seems that reflection loss within 21-27 GHz frequency range has increased, broadband efficiency is attained within K band resulting in improved potential EM wave absorption stability crucial for application side.

In Figure 4.34, transmission loss of 25 nm Ni / 50 nm Ni / 75 nm Ni / 100 nm Ni four layered structure and 25 nm Ni / 35 nm Ni/ 50 nm Ni / 75 nm Ni /100 nm Ni five layered structure is shown.

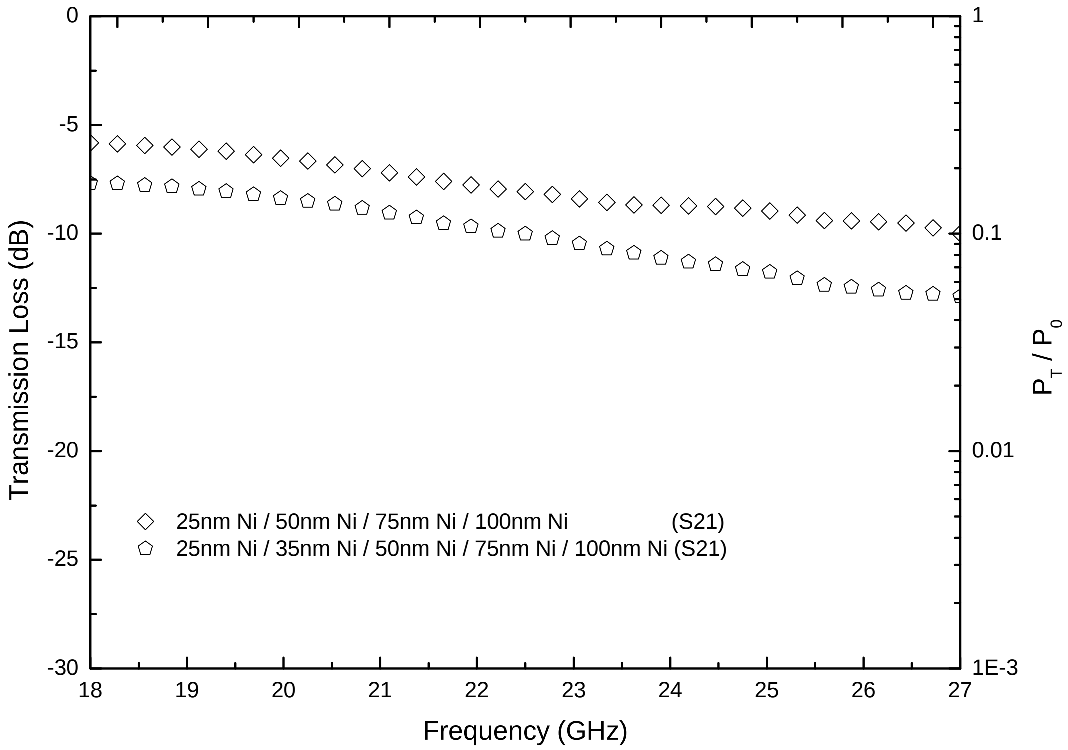

Figure 4.34 Transmission loss of 25 nm Ni / 35 nm Ni / 50 nm Ni / 75 nm Ni / 100 nm Ni five layered structure and its comparison with that of 25 nm Ni / 50 nm Ni / 75 nm Ni / 100 nm Ni four layered structure

As it is predicted, transmission loss decreases due to application of extra surface-modified layer while obtained reflection loss is still below 10 dB. Further improvement can be attained by additional layers with high reflection loss if required.

Simultaneous improvement of reflection and transmission loss has lead to improvement of overall EM wave absorption characteristics. In Figure 4.35, EM wave absorption percentages of 25 nm Ni / 50 nm Ni / 75 nm Ni / 100 nm Ni four layered and 25 nm Ni / 35 nm Ni/ 50 nm Ni / 75 nm Ni /100 nm Ni five layered structures are presented.

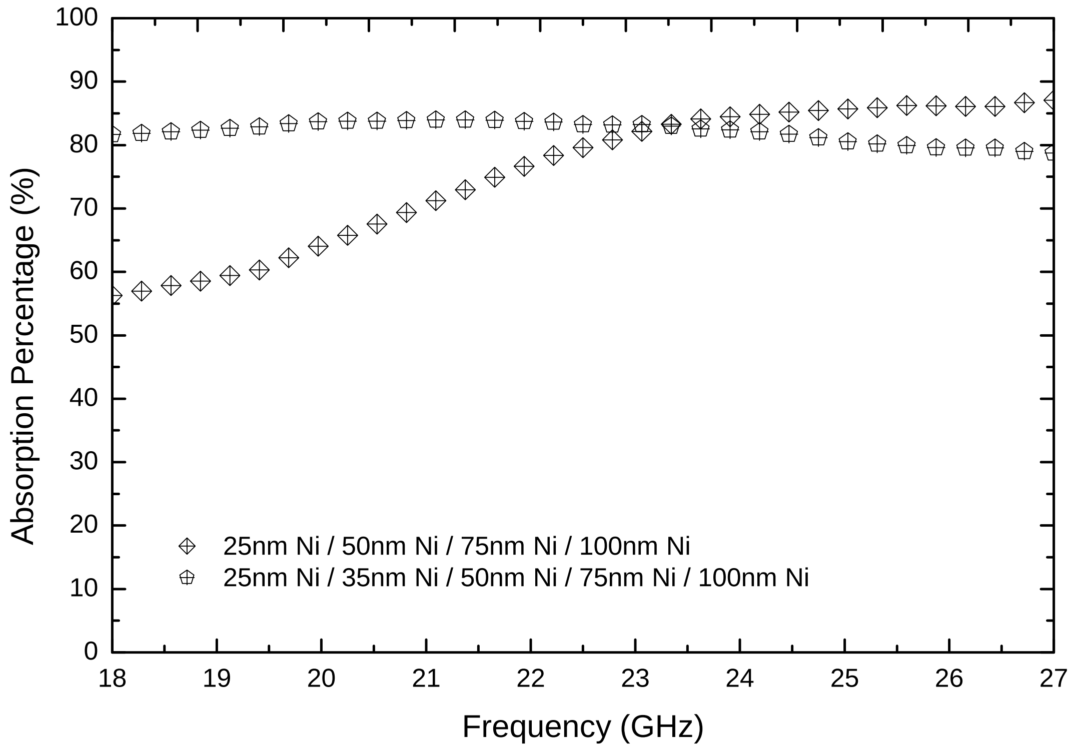

Figure 4.35 EM Wave absorption of 25 nm Ni / 35 nm Ni / 50 nm Ni / 75 nm Ni / 100 nm Ni five layered structure compared to that of 25 nm Ni / 50 nm Ni / 75 nm Ni / 100 nm Ni four layered structure

From Figure 4.35, improvement in EM wave absorption properties is clearly seen. Especially in 18-24 GHz range, improvement of EM wave absorption potential after the application of 35 nm Ni surface-modified layer is evidenced. Development of EM wave absorption stability within a wide frequency range is also demonstrated with the results presented in this figure. Computational methods have shown great success in predicting EM wave absorption characteristics of multilayered structures. In Figure 4.36, comparison of estimated and measured EM wave absorption characteristic is represented.

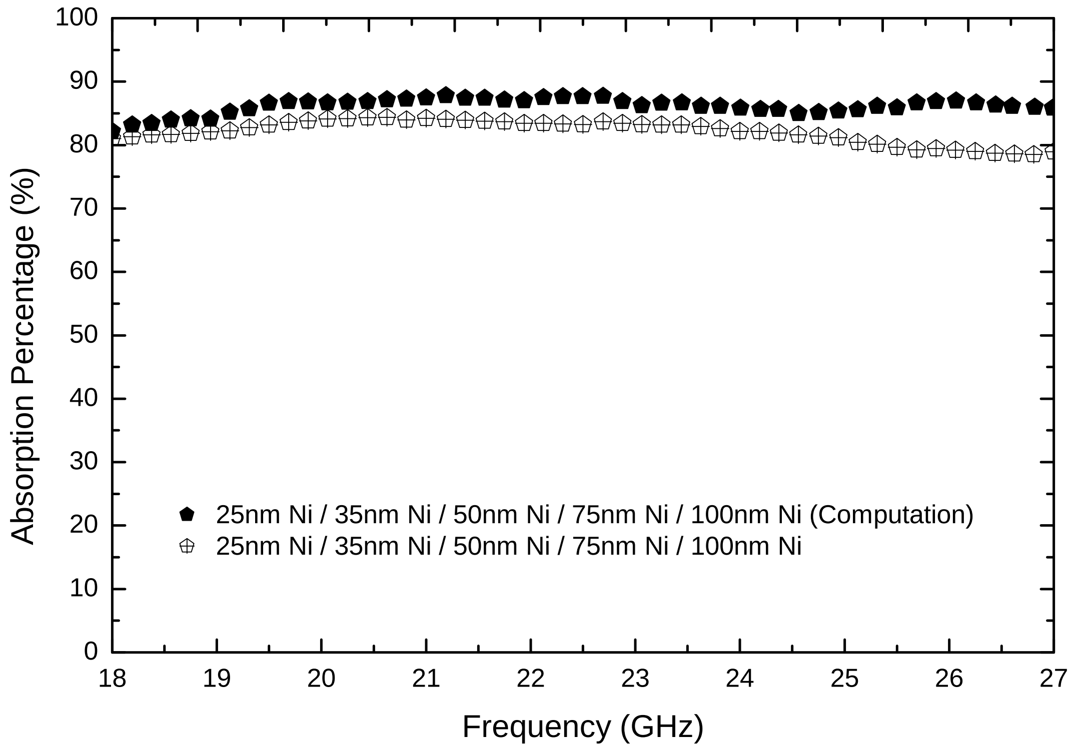

Figure 4.36 Comparison of estimated and measured EM wave absorption of 25 nm Ni / 35 nm Ni / 50 nm Ni / 75 nm Ni / 100 nm Ni five layered multilayer structure.

By this representative analysis on the five layered structure, verification of computation method has been repeated, and reliability of the computation system has also been retested. Computations conducted on four and five layered structures have provided results highly compatibility with the experimental data. Computer aided computation of multilayered structures can be used as an effective tool in designing and engineering of EM wave characteristics for GFRP composite materials.

4.5.2. Further Development of Electromagnetic Properties by the Use of Computer Aided Methods

Further improvements in the EM wave absorption behavior of multilayered structures can be achieved using computational methods. Necessary changes in the extent of the surface modifications along with the arrangements and number of individual layers in the multilayered structures can be previewed by the application of computation method to further enhance reflection, transmission and absorption characteristics. For example, development of the symmetry of the absorption characteristic for the four layered system shown in Figure 4.15 can be predicted by the insertion of additional surface-modified layers in an inverse order. Electromagnetic characterization of obtained eight layered structure can be conducted by the presented computation method. In practice, experimental characterization of such a structure by free-space is rather time taking and demanding. Consequently, in order to overcome such practical limitations effect of additional surface-modified layers on the overall EM wave transmission/reflection characteristic of the multilayered structures can be monitored via computations.

CHAPTER 5

CONCLUSION

In the current study, electromagnetic wave absorption potential of gold and nickel coating surface-modified single and multilayered fiber glass woven fabric reinforcement structures was investigated within 18 - 27 GHz frequency range by free-space measurement method. Quadriaxially woven fiber glass fabric (Q625) surfaces were modified by gold and nickel conductive thin film deposition applied by sputter deposition technique. First of all, effect of coating thickness up to 100 nm on the EM wave reflection/transmission, and hence absorption of single layer fabrics has been investigated. Surface-modified layers with tailored electromagnetic properties were proposed to be utilized in multilayer form in composite material design. Principles of multilayered arrangement for maximized and broadband effective EM wave absorption were discussed in detail. Remarkable EM wave absorption within 18 - 27 GHz frequency band has been achieved by successive ordering of surface-modified layers in the form of multilayered structures. Combinations of surface-modified layers up to 5 layers were examined in this study. Furthermore, a computer aided computation method for the prediction of EM wave interaction properties of multilayer structures based on the data of single layers forming the structure has been introduced. The mathematical basis of the computation has been provided. Properties of multilayers were computed by multiplication of transmission matrices measured on single layers. In this study, predicted and experimentally determined EM wave absorption properties of multilayer structures have been compared. Comparisons exhibited considerable compatibility between experimental and computational data. In summary, following conclusions were drawn:

- Fiber glass woven fabric reinforcements are transparent to EM waves in as-received state. As conductive surface coating is applied, electromagnetic transparency is weakened. Reflection loss is observed to increase as transmission loss decreases.
- Electromagnetic properties can be tailored by controlling the thickness of surface modification. By surface modification, surface-modified layers with reflective, transmissive or lossy characteristic can be achieved.
- Effectiveness of electromagnetic absorption is higher in nickel treated Q625 woven fabric layers when compared to gold treated layers. Being a ferromagnetic material, nickel modified layers provided magnetic loss in addition to ohmic loss mechanism.
- Lower electrical conductivity of nickel caused reflection loss to be less dependent on coating thickness when compared to gold modified layers.
- Target materials to be used in the surface modification should exhibit low conductivity and low skin depth in order to achieve more controllable electromagnetic characteristics.
- Multilayered arrangement of surface-modified layers provided higher absorption percentage due to multiple interaction of EM waves reflected from different layers. EM wave absorption potential of single layers is further improved by multilayer formation as it is stated in the literature.
- Multilayered structure can designed based on three functional layer groups. First group is formed by impedance matching layers. By this group reflection loss from the structure is lowered. Second group is composed of electromagnetic lossy layers. Within these layers, electromagnetic power is suppressed by the

operative loss mechanisms. Third group is formed by reflective layers in order to prevent EM wave transmission.

- Gradual changes in complex permittivity and complex permeability between the layers forming the multilayer structure yields structures with intrinsic electromagnetic impedance comparable to that of free-space within frequency range under consideration. As a result, operational frequency range stability is attained and strong reflections from GFRP composite material at specific frequencies can be prevented.

- Electromagnetic interaction asymmetry between front and back faces of multilayered structures has been observed. Symmetry against EM waves can be attained by mirror image layering. Increment in multilayer thickness is expected to provide lower transmission loss and improved absorption performance from both sides.

- Precision of the results obtained by computer aided computation was observed to increase by increasing number of surface-modified layers

- Sharp reflection drops due to interlayer spacing or remarkable impedance difference and multiple reflections between successive layers cannot be predicted by the computation precisely. Especially for multilayers formed by three or less layers, prediction exhibited higher reflection loss compared to experimental data. Therefore, EM wave absorption prediction appeared to be less than experimental results which can be regarded as a safety margin in practice.

- Computer aided computation can be used in improving EM wave absorption potential of multilayered structures predesigned considering mechanical constraints. A representative work has been covered in the present study. By computer aided computation a solution has been offered for the development of multilayered structures with broadband EM wave absorption capability. Experimental results proved the success of the computation method in the design and development of such reinforcement structures.

REFERENCES

[1] P. S. Neelakanta, Handbook of Electromagnetic Materials (CRC Press, Washington D.C., 1995).

[2] E. F. Knott, J. F. Shaeffer and M. T. Tuley, Radar Cross Section (SciTech Publishing, 1993).

[3] IEEE, IEEE Standard Letter Designations for Radar-Frequency Bands, in "IEEE Std 521-2002 (Revision of IEEE Std 521-1984)" (2003) p. 0_1.

[4] D. C. Giancoli, Physics for Scientists & Engineers (Prentice Hall, New Jersey, 2000).

[5] M. Gupta and E. W. W. Leong, Microwaves and Metals (Wiley, 2007).

[6] IPAC, Infrared Windows, (Infrared Processing and Analysis Center, California, 2010).

[7] D. Pozar, Microwave Engineering (Wiley, 2004).

[8] J. Huo, L. Wang and H. Yu, Journal of Materials Science 44 (2009) 3917.

[9] W. Callister, Materials Science and Engineering: An Introduction (Wiley, 2006).

[10] A. T. Adams, Electromagnetics for Engineers (The Ronald Press Company, New York, 1971).

[11] J. F. Shackelford, Introduction to Material Science for Engineers (Prentice Hall, New Jersey, 2005).

[12] C. K. Yuzcelik, Radar Absorbing Materials Design, in "Systems Engineering " (Naval Postgraduate School, Monterey, 2003).

[13] L. F. Chen, C. K. Ong, C. P. Neo, V. V. Varadan and V. K. Varadan, Microwave Electronics Measurement and Characterization (John Wiley & Sons Ltd., 2004).

[14] D. Ebbing and S. D. Gammon, General Chemistry (Houghton Mifflin Company, New York, 2001).

[15] W. Mingzhong and et al., Journal of Physics D: Applied Physics 33 (2000) 2398.

[16] M. S. Pinho, M. L. Gregori, R. C. R. Nunes and B. G. Soares, European Polymer Journal 38 (2002) 2321.

[17] A. N. Yusoff, M. H. Abdullah, S. H. Ahmad, S. F. Jusoh, A. A. Mansor and S. A. A. Hamid, Journal of Applied Physics 92 (2002) 876.

[18] J. Li, J. Huang, Y. Qin and F. Ma, Materials Science and Engineering B: Solid-State Materials for Advanced Technology 138 (2007) 199.

[19] M. H. Shams, S. M. A. Salehi and A. Ghasemi, Materials Letters 62 (2008) 1731.

[20] A dictionary of science, in "Oxford paperback reference", edited by J. Daintith (Oxford University Press, Oxford :, 2005).

[21] Y. Qing, W. Zhou, F. Luo and D. Zhu, Journal of Magnetism and Magnetic Materials 321 (2009) 25.

[22] Y. Fan, H. Yang, X. Liu, H. Zhu and G. Zou, Journal of Alloys and Compounds 461 (2008) 490.

[23] D. K. Ghodgaonkar, V. V. Varadan and V. K. Varadan, IEEE Transactions on Instrumentation and Measurement 39 (1990) 387.

[24] N. Gürkan, Studies on interaction of electromagnetic waves with barium hexaferrite ceramics, in "Department of Metallurgical and Materials Engineering" (Middle East Technical University, Ankara, 2008).

[25] C.-Y. Huang and C.-C. Wu, European Polymer Journal 36 (2000) 2729.

[26] N. Dishovsky and M. Grigorova, Materials Research Bulletin 35 (2000) 403.

[27] W. S. Chin and D. G. Lee, Journal of Composite Materials 41 (2007) 403.

[28] K. K. Chawla, Composite Materials: Science and Engineering (Springer London London, 2008).

[29] S. K. Mazumdar, Composites Manufacturing : Materials, Product, and Process

Engineering (CRC Press, Florida, 2002).

[30] T. F. Wallenberger, J. C. Watson and H. Li, in "ASM Metals Handbook", edited by A. I. H. Committee (ASM International, 2001) p. 77

[31] ASTM, Standard Specification for Glass Fiber Strands, (2005).

[32] K. B. Cheng, S. Ramakrishna and K. C. Lee, Composites Part A: Applied Science and Manufacturing 31 (2000) 1039.

[33] W. S. Chin and D. G. Lee, Composite Structures 77 (2007) 457.

[34] J. H. Oh, K. S. Oh, C. G. Kim and C. S. Hong, Composites Part B: Engineering 35 (2004) 49.

[35] E. Tan, Characterization of Electromagnetic Wave Absorbing Properties of SiC - Based and Alumina Ceramic Woven Fabrics, in "Department of Metallurgical and Materials Engineering " (Middle East Technical University, Ankara, 2008).

[36] METYX Glass Fiber Reinforcement Catalog, (2005).

[37] N. Gagnon, Design and Study of a Free - Space Quasi Optical Measurement System, in "Institute for Electrical and Computer Engineering" (University of Ottawa, Ottawa, 2002).